

**DECIPHERING SOIL NITROGEN BIOGEOCHEMICAL PROCESSES
USING NITROGEN AND OXYGEN STABLE ISOTOPES**

by

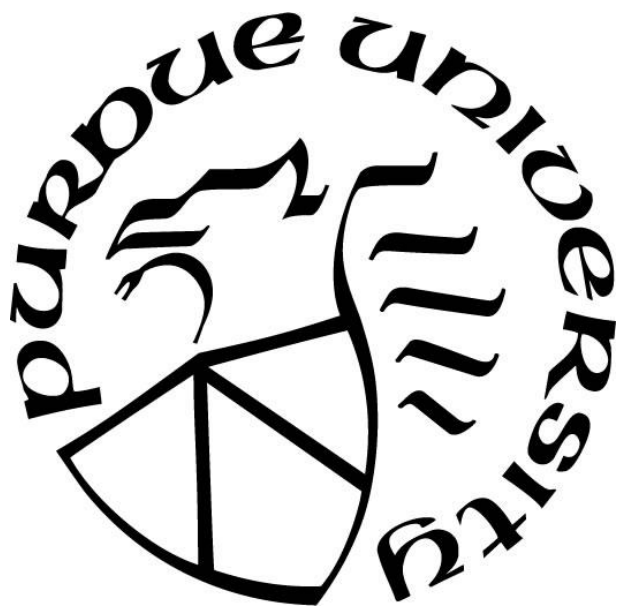
Benjamin Paul Wilkins

A Dissertation

Submitted to the Faculty of Purdue University

In Partial Fulfillment of the Requirements for the degree of

Doctor of Philosophy



Department of Chemistry

West Lafayette, Indiana

May 2019

THE PURDUE UNIVERSITY GRADUATE SCHOOL
STATEMENT OF COMMITTEE APPROVAL

Dr. Greg Michalski, Chair

Department of Earth, Atmosphere, and Planetary Sciences

Dr. Lisa Welp

Department of Earth, Atmosphere, and Planetary Sciences

Dr. Richard Grant

Department of Agronomy

Dr. Alexander Laskin

Department of Chemistry

Approved by:

Dr. Christine Hrycyna

Head of the Graduate Program

To My Wife
For her unconditional love and support

ACKNOWLEDGMENTS

First and foremost, I'd like to express my deep gratitude and appreciation towards my advisor Dr. Greg Michalski for his patience, mentorship, guidance, and knowledge over these past 5 years. This work would not have been possible without him. His excitement and enthusiasm for science has transformed me into the researcher and problem solver I am today.

I'd also like to thank my committee members, Dr. Richard Grant, Dr. Alex Laskin, and Dr. Lisa Welp, for sharing their knowledge and suggestions. Appreciation is also due towards my lab mates and managers over the years for their research and laboratory help, input, suggestions, and guidance. Thanks, are also in order for all the undergraduates I have been able to guide and work beside as we completed numerous projects.

Special thanks are due the American Society for Engineering Education Department of Defense Science Mathematics and Research for Transformation Scholarship (ASEE-DOD-SMART), U.S. Department of Homeland Security HS-STEM, Purdue Climate Change Research Center (PCCRC), and the Purdue Department of Chemistry for their financial support allowing me to pursue and conduct independent research and attend academic conferences leading to my intellectual growth.

TABLE OF CONTENTS

LIST OF TABLES	8
LIST OF FIGURES	9
ABSTRACT	12
CHAPTER 1. INTRODUCTION	14
1.1 Objectives	14
1.2 Chapter Organization	16
CHAPTER 2. LITERATURE REVIEW OF THE SOIL NITROGEN CYCLE AND APPLICATION OF STABLE ISOTOPES	18
2.1 Soil Nitrogen Cycle.....	18
2.2 Stable Isotopes	26
2.3 Isotope Mixing Models.....	29
2.4 Isotope Effects on Production and Consumption of Nitrogen Compounds.....	32
2.5 Rayleigh Distillation	39
CHAPTER 3. DETERMINING THE ¹⁵ N ENRICHMENT AND SOURCES OF OXYGEN IN NITRATE PRODUCED BY NITRIFICATION IN AN AGRICULTURAL SOIL	42
3.1 Abstract	42
3.2 Introduction.....	43
3.3 Materials and Methods.....	49
3.3.1 Nitrification Incubations	49
3.4 Results.....	52
3.5 Discussion.....	54
3.5.1 Nitrification Rates.....	54
3.5.2 ¹⁵ N Enrichment Factor of Nitrification.....	56
3.5.3 Sources of ¹⁸ O incorporated into NO ₃ ⁻ during nitrification	59
3.6 Conclusion	62
CHAPTER 4. DETERMINATION OF THE ¹⁵ N ENRICHMENT OF NITRATE AND NITRITE REDUCTION DURING DENITRIFICATION BY EXPERIMENTAL AND KINETIC MODELS	64
4.1 Abstract	64

4.2	Introduction.....	64
4.3	Materials and Methods.....	68
4.3.1	Denitrification Incubations	68
4.4	Results.....	71
4.5	Discussion.....	72
4.5.1	Accumulation of Nitrite in Denitrification Incubations.....	72
4.5.2	Modeling Denitrification Concentration by Zero, First, and Michealis-Menten Kinetics	74
4.5.3	The $\delta^{15}\text{N}$ of $\text{NO}_3/2$ During Denitrification Incubations	81
4.6	Conclusion	95
CHAPTER 5. QUANTIFICATION OF FIELD-SCALE DENITRIFICATION BY STABLE ISOTOPE ANALYSIS OF NITRATE AND WATER FROM TILE DRAIN DISCHARGE.....		98
5.1	Abstract.....	99
5.2	Introduction.....	99
5.3	Materials and Methods.....	103
5.3.1	Site description	103
5.3.2	Meteorological and Soil Data	104
5.3.3	Sample Collection and Storage.....	105
5.4	Results.....	106
5.4.1	Hydrology and Chemistry of Discharge Overview	106
5.5	Discussion.....	112
5.5.1	Qualitative Evidence of Denitrification.....	112
5.5.2	Rayleigh Distillation Model	120
5.6	Conclusion	130
5.7	Acknowledgments.....	134
CHAPTER 6. CONCLUSION AND FUTURE DIRECTIONS		135
6.1	$^{15}\epsilon_{\text{NO}_3^-/\text{NH}_4^+}$ of nitrification and source of oxygen	135
6.2	$^{15}\epsilon_{\text{NO}_3^-}$ and $^{15}\epsilon_{\text{NO}_2^-}$ of denitrification.....	137
6.3	Qualitative identification and quantification measured of denitrification by stable isotopes within an agricultural soil	137
6.4	Future Outlook	138

REFERENCES	140
APPENDIX.....	161
VITA.....	163

LIST OF TABLES

Table 2-1 The oxidation states of nitrogen in common compounds.....	19
Table 2-2 The rare and common stable isotope, its natural abundance, international standard, and atomic ratios of standards	27
Table 2-3 Nitrogen and oxygen isotope enrichment factors of microbial and physical processes	33
Table 3-1 Experiment conditions used throughout incubations	49
Table 3-2 $\delta^{18}\text{O}$ Values of various H_2O and O_2 used in Experiments	52
Table 3-3 NH_4^+ and initial and final NO_3^- $\delta^{15}\text{N}$ values of nitrification experiments.....	59
Table 4-1: The experimental $^{15}\epsilon_{\text{NO}_3/2}$ and $^{15}\epsilon_{\text{NO}_2^-}$ values determined using measured $\delta^{15}\text{N}$ values with fraction of $\text{NO}_3/2$ remaining.	83
Table 4-2 The reactions and rate constants for all denitrification isotope enrichment models. The α value represents the fractionation factor or the relative reaction rate of the heavier isotope to the lighter isotope. The reaction rate for the heavier isotope was determined by multiplying the rate of the light isotope by the α value. Though arbitrary, the initial concentrations were set to best represent the initial NO_3^- concentration in our incubations. The critical part in this model is that the $^{15}\text{N}/^{14}\text{N}$ ratios are equal to the $\delta^{15}\text{N}$ of NO_3^- added to our soils. Therefore, initial ratios of $^{15}\text{N}/^{14}\text{N}$ here were set to equal 0.5‰, the $\delta^{15}\text{N}$ value of the NaNO_3 added to soil during incubations.	85

LIST OF FIGURES

- Figure 2-1 A simplified nitrogen cycle showing major N transformations and processes. 19
- Figure 2-2 Normal ranges of $\delta^{15}\text{N}$ and $\delta^{18}\text{O}$ of NO_3^- from fertilizer, atmospheric deposition, and soil. The purple circle represents a two source nitrate mixture of nitrate from fertilizer and deposition. The length of the line away from a source represents the fraction contribution of one source relative to another. The red circle represents a three source mixing between fertilizer, atmospheric deposition, and soil NO_3^- . The dashed triangle area represents the possible values for a mixture of fertilizer, atmospheric deposition, and soil NO_3^- . The black arrow indicates the dual isotope enrichment that is caused by denitrification and indicates how isotopic enrichment by denitrification can be mistaken as source mixing. 32
- Figure 2-3 All major sources, sinks and transformation of nitrogen in the nitrogen cycle. All forms and sources of nitrogen in soil are in black text and their $\delta^{15}\text{N}$ and $\delta^{18}\text{O}$ values in white text. Microbial processes are shown in yellow text and the isotopic enrichment of the process in light blue text. Sinks of N are shown in red text along with their corresponding enrichment in light blue text. See table 2-3 for references. 39
- Figure 2-4 Isotopic change in $\delta^{18}\text{O}$ of H_2O in both a closed and an open Rayleigh system with an $\epsilon = -10$. Lines A, B, and C are the observed curves in an open system where A is the remaining liquid, B is the instantaneous product vapor, and C is the accumulated vapor product. Lines D and E represent a closed Rayleigh system where D is the liquid reactant remaining and E is the equilibrated vapor product. Image modified from Gat and Gonfiantini (1981). 40
- Figure 3-1 NO_3^- accumulation over time during nitrification and control incubations. 54
- Figure 4-1 Concentrations of NO_2^- , NO_3^- , and $\text{NO}_{3/2}$, throughout the 24-hour denitrification incubations. The concentrations predicted by the first (black lines) and zero (blue lines) order, Michaelis-Menten (red lines), and Transient Coupled Michaelis-Menten (purple lines) kinetic models. 71
- Figure 4-2. The average $\delta^{15}\text{N}$ value of $\text{NO}_{3/2}$ throughout the 24-hours denitrification incubations of all 5 incubation trials. The increase in standard deviation of samples with time is due to higher isotope and concentration standard deviations at low concentrations of $\text{NO}_{3/2}$ 81
- Figure 4-3 The enrichment factors were determined by plotting the measured $\delta^{15}\text{N}$ values of $\text{NO}_{3/2}$ ($\text{NO}_2^- + \text{NO}_3^-$) against the natural logarithm of the fraction of remaining $\text{NO}_{3/2}$. This was performed for each incubation trial and the slope ($^{15}\epsilon_{\text{NO}_{3/2}}$) is recorded in table 4-3. 83
- Figure 4-4 Three first order *Kintecus* models were used, one with only enrichment during NO_3^- reduction (A), one with only enrichment during NO_2^- reduction (B), and another with enrichment during the reduction of both NO_2^- and NO_3^- (C). The NO_3^- line predicts the change in $\delta^{15}\text{N}$ of NO_3^- throughout the incubations, NO_2^- predicted the change in the $\delta^{15}\text{N}$ of NO_2^- throughout incubations, the $\text{NO}_{3/2}$ is the $\delta^{15}\text{N}$ that would be measured if both NO_2^- and NO_3^- molecules are not separated during the bacteria method, and the gaseous nitrogen is the $\delta^{15}\text{N}$ of the final

gaseous nitrogen products produced at the end of denitrification. The fraction of NO_3^- and NO_2^- in total N graph (D) demonstrates the importance of accurate modeling of NO_2^- and NO_3^- fractions, because data points that do not fall along this predicted fraction are poorly modeled by the first order model. Results show that if only one of the enrichments is considered predicted $\delta^{15}\text{N}$ values of $\text{NO}_{3/2}$ are too low. The model best predicted experimental results when enrichment by both NO_2^- and NO_3^- was considered. During all models after all NO_3^- and NO_2^- has been consumed the $\delta^{15}\text{N}$ of gaseous N all returned to 0.5‰ indicating conservation of all N to gaseous N. 87

Figure 4-5 The change of $\delta^{15}\text{N}$ of $\text{NO}_{3/2}$ with decreasing fraction of remaining N of experimental denitrification incubation and computational models. The fraction of remaining N consisted of both the remaining amount of NO_2^- and NO_3^- compared to the initial amount of N added. Hollow squares are experiment values and the dash, dot, and solid lines are values generated by computational models. Models consisted of zero order (blue dash line), first order (black dot line), Michaelis-Menten (red dot dash line), and Transient Coupled Michaelis-Menten (purple solid line). R^2 values can be found in figure 4-6. 91

Figure 4-6 Experimental $\delta^{15}\text{N}$ of $\text{NO}_{3/2}$ versus modeled $\delta^{15}\text{N}$ of $\text{NO}_{3/2}$. Experimental values are the measured $\delta^{15}\text{N}$ values of $\text{NO}_{3/2}$ from different fractions of N remaining measured from denitrification incubations sampled at 6 different incubation times. Modeled values are the computational calculated $\delta^{15}\text{N}$ values of $\text{NO}_{3/2}$ at the measured fractions of N remaining during denitrification incubations. Models performed were zero order (red circles), first order (black squares), Michaelis-Menten (blue triangles), and Transient Coupled Michaelis-Menten (green upside down triangle). 93

Figure 4-7 Fractions of NO_3^- and NO_2^- in fraction of total N ($\text{NO}_{3/2}$) remaining during denitrification of the first order, Michaelis-Menten and TRMM kinetic models compared to experimental results. The Michaelis-Menten model best predicts the fractions of NO_2^- and NO_3^- at fraction of total N remaining at 0.7. The TRMM model more accurately predicts fractions of NO_2^- and NO_3^- at fraction of total N remaining at 0.5 to 0. Proper modeling of molar fraction of NO_3^- and NO_2^- of $\text{NO}_{3/2}$ is critical for accurate modeling of $\delta^{15}\text{N}$ values of $\text{NO}_{3/2}$ 94

Figure 5-1 (A) $\delta^{15}\text{N}$ - NO_3^- (red triangles) and $\delta^{18}\text{O}$ - NO_3^- values (blue circles) and precipitations amounts (black lines). (B) nitrate concentrations as N (purple diamonds), $\delta^{18}\text{O}$ - H_2O (orange squares), and tile flow (blue lines) throughout the year. Red lines separate each of the four periods (Spring, Transition, Summer, and Fall). 110

Figure 5-2 A dual isotope plot of tile drain nitrate and all potential sources of nitrogen within the experimental plot. Sources of nitrogen added directly to the land as NO_3^- include atmospheric deposition (red box) and UAN (yellow box). The green and orange line are sources of reduced N added to the system that might be nitrified. The light blue box is the NO_3^- $\delta^{18}\text{O}$ values of nitrification assuming all oxygen in NO_3^- was derived from H_2O and the theorized $\delta^{15}\text{N}$ isotope values of nitrate formed by nitrification of urea, NH_4/NH_3 and soil N. The red hollow circles are tile drain NO_3^- $\delta^{15}\text{N}$ and $\delta^{18}\text{O}$ values in the Spring and the blue hollow circles are those in Summer and Fall. The solid blue square is the estimated starting value of $\delta^{15}\text{N}$ and $\delta^{18}\text{O}$ determined by mass balance of all inputs (see discussion). The solid black line with a slope of

0.82 is the increase of $\text{NO}_3^- \delta^{15}\text{N}$ relative to $\delta^{18}\text{O}$. The arrows labeled nitrification and volatilization are the potential enrichment in $\delta^{15}\text{N}$ that can occur by those processes. 111

Figure 5-3 The $\delta^{18}\text{O}\text{-H}_2\text{O}$ vs. $\delta^{18}\text{O}\text{-NO}_3^-$ in tile discharge. Nitrification using tile water as the oxidant source would produce $\delta^{18}\text{O}\text{-NO}_3^-$ values that follow the predicted nitrification line. Changes in tile $\delta^{18}\text{O}\text{-H}_2\text{O}$ are caused by a combination of variations in precipitation $\delta^{18}\text{O}$ values and ^{18}O enrichment caused by evaporation. A shift to the right increases $\delta^{18}\text{O}\text{-NO}_3^-$, with no change in $\text{H}_2\text{O} \delta^{18}\text{O}$, suggesting denitrification..... 112

Figure 5-4 The study site's soil temperature (A) and soil moisture (B) at three depths (5cm, 20cm and 60cm) over a year..... 125

Figure 5-5(A) The fraction of nitrate loss through denitrification by the Rayleigh isotopic distillation model. Error bars are every other measurement point. (B) The cumulative loss of nitrate through leaching (red squares) and denitrification (blue diamonds) over the season. The grey area represents the error. The absence of data around 6/1 in figure 5B is due to no tile flow data collection 128

ABSTRACT

Author: Wilkins, Benjamin, P. PhD

Institution: Purdue University

Degree Received: May 2019

Title: Deciphering the Soil Nitrogen Biogeochemical Processes Using Nitrogen and Oxygen Stable Isotopes

Committee Chair: Greg Michalski

Variations in stable isotope abundances of nitrogen ($\delta^{15}\text{N}$) and oxygen ($\delta^{18}\text{O}$) of nitrate are a useful tool for determining sources of nitrate as well as understanding the transformations of nitrogen within soil (Chapter 2). Various sources of nitrate are known to display distinctive isotopic compositions, while nitrogen transformation processes fractionate both N and O isotopes and can reveal the reaction pathways of nitrogen compounds. However, to fully understand the $\delta^{15}\text{N}$ and $\delta^{18}\text{O}$ values of nitrate sources, we must understand the chemistry and the isotopic fractionations that occur during inorganic and biochemical reactions. Among all N cycle processes, nitrification and denitrification displayed some of the largest and most variable isotope enrichment factors, ranging from -35 to 0‰ for nitrification, and -40 to -5‰ for denitrification. In this dissertation, I will first characterize the isotopic enrichment factors of ^{15}N during nitrification and denitrification in a Midwestern agricultural soil, two important microbial processes in the soil nitrogen cycle. Nitrification incubations found that a large enrichment factor of -25.5‰ occurs during nitrification $\text{NH}_4^+ \rightarrow \text{NO}_3^-$, which agrees well with previous studies (Chapter 3). Additionally, oxygen isotopic exchange that occurs between nitrite and water during nitrification was also quantified and found that 82% of oxygen in NO_3^- are derived from H_2O , much greater than the 66% predicted by the biochemical steps of nitrification. The isotopic enrichment that occurs during denitrification was assessed by measuring the change in $\delta^{15}\text{N}$ as the reactant NO_3^- was reduced to N_2 gas (Chapter 4). The incubations and kinetic models showed

that denitrification can cause large isotopic enrichment in the $\delta^{15}\text{N}$ of remaining NO_3^- . The enrichment factor for $\text{NO}_2^- \rightarrow$ gaseous N was -9.1‰ , while the enrichment factors for $\text{NO}_3^- \rightarrow \text{NO}_2^-$ were between -17 to -10‰ , both of which were within the range of values reported in literature. The results demonstrated that nitrification and denitrification caused large isotope fractionation and can alter the presumed $\delta^{15}\text{N}$ and $\delta^{18}\text{O}$ values of nitrate sources, potentially leading to incorrect apportionment of nitrate sources.

The results of the denitrification incubation experiments were applied to a field study, where the measured enrichment factor was utilized to quantify loss of N by field-scale denitrification (Chapter 5). Field-based estimates of total denitrification have long been a challenge and only limited success has been found using N mass balance, N_2O gas flux, or isotope labeling techniques. Here, the flux of nitrate and chloride from tile drain discharge from a small field was determined by measuring both dissolved ions (ion chromatography) and monitoring water discharge. The $\delta^{15}\text{N}$ and $\delta^{18}\text{O}$ of tile nitrate was also measured at a high temporal resolution. Fluxes of all N inputs, which included N wet and dry deposition, fertilizer application, and soil mineralization were determined. The $\delta^{15}\text{N}$ and $\delta^{18}\text{O}$ values of these nitrate sources were also determined. Using this data, I first detected shifts in $\delta^{15}\text{N}$ and $\delta^{18}\text{O}$ values in the tile drain nitrate, which indicated variable amounts of denitrification. Next, a Rayleigh distillation model was used to determine the fraction of NO_3^- loss by field scale denitrification. This natural abundance isotope method was able to account for the spatial and temporal variability of denitrification by integrating it across the field scale. Overall, I found only 3.3% of applied N was denitrified. Furthermore, this study emphasized the importance of complementary information (e.g. soil moisture, soil temperature, precipitation, isotopic composition of H_2O , etc.), and the evidence it can provide to nitrogen inputs and processes within the soil.

CHAPTER 1. INTRODUCTION

This introduction briefly outlines the questions and research needs to deepen our understanding of the nitrogen cycle within soil and the impacts of anthropogenic reactive nitrogen additions to intensively managed landscapes. Below are the objectives of this dissertation followed by the organizational layout.

1.1 Objectives

1. Improve and constrain the ^{15}N enrichment factor and the sources of oxygen of nitrate formed during soil nitrification in a midwestern agricultural soil.

Nitrification is a microbial process that occurs under aerobic conditions in soils and oxidizes NH_4^+ to NO_3^- . The stable isotopes of NO_3^- ($\delta^{15}\text{N}$ and $\delta^{18}\text{O}$) are frequently used to delineate between different sources of NO_3^- in soils and marine environments, such as nitrification. The $\delta^{15}\text{N}$ value of NO_3^- derived from nitrification is often assumed to directly reflect the $\delta^{15}\text{N}$ value of the nitrogen sources (manure, soil N, NH_4^+ fertilizers). In contrast, the NO_3^- $\delta^{18}\text{O}$ value is often assumed to be proportional to the $\delta^{18}\text{O}$ values of the sources of oxygen used during nitrification, which include H_2O and O_2 . Here we measured the isotope enrichment that occurs in ^{15}N and the sources of oxygen in the final NO_3^- product from nitrification in water runoff from a Midwestern cultivated field. This was evaluated by performing aerobic incubations of soil amended with high concentrations of ammonium mixed with isotopically variable H_2O . Results showed that the enrichment factor of $\delta^{15}\text{N}$ from nitrification is large. Additionally, during these incubations we found that the fraction of oxygen from H_2O used during nitrification do not always hold. The fraction of oxygen derived from H_2O found in the NO_3^- product was

consistently higher than the theoretical value of 0.66. The fractions of oxygen in NO_3^- from H_2O were 0.82, indicating isotope exchange between H_2O and the nitrification intermediate NO_2^- is rapid in agricultural soils amended with ammonium.

2. Quantify the ^{15}N enrichment factor for nitrate and nitrite reduction during denitrification in a midwestern agricultural soil by experimental and kinetic models.

Nitrogen stable isotopes are often used to delineate between different sources of nitrate and nitrite in soils and marine environments. In isotope mixing models the nitrogen isotope ratios in nitrate and nitrite from different sources are often assumed conservative. However, a process such as denitrification, the reduction of NO_3^- to N_2 , can cause substantial changes in the nitrogen stable isotope ratios, causing error in nitrate and nitrite source apportionment when using isotope mixing models. Because nitrate and nitrite are reduced by different enzymes they have different degrees of isotope enrichment and studies have demonstrated the overall rate of reduction can vary due to environmental conditions. Here we report the nitrogen isotope enrichment factor for both nitrate and nitrite reduction in a Midwestern agricultural soil. Enrichment values were determined by performing denitrification incubations using agricultural soils collected and measuring the change in nitrite and nitrate concentrations and their nitrogen isotope ratios as a function of time. Data was then fit to models using a kinetic compiler, *kinetcus*, to determine the nitrate and nitrite isotope enrichment values using first order, zero order, and Michaelis-Menten models.

3. Quantifying field-scale denitrification by measuring the change in concentration and $\delta^{15}\text{N}$ of field NO_3^- and applying a Rayleigh distillation model

Denitrification is a microbial process that occurs in anaerobic conditions reducing NO_3^- / NO_2^- in solution to N_2 and N_2O gases. This process removes reactive nitrogen species resulting in the undesired loss of N from intensively managed landscapes (IML). Quantifying the amount of N loss by denitrification within IMLs is difficult. Current chamber and open-path optical methods can be time-consuming and limited in spatial and temporal resolution. Here we present an isotopic approach to quantify denitrification that is able to integrate spatial and temporal variability across the field scale. Tile drain discharge was collected at an IML site between May and November and was analyzed for ion concentrations (NO_3^-) and isotopic composition of H_2O ($\delta^2\text{H}$ and $\delta^{18}\text{O}$) and NO_3^- ($\delta^{15}\text{N}$ and $\delta^{18}\text{O}$). The amount of NO_3^- leached from the beginning of May to the end of October was 31 kg N ha^{-1} , while denitrification was 7.6 kg N ha^{-1} . Seasonal estimates of denitrification N loss were 2.0 , 4.7 , and 0.9 kg N ha^{-1} for Spring, Summer, and Fall respectively.

1.2 Chapter Organization

This dissertation is comprised of six chapters, including this introduction, and is organized as the following:

- Chapter 2: Literature Review of the Soil Nitrogen Cycle and Applications of Stable Isotopes
- Chapter 3: Determination of the ^{15}N Enrichment and Sources of Oxygen in Nitrate Produced by Nitrification in an Agricultural Soil.
- Chapter 4: Determination of the ^{15}N Enrichment of Nitrate and Nitrite Reduction During Denitrification by Experimental and Kinetic Models
- Chapter 5: Quantification of Field-Scale Denitrification by Stable Isotope Analysis of Nitrate and Water from Tile Drain Discharge

- Chapter 6: Conclusion and Future Directions

CHAPTER 2. LITERATURE REVIEW OF THE SOIL NITROGEN CYCLE AND APPLICATION OF STABLE ISOTOPES

2.1 Soil Nitrogen Cycle

Nitrogen (N) is a necessary element for life, since it is a major element in amino acids that make up proteins (Hatfield & Keeney, 2008). Despite the fact that nitrogen accounts for 79% of the Earth's atmosphere, only a few specialized bacteria, archaea, and fungi can utilize N_2 from the atmosphere (Franche et al., 2009). The biological inaccessibility of N_2 is due to the high energy (942 kJ/mol) required to break the N_2 triple bond (Cottrell, 1958). A few microorganisms (biological) and lightening (physical) are the only natural processes that can convert N_2 to biologically available N, which is referred to as "fixed N". Fixed N exists as either an inorganic compound, such as ammonium (NH_4^+) and nitrate (NO_3^-), or as organic compounds, such as urea ($(NH_2)_2CO$), amino acids, and complex biologic material. The variety of N compounds demonstrate the versatility of N because it can exist in several oxidation states, ranging from +5 to -3 (Table 2.1). Nitrogen can transition between these oxidation states through biogeochemical redox reactions while cycling through the atmosphere, biosphere, hydrosphere, and geosphere. This cycling makes up the nitrogen cycle (Figure 2-1). The biologic nitrogen cycle consists of 5 main biological processes: Nitrogen fixation, assimilation, mineralization, nitrification, and denitrification (Bothe et al., 2006). These processes are driven by environmental factors such as temperature, soil moisture, and resource availability (Bothe et al., 2006).

The Nitrogen Cycle

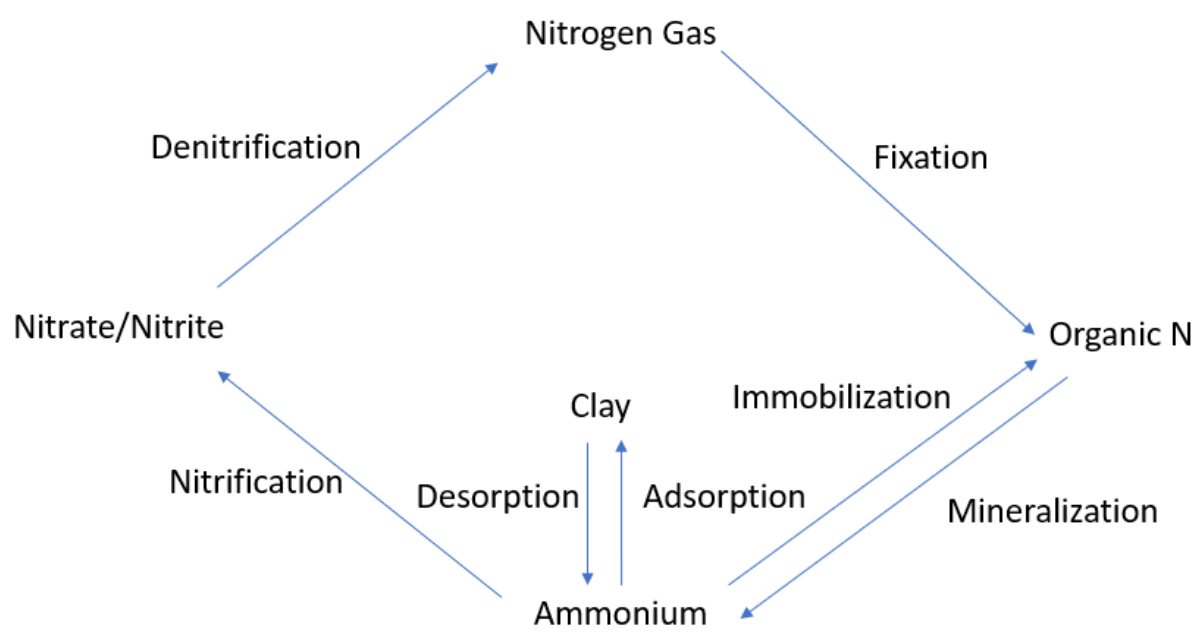


Figure 2-1 A simplified nitrogen cycle showing major N transformations and processes.

Table 2-1 The oxidation states of nitrogen in common compounds

Nitrogen Compounds	Nitrogen Oxidation State
$\text{NH}_3/\text{NH}_4^+$	-3
NH_2OH	-1
N_2	0
N_2O	+1
NO	+2
NO_2^-	+3
NO_3^-	+5

Biological fixation is the microbial process of converting N_2 into biologically available NH_3 (Eq. 1). Despite the presence of the FeMo cofactor, which lowers the activation energy, this reaction is still energy demanding and requires sixteen ATP molecules to break the N_2 triple bond (Berg et al., 2002; Hoffman et al., 2014).



Where ATP is adenosine triphosphate, an energy source in cells, ADP is adenosine diphosphate, and P_i is an inorganic phosphate (orthophosphate). Consequently, few microorganisms can perform this reaction, but those that do are prolific producers of fixed N. These terrestrial and oceanic microorganisms naturally fix approximately 107 Tg N yr^{-1} , far more than the 5.4 Tg N yr^{-1} fixed by lightening (Galloway et al., 2004). Humans have enhanced biological fixation through the cultivation of legumes that have a symbiotic relationship with nitrogen fixing microorganisms. Estimates of global anthropogenic N fixed by legume cultivation are on the order of $31.5 \text{ Tg N yr}^{-1}$ (Galloway et al., 2002).

Assimilation is the creation of organic N from inorganic N by microorganisms (also called immobilization) or plants (uptake). Organic N is often viewed as a temporary storage, or reservoir, of nitrogen (N), because it will eventually return to biologically available N through mineralization (see below). The rate of soil N immobilization is controlled by several factors within the soil such as temperature, moisture, total organic content, pH, soil type, and the carbon/nitrogen (C/N) ratio of soils (Geisseler et al., 2010). Among these variables the C/N ratio has the strongest control on whether immobilization will result in a net sink of N, because microbes will either further decompose releasing N or will use the excess C to uptake N (Geisseler et al., 2010). Research suggest that C/N greater than 40 will lead to net immobilization (organic N), while a ratio below 20 leads to net N mineralization (NH_4^+).

N mineralization is the counter process to immobilization, meaning organic N is transformed back into biologically available inorganic N (organic N \rightarrow NH_4^+) by heterotrophic fungi and bacteria. The rate of organic N turnover is driven by the mineralization rate (Luxhøi et al., 2008). Mineralization is composed of two processes aminization and ammonification. Aminization is the first step when bacteria break complex proteins into simpler amino acids, amides, and amines as a means of gaining energy (proteins \rightarrow $\text{R-NH}_2 + \text{CO}_2 + \text{Energy}$). Ammonification is when bacteria degrade these simple compounds into NH_3 ($\text{R-NH}_2 + \text{H}_2\text{O} \rightarrow \text{NH}_3 + \text{R-OH} + \text{Energy}$). This newly formed NH_3 can then rapidly react with H_2O to form NH_4^+ . This reaction is often considered desirable, because NH_4^+ does not readily leach from soils like other inorganic forms of N, since it is attracted to the negatively charged particles in clay soils. Like immobilization, mineralization is controlled by several factors such as soil temperature and moisture, total organic content, pH, soil type, and C/N ratio (Geisseler et al., 2010). As mentioned above the C/N ratio will determine if mineralization is a net source of N.

Nitrification is a microbial oxidation process that converts NH_4^+ to NO_3^- as a means to extract chemical energy. This process occurs in two steps, the first is ammonia oxidation to nitrite by either chemolithic autotrophic ammonia oxidizing bacteria (AOB) or ammonia oxidizing archaea (AOA). The second step is by nitrite oxidizing bacteria (NOB) that oxidize nitrite into nitrate (Aleem et al., 1965; Andersson & Hooper, 1983; Hollocher, 1984; Kumar et al., 1983; Yoshinari & Wahlen, 1985a). The first step is performed by AOB or AOA (e.g. *Nitrosomonas* or *Nitrosospira*) where NH_3 is oxidized to NO_2^- by two redox reactions (Eq. 2A and 2B) (Andersson & Hooper, 1983).



The second step is performed through NOB (e.g. *Nitrobacter* or *Nitrospira*) oxidizing NO_2^- to NO_3^- (Eq. 3) (Kumar et al., 1983; Xia et al., 2011).



Step 1 is often the rate limiting step, hence NO_2^- accumulation within soils is rare, and when it is observed, is believed to be the result of a decreased or suppressed NOB population (Norton & Stark, 2010; Venterea & Rolston, 2000). Nitrification produces 5 free H^+ and can acidify soils when nitrification is intense such as in agricultural fields where NH_3 fertilizers are applied.

Denitrification is often viewed as the last step of the nitrogen cycle as bioavailable N is returned to the atmosphere as N_2 by heterotrophic bacteria. Denitrification occurs under anaerobic conditions where NO_3^- is used in the absence of O_2 as a terminal electron acceptor during respiration (equation 4) (Martens, 2005).



However, incomplete denitrification can produce important atmospheric gases, N_2O and NO , Eq. 5A-D (Firestone & Davidson, 1989).



N_2O is a greenhouse gas with 298 times the heat trapping ability of CO_2 , and is the main source of NO_x in the stratosphere, which causes catalytic destruction of stratospheric ozone (Crutzen, 1974). The NO by-product reacts in the troposphere, where it participates in the direct removal of 1 troposphere ozone molecule and indirectly removes an additional ozone or hydroxide radical through a series of reactions, where the NO is ultimately oxidized to HNO_3 or aerosol NO_3^- .

Additionally, NO can react with volatile organic compounds (VOCs) in the troposphere ultimately producing ozone, a harmful compound to both plants and humans.

Human activity has had a profound effect on the nitrogen cycle, more than doubling bioavailable terrestrial and marine nitrogen since the 1860s (Galloway et al., 2004). This increase is driven by both agricultural and industrial activity/energy production. Anthropogenic N increases in agriculture are due a growing world population which is reliant on industrial fertilizers and legume cultivations to satisfy nitrogen needs. Anthropogenic N inputs in agriculture are estimated to have increased by over 115 Tg N yr⁻¹ globally since 1860 to a total of 131.5 Tg N yr⁻¹. Industrial inputs, driven by energy demands of first world countries, are estimated to have increased by another 24 Tg N yr⁻¹ globally since 1860 years (Galloway et al., 2002, 2004; Kuypers et al., 2018).

While anthropogenic N is necessary for supporting an increasing world population, it also has many negative environmental impacts, some of which are not completely understood. Most acute human health impacts from anthropogenic N are well known. For example, high concentration exposure to atmospheric NO_x increases the risk of respiratory infections, while high consumption of nitrate in drinking water can cause methemoglobinemia (Powlson et al., 2008). The effects from chronic nitrate exposure are still debated, particularly for nitrate consumption where studies have shown it leads digestive tract cancers (Schlesinger, 2009). Some environmental repercussions are evident and depend on the form of N. Excess addition of fixed N leads to the production of N₂O by incomplete nitrification and denitrification that enhances global warming. NO₃⁻ can leach from soils to waterways and causes eutrophication in both coastal waters and estuaries and the degradation of surface and ground waters (Selman et al., 2008). The nitrogen cycle is complex, which makes tracking and tracing anthropogenic N

difficult. However, an understanding of this is critical, due to nitrogen importance to life and the detrimental environmental impact excessive nitrogen can cause.

One of the objectives of this dissertation is to use stable isotopes to better understand nitrification. While the biochemical steps of nitrification are generally well understood many unknowns still exist. Currently most nitrification research is attempting to understand how it contributes to N pollution in the atmosphere through $\text{NO} + \text{N}_2\text{O}$ release and in aquatic and soil systems. Nitrification is often considered a negative process in soil systems because it transforms clay bound NH_4^+ to easily leachable NO_3^- . Research is focused on field conditions and applications (moisture, tillage, crop, forms of N etc.) and how management practice can be used to minimize the amount of nitrification. Nitrification inhibitors, such as 3-4-dimethylpyrazole phosphate (DMPP) and dicyandiamide (DCA), are added during field application of NH_3 to prevent or reduce the rate of nitrification within the field, because they prevent the initial ammonium oxidation step to NO_2^- . Like denitrification, nitrification produces the reaction by-product N_2O that can be released from the cell into the atmosphere. While the contribution of N_2O from nitrification is often considered minor compared to denitrification, recent research using bacteria cultures have shown that N_2O production by nitrifiers may be significant under proper conditions (Goreau et al., 1980; Linn & Doran, 1982; Moir, 2011). Research by Khalil et al (2004), demonstrated that over 1.5% of nitrified N will end up as N_2O . Soil conditions not only effect the amount of nitrification but also effect how much of the intermediates, NO and N_2O , are released to the atmosphere. For example, as water filled pore space (WFPS) increases from 0 to 50%, N_2O production increases exponentially, but after 50% WFPS N_2O from nitrification rapidly decreases and ceases at 70% WFPS (Bouwman, 1998). Additionally, with the discovery of new heterotrophic nitrifiers, such as *Alcaligenes Faecalis*,

research is needed to understand their contributions to nitrification. In Chapter 3 we will use stable isotopes to better understand nitrification within a Midwestern agricultural soil.

The other major subject of this dissertation, in part, is to use stable isotopes to reduce the uncertainties in the denitrification part of the N cycle. Most research on denitrification has tried to quantify total denitrification, but this has proven difficult because denitrification depends on environmental factors, such as temperature, moisture, pH, and oxygen availability, which can have large spatial and temporal variability within a field (Hofstra & Bouwman, 2005; Woo & Kumar, 2017). This variability has led to a wide range of global estimates of denitrification from 22 to 185 Tg N yr⁻¹ (Bouwman et al., 2013; Hofstra & Bouwman, 2005; Tiedje, 1988). Additionally, denitrification at the field scale has shown large variability, ranging from 8 to 51 kg N ha⁻¹ (Hofstra & Bouwman, 2005). Much of this variability is due to denitrification “hot spots” and “hot moments” (Parkin, 1987) but can also be attributed to methods for measurement. For example, Hofstra & Bouwman (2005) compared four different methods, and found that the estimated denitrification rates could vary by more than 50%. In addition to loss of N by denitrification, production of the greenhouse gas N₂O during denitrification and contributes to climate change. Denitrification is the primarily contributor of biogenic N₂O and its contribution to the global N₂O budget ranges from 4.3 to 5.8 Tg N yr⁻¹ (Crutzen et al., 2007; Davidson, 2009; Syakila et al., 2011) and much of this variability is driven by environmental conditions (Syakila et al., 2011), and research is needed to better understand the field conditions that influence N₂O production over N₂. In Chapter 4 we will use stable isotopes to better understand denitrification within a Midwestern agricultural soil.

Nitrate pollution in surface and ground waters have a variety of N sources. The primarily sources are atmospheric deposition, sewage, manure, and fertilizers. Traditionally nitrogen

pollution in bodies of water and water ways were determined by land usage. This method is reliant on proper and accurate recording of land management, such as crop and fertilizer application or the raising of cattle or swine. However, this approach has proven difficult to properly source nitrate because not only is an accurate inventory difficult to determine but also all nitrogen compounds can be affected by physical, chemical, and biological processes during land to stream transport. These processes can alter the amount of nitrogen that reaches a water way. At the field scale multiple sources of nitrate are added, including large annual application of anhydrous ammonium to agricultural lands, steady continuous wet and dry deposition of N and N fixation by rhizobia bacteria. With many possible sources of nitrate and the amount of that is leached or uptake is highly variable on crops and climate patterns. Therefore, it can be difficult to accurately determine inputs and outputs of nitrate at the field scale. In Chapter 5 we will use stable isotopes to better understand sources of nitrate in discharge from a small Midwestern agricultural field growing corn.

2.2 Stable Isotopes

Stable isotope analysis is an established tool used to understand the sources, sinks, and transformation of elements within biogeochemical cycles, including the nitrogen cycle. Compounds with the same molecular formula but different isotopic mass are called isotopologues. For most elements, the natural abundance of the heavier isotope is usually extremely small compared to the lighter isotope (Table 2.2). These extremely small abundances of the minor (heavy) isotope make accurate absolute measurements difficult, and to avoid these difficulties the ratio (R) of the minor to major isotope abundances are measured. The small differences in the R 's in the sample and standard are reported in dimensionless per mille (‰) values, Eq.6.

$$\delta(\text{‰}) = \left(\frac{R_{\text{Sample}} - R_{\text{Standard}}}{R_{\text{Standard}}} \right) \times 1000 \quad \text{Eq. 6}$$

Where R refers to the atomic ratio of heavy/rare to light/common isotopes (e.g., $^{15}\text{N}/^{14}\text{N}$), sample refers to the sample measured, and standard is the R value of the appropriate international standard (Table 2.2).

Table 2-2 The rare and common stable isotope, its natural abundance, international standard, and atomic ratios of standards

Isotope	Atomic Ratio (Rare/Common)	International Standard	Abundance ratio in Standard
$\frac{D}{H}$	0.00015576	Vienna Standard Mean Ocean Water (VSMOW) $\delta^{18}\text{O}$, $\delta^{17}\text{O}$, δD	$\frac{0.00015574}{0.99984426}$
$\frac{^{17}\text{O}}{^{16}\text{O}}$	0.000373		$\frac{0.00037286}{0.99962714}$
$\frac{^{18}\text{O}}{^{16}\text{O}}$	0.00200520		$\frac{0.00200119}{0.99799881}$
$\frac{^{13}\text{C}}{^{12}\text{C}}$	0.0112372	PeeDEE Belemnite (PDB) $\delta^{13}\text{C}$	$\frac{0.01111233}{0.98888767}$
$\frac{^{15}\text{N}}{^{14}\text{N}}$	0.0036765	Air N_2 $\delta^{15}\text{N}$	$\frac{0.00366303}{0.99633697}$
$\frac{^{34}\text{S}}{^{32}\text{S}}$	0.0450045	Canyon Diablo Troilite (CDT) $\delta^{34}\text{S}$	$\frac{0.04306632}{0.95693368}$

The different reaction rate of one isotope over another in chemical, physical, and biological processes is quantified by an isotope fractionation factor (α). The α value is defined as the ratio of the reaction rates of individual isotopes (k), product and reactant isotope ratios (R), or

the isotope-specific equilibrium constants (K). For example, the α value for denitrification can be defined as Eq. 8A.



$$\alpha = \frac{^{15}k}{^{14}k} = \frac{k_H}{k_L} \quad \text{Eq. 8A}$$

Where the k's are the rate constants of denitrification for each isotopologue. The α is always a ratio of the rate constants but the definition of the fractionation factor is arbitrary, either k can go into the numerator (or the denominator), and is defined differently between different fields of science. Physical chemists and biologist often define $\alpha = \frac{k_L}{k_H}$, while geochemist and other Earth scientists typically define $\alpha = \frac{k_H}{k_L}$, where L is the light isotope and H is the heavy isotope. This can cause considerable confusion when comparing literature α values if the reader is not careful to understand how the author defines α . For example, consider the first order kinetic reaction of N_2O_5 decomposition to NO_2 and NO_3 . Here the reaction rate of the ^{14}N isotopes (k_{14}) is 6.220×10^{-4} , while the ^{15}N reaction rate (k_{15}) is 6.158×10^{-4} . If these rates are plugged into the standard chemist convention a value of 1.010 is found while the geochemist convention produces a value of 0.990. Neither is an incorrect notation, and both suggest that the lighter isotope reacts faster, however if a reader is not careful they may misunderstand the finding of the author. Likewise, to avoid any unnecessary confusion an author needs to define α and remain consistent. Therefore, within this dissertation, to minimize confusion, α will be written using the common geochemist (Eq. 8b).

$$\alpha_{H-L} = \frac{k_H}{k_L} = \frac{R_A}{R_B} = \frac{\beta_H}{\beta_L} \quad \text{Eq. 8B}$$

Often the α value is converted into per mille notation (‰) and is referred to as the isotope enrichment factor (ϵ) Eq. 9.

$$\epsilon_{A-B} (\text{‰}) = (\alpha_{A-B} - 1) * 1000 \quad \text{Eq. 9}$$

This notation will be used throughout this dissertation for isotopic fractionation, unless otherwise noted, and will be referred to as either $^{15}\epsilon_{A-B}$ (for N isotopes) or $^{18}\epsilon_{A-B}$ (for O isotopes), where A is the product and B is the reactant. Because ϵ is dependent on the α value, confusion can occur by lack of universal convention. For example, oxygen equilibrium exchange (discussed below) between H_2O and NO_2^- is often written as $^{18}\epsilon_{\text{ex}} = 14\text{‰}$, however without a definition of what is in the numerator and denominator, one cannot tell in which compound the ^{18}O is accumulating. However, by using $^{18}\epsilon_{\text{NO}_2\text{-H}_2\text{O}}$ it is clear that the ^{18}O accumulates in NO_2^- , relative to H_2O .

There are two ways that isotopic fractionation is known to occur: kinetics and equilibrium. The first is the preference of a light isotopologue to react faster in unidirectional reactions and is called the kinetic isotopic effect (KIE). An example of this is denitrifying bacteria's preferential use of the lighter ^{14}N over the heavier ^{15}N when reducing NO_3^- to N_2 (Mariotti et al., 1981). The type of isotopic fractionation is equilibrium isotopic exchange (EIE). Here, no new chemical compounds are formed but instead kinetically favorable isotopic repositioning occurs between two isotopologues in equilibrium. An example of this is ^{18}O exchange between nitrite and water: $^{14}\text{N}^{16}\text{O}^{16}\text{O} + \text{H}_2^{18}\text{O} \leftrightarrow ^{14}\text{N}^{16}\text{O}^{18}\text{O} + \text{H}_2^{16}\text{O}$ (Casciotti et al., 2007). This isotope exchange reaction will be discussed in Chapter 3.

2.3 Isotope Mixing Models

When there are two or more sources of a compound, such as nitrate, in a mixed system (lake, river, soil) then isotope mixing models can be used determine what fraction of the compound that comes from each source. This approach requires that the δ value of each source is

isotopically known, distinct, and acts conservatively. These values are used as isotopic “end-members” in isotope mixing models, that utilize $\delta^{15}\text{N}$, $\delta^{18}\text{O}$, and δD .

The simplest isotope mixing model assumes two sources (Eq. 10A and 10B). For example, using $\delta^{18}\text{O}$ to determine the relative contribution of two nitrate sources (e.g atmospheric and fertilizer) in a mixture

$$F_{\text{atm}} + f_{\text{fert}} = 1 \quad \text{Eq. 10A}$$

$$f_{\text{atm}} * \delta^{18}\text{O}_{\text{atm}} + f_{\text{fert}} * \delta^{18}\text{O}_{\text{fert}} = \delta^{18}\text{O}_{\text{mix}} \quad \text{Eq. 10B}$$

Where the f s are the molar (or mass) fractions of the two nitrate sources (atmospheric and fertilizer) and the $\delta^{18}\text{O}$ are the $\delta^{18}\text{O}$ values of the two nitrate sources. This two isotope mixing model is represented graphically in Figure 2-2. Equation 10A can be rearranged and substituted into equation 10B to give equation 10C, which can be used to solve for f_{fert} (or f_{Atm}). The known fraction can then be plug into Eq. 10A to solve for the unsolved f_{Atm} (or f_{fert}).

$$F_{\text{fert}} = \frac{\delta^{18}\text{O}_{\text{mix}} - \delta^{18}\text{O}_{\text{atm}}}{\delta^{18}\text{O}_{\text{fert}} - \delta^{18}\text{O}_{\text{atm}}} \quad \text{Eq. 10C}$$

Mixing models can also consist of 3 or more end-members (Eq. 11A). For a three-end member mixing model, two conservative tracers are needed (Eq. 11B & C), so a second isotope can be used, if it provides unique info about the sources. For example, a system containing three nitrate sources (e.g. fertilizer, atmospheric deposition, and soil N) the both $\delta^{18}\text{O}$ and $\delta^{15}\text{N}$ can be applied (Eq.11A-11C)

$$f_{\text{atm}} + f_{\text{fert}} + f_{\text{soil}} = 1 \quad \text{Eq. 11A}$$

$$f_{\text{atm}} * \delta^{15}\text{N}_{\text{atm}} + f_{\text{fert}} * \delta^{15}\text{N}_{\text{fert}} + f_{\text{soil}} * \delta^{15}\text{N}_{\text{soil}} = \delta^{15}\text{N}_{\text{mix}} \quad \text{Eq. 11B}$$

$$f_{\text{atm}} * \delta^{18}\text{O}_{\text{atm}} + f_{\text{fert}} * \delta^{18}\text{O}_{\text{fert}} + f_{\text{soil}} * \delta^{18}\text{O}_{\text{soil}} = \delta^{18}\text{O}_{\text{mix}} \quad \text{Eq. 11C}$$

These three equations can be substituted into each to solve for one fraction through Eq. 11D.

$$f_{\text{atm}} = \frac{(\delta^{15}\text{N}_{\text{mix}} - \delta^{15}\text{N}_{\text{soil}})(\delta^{18}\text{O}_{\text{fert}} - \delta^{18}\text{O}_{\text{soil}}) - (\delta^{15}\text{N}_{\text{fert}} - \delta^{15}\text{N}_{\text{soil}})(\delta^{18}\text{O}_{\text{mix}} - \delta^{18}\text{O}_{\text{soil}})}{(\delta^{15}\text{N}_{\text{atm}} - \delta^{15}\text{N}_{\text{soil}})(\delta^{18}\text{O}_{\text{fert}} - \delta^{18}\text{O}_{\text{soil}}) - (\delta^{15}\text{N}_{\text{fert}} - \delta^{15}\text{N}_{\text{soil}})(\delta^{18}\text{O}_{\text{atm}} - \delta^{18}\text{O}_{\text{soil}})} \quad \text{Eq. 11D}$$

The second fraction can then be solved by Eq. 11E

$$f_{\text{fert}} = \frac{(\delta^{15}\text{N}_{\text{mix}} - \delta^{15}\text{N}_{\text{soil}}) - (\delta^{15}\text{N}_{\text{atm}} - \delta^{15}\text{N}_{\text{Csoil}})}{(\delta^{15}\text{N}_{\text{fert}} - \delta^{15}\text{N}_{\text{soil}}) - (\delta^{15}\text{N}_{\text{fert}} - \delta^{15}\text{N}_{\text{soil}})} f_{\text{atm}} \quad \text{Eq. 11E}$$

The last fraction can then be solved through Eq. 11A using the two known f_s , determined through Eq. 11D and 11E. Graphically this three component mixture of nitrate from three sources is represented graphically in Figure 2-2 and is often referred to as the dual isotope approach. An isotope mixing model is used to understand sources of nitrate (Chapter 3 and Chapter 6) in this dissertation. The dual isotope approach relies on each nitrate source having a unique range of $\delta^{15}\text{N}$ and $\delta^{18}\text{O}$ values. However, physical and microbial processes can create a range of δ values for each source, adding ambiguity, causing misinterpretation and error in source apportionment (Figure 2.2). These processes control or influence the observed $\delta^{15}\text{N}$ and $\delta^{18}\text{O}$ values of NO_3^- (Table 2.3) (Figure 2.3).

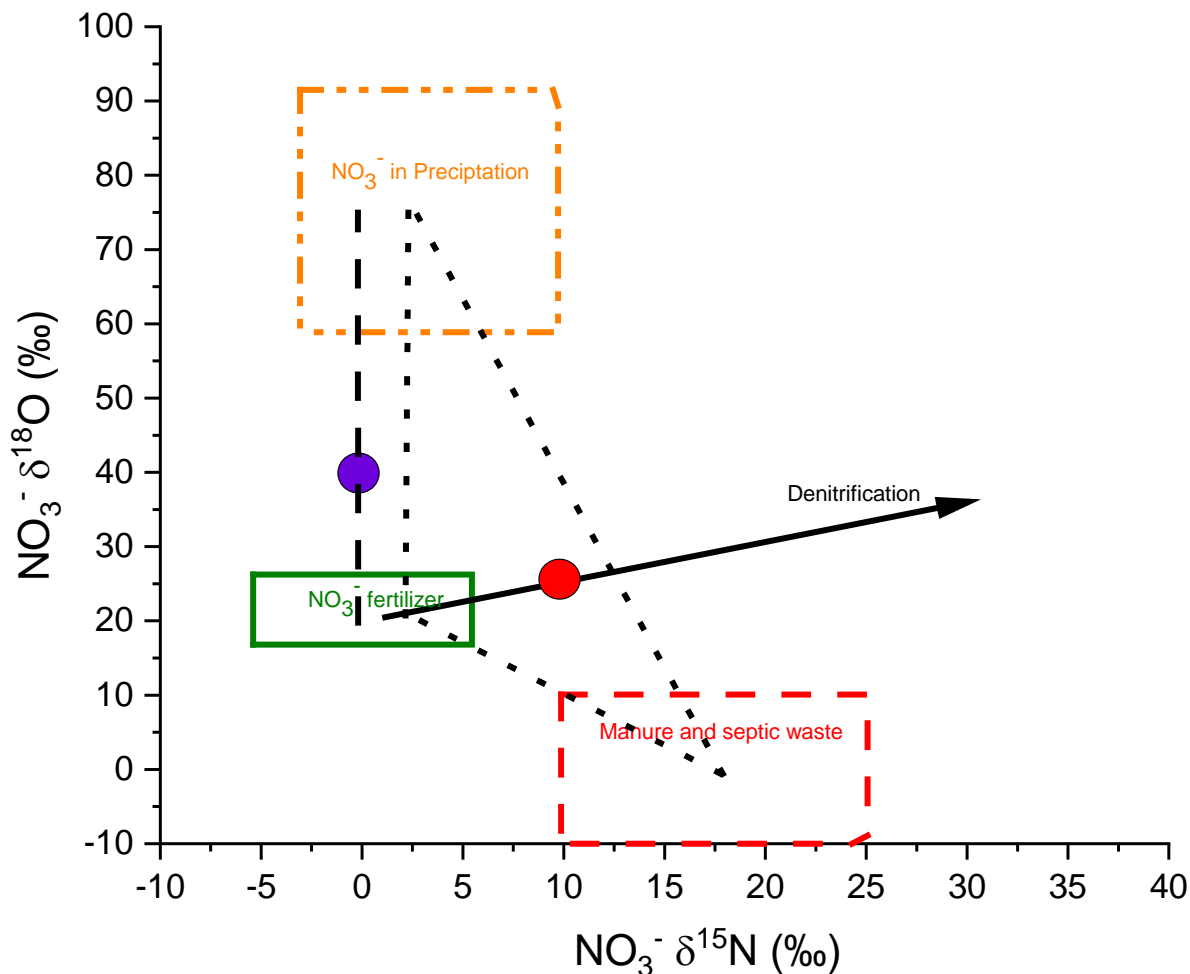


Figure 2-2 Normal ranges of $\delta^{15}\text{N}$ and $\delta^{18}\text{O}$ of NO_3^- from fertilizer, atmospheric deposition, and soil. The purple circle represents a two source nitrate mixture of nitrate from fertilizer and deposition. The length of the line away from a source represents the fraction contribution of one source relative to another. The red circle represents a three source mixing between fertilizer, atmospheric deposition, and soil NO_3^- . The dashed triangle area represents the possible values for a mixture of fertilizer, atmospheric deposition, and soil NO_3^- . The black arrow indicates the dual isotope enrichment that is caused by denitrification and indicates how isotopic enrichment by denitrification can be mistaken as source mixing.

2.4 Isotope Effects on Production and Consumption of Nitrogen Compounds

Isotope effects are observed in most physical and chemical reactions. When reactions are incomplete the δ value of the product will be different from the reactant. The difference between δ of the reactant and the instantaneous product is determined by the enrichment factor. Furthermore, for reactions that involve intermediate products $[A \rightarrow B \rightarrow C]$ each step can have

an associated enrichment factor, causing the δ of A, B, and C to differ. During these processes the N fractions and the $\delta^{15}\text{N}$ values can change, but the weighted average of $\delta^{15}\text{N}$ throughout the system will remain the same, assuming no addition or loss of N from the system. These changes in $\delta^{15}\text{N}$ are driven by the KIE and EIE described above. However, when the reaction has gone to completion, the $\delta^{15}\text{N}$ of C will equal the initial $\delta^{15}\text{N}$ of A.

Table 2-3 Nitrogen and oxygen isotope enrichment factors of microbial and physical processes

Process	Reaction	$^{15}\epsilon_{A/B}$ (‰)	$^{18}\epsilon_{A/B}$ (‰)	References
Nitrate Reduction (Denitrification)	$\text{NO}_3^- \rightarrow \text{NO}_2^-$	-40 - -5	-32 - -5	(Delwiche & Steyn, 1970a; Granger et al., 2006; Granger & Wankel, 2016; Mariotti et al., 1981; Nikolenko et al., 2018)
Nitrite Reduction (Denitrification)	$\text{NO}_2^- \rightarrow \text{NO}$	-20 - 0	-20 - 0	(Bryan et al., 1983; Casciotti, 2009)
Nitrous Oxide Reduction (Denitrification)	$\text{N}_2\text{O} \rightarrow \text{N}_2$	-10 - -5	*	(Ostrom et al., 2007)
Nitrogen Fixation	$\text{N}_2 \rightarrow \text{N}_{\text{Org}}$	-2 - 2	*	(Delwiche & Steyn, 1970a; Hoering & Ford, 1960)
Mineralization	$\text{N}_{\text{org}} \rightarrow \text{NH}_4^+$	-1 - 0	*	(Högberg, 1997)
Ammonium Oxidation (Nitrification)	$\text{NH}_4^+ \rightarrow \text{NO}_2^-$	-38 - -14	-38 - -18	(Casciotti et al., 2010; Delwiche & Steyn, 1970a; Granger & Wankel, 2016; Mariotti et al., 1981; Nikolenko et al., 2018)
Nitrite Oxidation (nitrification)	$\text{NO}_2^- \rightarrow \text{NO}_3^-$	0 - 35	3 - 7	(Casciotti et al., 2010; Granger & Wankel, 2016)

Table 2-3 Continued

Ammonia Volatilization	$\text{NH}_3 \leftrightarrow \text{NH}_4^+$	-36 - -15	*	(Högberg, 1997; Nikolenko et al., 2018)
Ammonium Ion Equilibrium	$\text{NH}_4^+ \leftrightarrow \text{NH}_3$ (solution)	-27 - -20	*	(Högberg, 1997)
Industrial Fixation	$\text{N}_2 \rightarrow \text{NH}_3$	0	*	(Bateman & Kelly, 2007; Michalski et al., 2015)
Lightning Fixation	$\text{N}_2 \rightarrow \text{NO}_x$	0	†	(Bateman & Kelly, 2007; Michalski et al., 2015)
Clay absorption/desorption	$\text{NH}_4^+ \leftrightarrow \text{NH}_4^+(\text{clay})$	0 - 8	*	(Delwiche & Steyn, 1970a; Högberg, 1997)

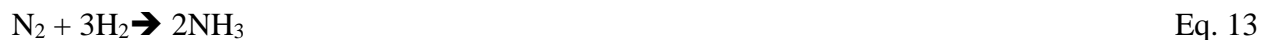
* Denotes that no oxygen is present in the compound

† Denotes that the ϵ is not well understood

Fixation, mineralization, and assimilation effect on $\delta^{15}\text{N}$ are small and often assumed to be zero (Bergersen, 1986; Delwiche & Steyn, 1970a; Doughton et al., 1992; Hoering & Ford, 1960; Högberg, 1997; Ledgard, 1989; Steele et al., 1983; Unkovich, 2013). These enrichment factors near zero mean the $\delta^{15}\text{N}$ of the original compound is preserved during transformations (Högberg, 1997; Hogberg et al., 1996; Nadelhoffer & Fry, 1994). Although a few studies have observed both normal and inverse enrichment factors (enrichment were the heavier isotope is preferentially used) during fixation and mineralization, these are attributed to specific bacterial strains, nutrient sources, and environmental settings and are not applicable in a soil setting (Ledgard, 1989; Steele et al., 1983; Unkovich, 2013).

Industrial fixation of N occurs through the Haber-Bosch process where N_2 is fixed to NH_3 . This process occurs at high temperatures and pressures over an iron catalyst (Eq. 13), where

methane is used as a hydrogen source. Due to the extreme conditions and high efficiency of this process little to no isotope enrichment occurs (Bateman & Kelly, 2007; Michalski et al., 2015),



Likewise, during the oxidization of NH_3 by O_2 in HNO_3 via the Ostwald process (Eq. 14) eliminates any ^{18}O enrichment (Michalski et al., 2015).



Atmospheric NO_3^- is produced from oxidation of NO_x (NO and NO_2). The mechanisms of atmospheric oxidation are out of the scope of this dissertation. But in short, NO_x oxidation proceeds through oxidation by HO_2 , ROO , O_3 , and OH (Rihn, 2013). These oxidation pathways control the observed $\delta^{18}\text{O}$ of atmospheric nitrate which can range from 70 to +100‰ (Michalski et al., 2002). While $\delta^{15}\text{N}$ is controlled by the source of NO_x (e.g. lightening, agricultural, or fossil fuel combustion) it has a measured values that ranges from -45 to 10‰ (Elliott et al., 2007; Freyer, 1991; Hastings et al., 2003; Moore, 1977; Nadelhoffer & Fry, 1994). Eventually this nitrate will dissolve in rain and reach the soil through wet deposition as NO_3^- or as a dry deposition aerosol as HNO_3 .

The two steps of nitrification, ammonium oxidization by AOB/AOA and nitrite oxidation by NOB, both have a ^{15}N enrichment factor. Ammonium oxidization has an ^{15}N enrichment factor ($^{15}\epsilon_{\text{NH}_4^+/\text{NO}_2^-}$) that ranges between -38 and -14‰, while nitrite oxidation has an inverse KIE ^{15}N enrichment factor ($^{15}\epsilon_{\text{NO}_2^-/\text{NO}_3^-}$) that ranges between 0 and 35‰ (Delwiche & Steyn, 1970a; Granger & Wankel, 2016; Mariotti et al., 1981). Högberg (1997) proposed since nitrite oxidation is often not the rate limiting step in nitrification, the nitrite oxidation enrichment factor ($^{15}\epsilon_{\text{NO}_2^-/\text{NO}_3^-}$) is often not expressed. Therefore, complete nitrification, from NH_4^+ to NO_3^- , should have a ^{15}N enrichment factor similar to ammonium oxidization. Indeed this is true as the ^{15}N enrichment

of complete nitrification ($^{15}\epsilon_{\text{NH}_4^+/\text{NO}_3^-}$) ranges from -36 to -15‰ (Högberg, 1997; Mariotti et al., 1981). This wide range of fractionation values has been attributed to several causes including high N_2O yields (Yoshida, 1988), accumulation of intermediates (Casciotti et al., 2003; Yoshida, 1988), concentration of electron donors (Bryan et al., 1983), biodiversity (Casciotti et al., 2003) and environmental conditions (Mariotti 1981). The isotopic fractionation during nitrification is not often observed in nature. For example, in managed landscapes where ammonium is the primary source of N, large negative $\delta^{15}\text{N-NO}_3^-$ values are not often observed (Keller et al., 2008; Kellman, 2005; Kellman & Hillaire-Marcel, 2003; Ostrom et al., 1998; Smith & Kellman, 2011). The absence of very negative $\delta^{15}\text{N}$ values has been suggested to be a result of rapid and complete conversion of all free NH_4^+ in to NO_3^- by bacteria (Kendall & McDonnell, 1998). Clay absorption of NH_4^+ may also act as a sink, since positively charged NH_4^+ bonds to soil clay particles (Karamanos & Rennie, 1978). The ^{15}N enrichment factor of clay desorption ($^{15}\epsilon_{\text{NH}_4^+/\text{NH}_4^+(\text{clay})}$) has been measured to range from 0 - 8‰ (Delwiche & Steyn, 1970a; Högberg, 1997). Thus, desorption of NH_4^+ from soils could alter observed $\delta^{15}\text{N}$ of NO_3^- , how much though will hinge on the amount of NH_4^+ absorbed and the value of ($^{15}\epsilon_{\text{NH}_4^+/\text{NH}_4^+(\text{clay})}$). This topic of nitrification isotopic enrichment is investigated in Chapter 3 of this dissertation.

The $\delta^{18}\text{O}$ of nitrate produced by nitrification will reflect the sources oxygen incorporated into NO_3^- during ammonium oxidation, which is either H_2O or O_2 . In the first step of nitrification, ammonium is oxidized to hydroxylamine by O_2 (Equation 2A), followed by oxidation into NO_2^- using H_2O (Equation 2B) (Andersson & Hooper, 1983; Bothe et al., 2000; Zhang et al., 2012). During the second step, NOB oxidizes NO_2^- into NO_3^- using H_2O as the oxygen source (Equation 3) (Kumar et al., 1983; Xia et al., 2011). From this stoichiometry the final $\delta^{18}\text{O}$ of NO_3^- from nitrification can be theoretically calculated through Eq. 12

$$\delta^{18}\text{O}_{\text{NO}_3^-} = f_{\text{H}_2\text{O}} (\delta^{18}\text{O}_{\text{H}_2\text{O}}) + f_{\text{O}_2} (\delta^{18}\text{O}_{\text{O}_2}) \quad \text{Eq. 12}$$

Based on the stoichiometry the expected $\delta^{18}\text{O}$ of nitrification can be calculated using $f_{\text{H}_2\text{O}} = 0.66$ and $f_{\text{O}_2} = 0.33$. (Aleem et al., 1965; Buchwald et al., 2012; Hollocher, 1984; Kumar et al., 1983; Yoshinari & Wahlen, 1985a). The $\delta^{18}\text{O}$ value of O_2 does not significantly vary spatially or temporally and is well constrained at 23.5‰ (Dole et al., 1954; Horibe et al., 2018; Kroopnick & Craig, 1972). On the other hand, the $\delta^{18}\text{O}$ of soil water is highly variable due to the spatial and temporal variability of $\delta^{18}\text{O}$ of precipitation (Gat, 1996, 1998). In order to calculate the $\delta^{18}\text{O}$ of NO_3^- produced by nitrification in a soil, the $\delta^{18}\text{O}$ of the soil H_2O must also be known. Besides needing to know the $\delta^{18}\text{O}$ of soil H_2O and O_2 , the value of $\delta^{18}\text{O}$ can also be affected during each step of nitrification, because of the nitrification KIE (Casciotti et al., 2010; Granger & Wankel, 2016). Adding to the ambiguity, nitrification studies have observed oxygen isotope exchange between NO_2^- and H_2O (Buchwald & Casciotti, 2010; Casciotti et al., 2010; Kool et al., 2011). This would result in any initial $\delta^{18}\text{O}$ signal of NO_2^- generated during ammonium oxidation (equations 2A and 2B) being partially or completely masked and replaced by the $\delta^{18}\text{O}$ of H_2O , depending on the amount of exchange. For example, soil incubation experiments by Snider (2010) observed exchange up to 88%, while aquatic experiments by Casciotti (2010) observed 0 to 25%. This dissertation investigates the kinetic and equilibrium isotope effects on $\delta^{15}\text{N}$ and $\delta^{18}\text{O}$ of nitrate from nitrification within soil in Chapter 3.

Among all processes mentioned here, denitrification has been the most studied, yet many questions remain about the ^{15}N and ^{18}O enrichment factors ($^{15}\epsilon_{\text{NO}_3^-/\text{N}_2}$ and $^{18}\epsilon_{\text{NO}_3^-/\text{N}_2}$) and $^{15}\epsilon_{\text{NO}_3^-/\text{N}_2} / ^{18}\epsilon_{\text{NO}_3^-/\text{N}_2}$ ratios (Böhlke & Denver, 1995; Knöller et al., 2011; Mariotti et al., 1981, 1988; Osaka et al., 2018). Denitrification proceeds in two steps (nitrate reduction and nitrite reduction) with each step have its own ^{15}N and ^{18}O enrichment factor value. Nitrate reduction has reported

$^{15}\epsilon_{\text{NO}_3/\text{NO}_2}$ and $^{18}\epsilon_{\text{NO}_3/\text{NO}_2^-}$ values that range from -30 - -5‰ (Granger & Wankel, 2016; Mariotti et al., 1981) Nitrite reduction has reported $^{15}\epsilon_{\text{NO}_2/\text{N}_2}$ and $^{18}\epsilon_{\text{NO}_2/\text{N}_2}$ values ranging from -20 - 0‰ (Granger & Wankel, 2016). The $^{15}\epsilon_{\text{NO}_3/\text{N}_2}$ and $^{18}\epsilon_{\text{NO}_3/\text{N}_2}$ values of total denitrification ($\text{NO}_3^- \rightarrow \text{N}_2$) vary extensively from -40‰ to -5‰ and -32‰ to -5‰, respectively (Aravena & Robertson, 1998; Blackmer & Bremner, 1977; Böttcher et al., 1990; Fukada et al., 2003; Gillam et al., 2008; Knöller et al., 2011; Mariotti, 1982; Mariotti et al., 1988; Osaka et al., 2018). This wide range of literature enrichment factor values for nitrate, nitrite, and total denitrification can be attributed to changes in temperature (Mariotti et al., 1981), denitrification rates (Mariotti et al., 1981), differences in soil type (Blackmer & Bremner, 1977), substrate concentration (Shearer & Kohl, 1988), availability of electron donors (Bryan et al., 1983), and bacteria strains (Böttcher et al., 1990; Bryan et al., 1983; Knöller et al., 2011; Macko, 1987). Additionally, their coinciding enrichments ratios ($\delta^{15}\text{N}/\delta^{18}\text{O}$) also vary from 0.5 to 3 (Aravena & Robertson, 1998; Granger et al., 2008; Knöller et al., 2011; Osaka et al., 2018). These discrepancies have been attributed to different bacteria strains, different metal centers, nitrite re-oxidation, equilibrium isotopic exchange between H_2O and either nitrate or nitrite, and different environmental conditions including temperatures and concentrations of electron acceptors and donors (Casciotti et al., 2010; Högberg, 1997; Osaka et al., 2018; Wunderlich et al., 2013). Regardless of the cause, isotopic enrichment via denitrification occur in both ^{15}N and ^{18}O and proceeds through a Rayleigh fractionation distillation (Kendall & McDonnell, 1998; Mariotti et al., 1981). This topic is further investigated in Chapter 4 of this dissertation.

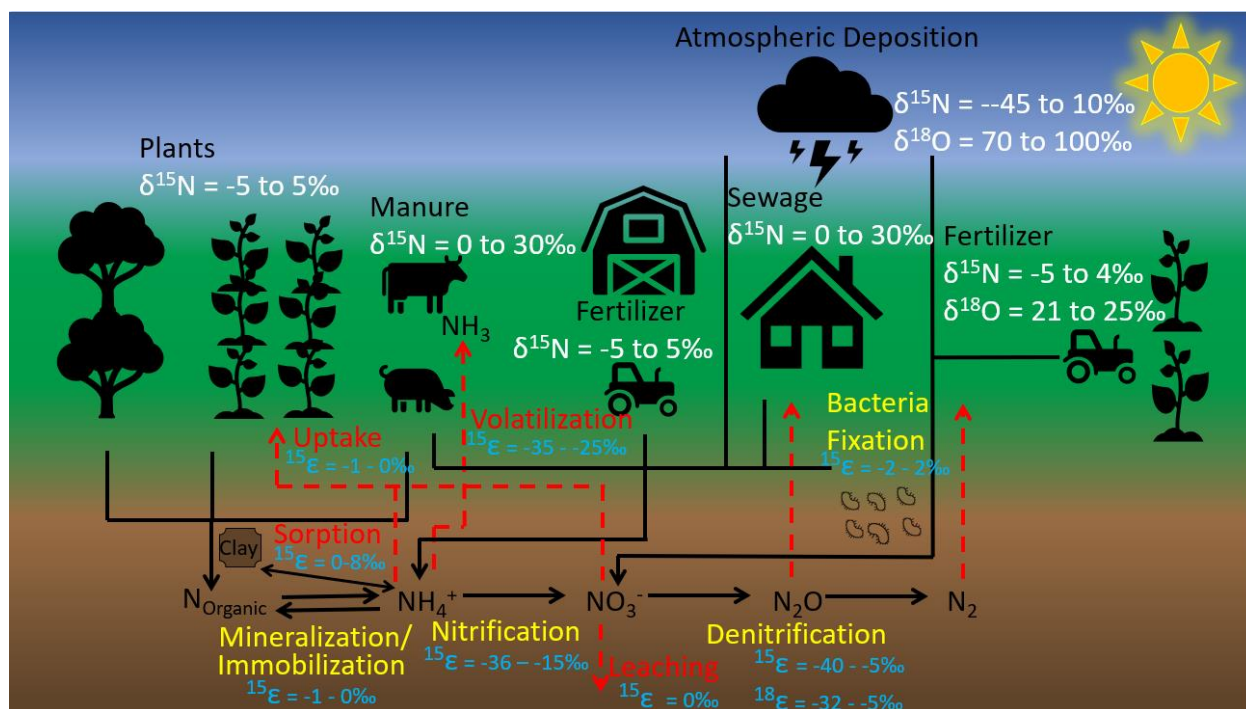


Figure 2-3 All major sources, sinks and transformation of nitrogen in the nitrogen cycle. All forms and sources of nitrogen in soil are in black text and their $\delta^{15}\text{N}$ and $\delta^{18}\text{O}$ values in white text. Microbial processes are shown in yellow text and the isotopic enrichment of the process in light blue text. Sinks of N are shown in red text along with their corresponding enrichment in light blue text. See table 2-3 for references.

2.5 Rayleigh Distillation

Rayleigh distillation models are often used to predict partitioning of isotopologues based on their different vapor pressure or rate constants. The Rayleigh equations were originally derived in order to predict separation progress of two solutions with different vapor pressures during a distillation. This method can be applied isotopes in both open and closed systems (Gat & Gonfiantini, 1981). A closed liquid system is bidirectional, meaning the distillate can equilibrate with the original liquid. The isotope fractionation that occurs in a closed system is a function of the fraction of liquid remaining (Eq. 15). Where δ_E is the delta value of the product, δ_0 is the delta value of the initial reactant, f is the fraction of reactant remaining, and ϵ is the enrichment factor.

$$\delta_E = \delta_0 - (1-f)\epsilon \quad \text{Eq. 15}$$

Open Rayleigh systems are unidirectional (Eq. 16) and the distillate never comes into equilibrium with the initial reservoir, because the vapor is removed from the system. This results in the δ value of the remaining liquid to increase exponentially (Figure 2-4).

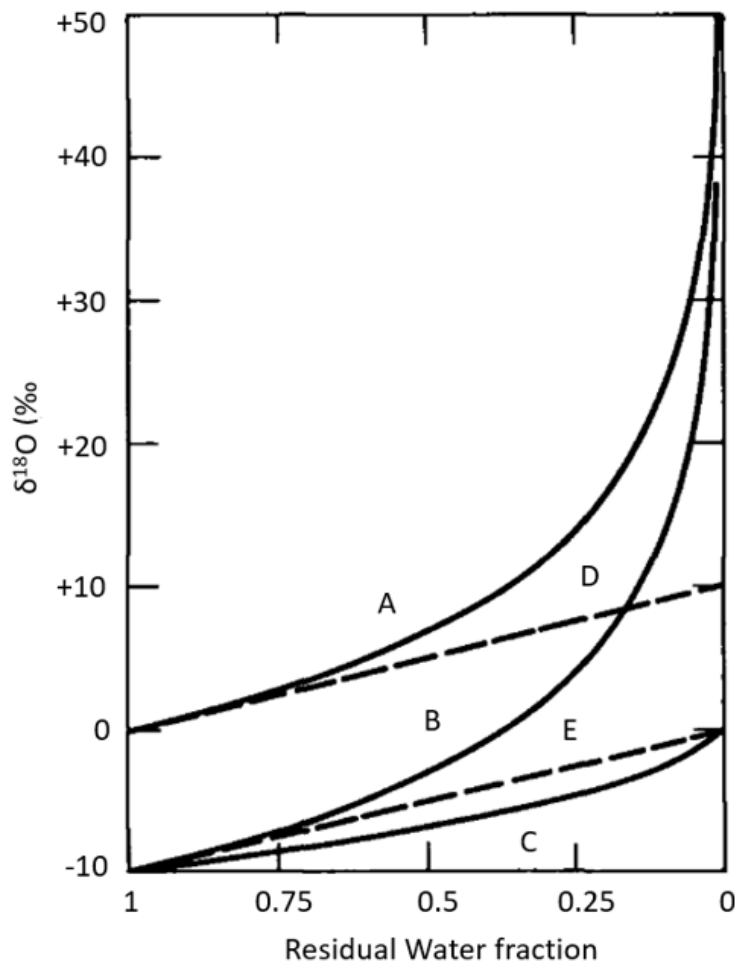


Figure 2-4 Isotopic change in $\delta^{18}\text{O}$ of H_2O in both a closed and an open Rayleigh system with an $\epsilon = -10$. Lines A, B, and C are the observed curves in an open system where A is the remaining liquid, B is the instantaneous product vapor, and C is the accumulated vapor product. Lines D and E represent a closed Rayleigh system where D is the liquid reactant remaining and E is the equilibrated vapor product. Image modified from Gat and Gonfiantini (1981).

Denitrification is an example of an open system because the gas products are quickly lost to the atmosphere. Here, the enrichment value (ϵ) between the original reservoir and the instantaneous product never change. Thus, Eq. 16 can calculate the final isotopic value of the initial reservoir based on fraction loss of an open system. Eq. 16 can be manipulated to Eq. 17, allowing for the fraction lost to be calculated.

$$\delta_f = \delta_0 + \epsilon \ln f \quad \text{Eq. 16}$$

$$f = e^{\frac{(\delta_f - \delta_0)}{\epsilon}} \quad \text{Eq. 17}$$

To apply this open Rayleigh model, the starting and final $\delta^{15}\text{N}$ and $\delta^{18}\text{O}$ values of NO_3^- need to be determined and the $^{15}\epsilon_{\text{NO}_3^-/\text{N}_2}$ and $^{18}\epsilon_{\text{NO}_3^-/\text{N}_2}$ values of denitrification need to be known. A Rayleigh distillation to monitor and quantify the progress of a reaction is used in Chapter 5 of this dissertation to quantify field scale denitrification.

CHAPTER 3. DETERMINING THE ^{15}N ENRICHMENT AND SOURCES OF OXYGEN IN NITRATE PRODUCED BY NITRIFICATION IN AN AGRICULTURAL SOIL

3.1 Abstract

Nitrification is a microbial process that occurs under aerobic conditions in soils and oxidizes NH_4^+ to NO_3^- . The stable isotopes of NO_3^- ($\delta^{15}\text{N}$ and $\delta^{18}\text{O}$) are frequently used to distinguish different sources of NO_3^- in soils and marine environments, such as nitrification. The $\delta^{15}\text{N}$ value of NO_3^- derived from nitrification is often assumed to directly reflect the $\delta^{15}\text{N}$ value of the NH_4^+ source (manure, soil N, NH_4^+ fertilizers). In contrast, the NO_3^- $\delta^{18}\text{O}$ value is often assumed to be proportional to the $\delta^{18}\text{O}$ values of the sources of oxygen used during nitrification. Here we measured the isotope enrichment that occurs in ^{15}N and the sources of oxygen in the final NO_3^- product from nitrification in a Midwestern cultivated agricultural soil. This was evaluated by performing aerobic incubations of soil amended with high concentrations of ammonium mixed with isotopically variable H_2O . Results showed that the enrichment factor of $\delta^{15}\text{N}$ from nitrification is large. Additionally, during these incubations we found that the fraction of oxygen from H_2O used during nitrification was consistently higher than the theoretical value of 0.66. The H_2O fraction measured were 0.82, indicating isotope exchange between H_2O and the nitrification intermediate NO_2^- is rapid in agricultural soils amended with ammonium.

3.2 Introduction

Nitrate is the main biologically available N source for plant uptake, yet it is often considered an undesirable form of nitrogen, because it readily leaches and can undergo denitrification, resulting in a loss of N from the biosphere. Nitrate's high solubility means it can leach from soil and can pollute nearby bodies of water causing harm to both terrestrial and aquatic life (Sobota et al., 2015). Nitrate in drinking water has been linked to health risk including methemoglobinemia and cancer (Fewtrell, 2004; World Health Organization, 2011). This toxicity extends to livestock where elevated nitrate concentrations can be poisonous (Davidson et al., 2006; Michalski et al., 2010). Nitrate pollution of drinking water has been estimated to cost \$19 billion while the impact on all freshwater systems is estimated at \$78 billion (Sobota et al., 2015). Furthermore, excess nitrate exported to coastal waters can cause eutrophication, reducing marine biodiversity and effecting commercially valuable fish (Yang et al., 2008). The cost of freshwater eutrophication in the US has been estimated at \$2.2 billion annually (Dodds et al., 2009). These adverse impacts have led the United States Environmental Protection Agency (US-EPA) and the World Health Organization (WHO) to monitor and place limits on nitrate concentrations in potable waters. Nitrate pollution has several potential sources, which includes livestock, agriculture, air pollution, and sewage (Kendall & McDonnell, 1998) but distinguishing the relative importance of these sources in mixed systems can be difficult (Kellman & Hillaire-Marcel, 2003).

Stable isotope analysis is a powerful forensic technique that can be used to determine the relative importance of various nitrate sources in mixed systems (Kendall & McDonnell, 1998). This technique uses variations in the abundance of stable isotopes of oxygen and nitrogen, contained in nitrate, that are often different depending on each nitrate source's mechanism of production. For example, nitrate produced by NO_x oxidation by ozone (Michalski et al., 2012) or

microbial nitrification (Högberg, 1997) will have different nitrogen ($^{15}\text{R} = ^{15}\text{N}/^{14}\text{N}$) and oxygen ($^{18}\text{R} = ^{18}\text{O}/^{16}\text{O}$) isotope ratios. The variation in these ratios (R) are small and measured relative to an accepted standard, and normally reported in delta notation in units of per mille where $\delta (\text{‰}) = [\text{R}_{\text{sample}}/\text{R}_{\text{standard}} - 1] * 1000$ (Kendall & McDonnell, 1998). The standard used to report $\delta^{15}\text{N}$ values is with respect to air N_2 ($^{15}\text{N}/^{14}\text{N}$) and for $\delta^{18}\text{O}$ values is with respect to Vienna Standard Mean Ocean Water (VSMOW) ($^{18}\text{O}/^{16}\text{O}$) (Bohlke & Coplen, 1995). Given that the δ values are often unique between nitrate from different sources, isotope mass balance mixing models are often used to determine the fraction contribution of each nitrate source in mixed systems (Kendall & McDonnell, 1998). For example, inorganic nitrate fertilizers have elevated $\delta^{18}\text{O}$ values ($23\text{‰} \pm 3$) due to their synthesis using O_2 , while nitrate from organic N has values closer to 0‰ (Bateman & Kelly, 2007; Kendall & McDonnell, 1998; Michalski et al., 2015). Both of these sources of nitrate are common in agricultural soils and if the $\delta^{15}\text{N}$ value of NO_3^- is measured, one can use isotope mass balance to determine their relative importance. This isotope mass balance technique has successfully been applied to source nitrate in soils, rivers, oceans, ground waters, and catchments (Böhlke et al., 2004; Böttcher et al., 1990; Chen et al., 2009; Cline & Kaplan, 1975; Fukada et al., 2003; Mariotti et al., 1988; Sebilo et al., 2006; Sigman et al., 2009; William, 1998). However, microbial processes such as nitrification can cause error when applying the isotope mass balance technique because the $\delta^{15}\text{N}$ is not conservative (Kendall & Aravena, 2000)

Nitrification is the microbial oxidation of ammonium that proceeds through several intermediates ($\text{NH}_4^+ \rightarrow \text{NH}_2\text{OH} \rightarrow \text{NO}_2^- \rightarrow \text{NO}_3^-$) (Johnson et al., 2005) and is the main source of NO_3^- in nature (Galloway, 1998). Each step of nitrification is associated with a kinetic isotope effect (KIE), where the lighter isotope is preferentially used over the heavier isotope (Mariotti et al., 1981). Quantitatively KIE can be defined as, $\text{KIE} = \alpha = k_{\text{H}}/k_{\text{L}}$ where k is the nitrification rate

constant for heavy (H) and light (L) isotope and α is called the isotope fractionation factor. The isotope fractionation factor (α) is often described in a permil notation and is referred to as the enrichment factor (ϵ) via $\epsilon_{A/B} (\text{‰}) = (\alpha_{A/B} - 1) * 1000$, where A is product and B is reactant. In short, the KIE of nitrification causes an increase in $\delta^{15}\text{N}$ value in the residual NH_4^+ pool (reactant) while producing NO_3^- (product) with a lower $\delta^{15}\text{N}$ value, relative to the initial reactant.

The observed enrichment factors of nitrification ($^{15}\epsilon_{\text{NO}_3^-/\text{NH}_4^+}$ and $^{18}\epsilon_{\text{NO}_3^-/\text{H}_2\text{O}}$) will be composed of the cumulative enrichment caused by each step of nitrification (Eq. 1-3).



Though it is written as three individual reactions, nitrification actually occurs through a 2 step processes using two different bacteria/Archaea. The first step is oxidation of ammonia to nitrite (Eq. 1 and 2) that is facilitated by either ammonia-oxidizing bacteria (AOB) or ammonia oxidizing Archaea (AOA). In this first step, NH_3 is oxidized to NH_2OH using O_2 through the ammonia monooxygenase enzyme (AMO) (Andersson & Hooper, 1983; Bothe et al., 2000; Zhang et al., 2012). NH_2OH is subsequently oxidized by H_2O to NO_2^- (equation 2) via the hydroxylamine oxidoreductase enzyme (HAO) (Bothe et al., 2000). The NO_2^- is then released by the AOB/AOA and taken up by nitrite oxidizing bacteria (NOB) that oxidizes NO_2^- into NO_3^- using H_2O via the nitrite oxidizing reductase (NOR) enzyme (equation 3) (Kumar et al., 1983; Xia et al., 2011).

If each reaction in a series has an associated isotopic fraction factor, then each subsequent product will be isotopically lighter relative to the reactant. For example, the NO_2^- product formed during the first step of nitrification (Eq. 1 and 2) will be lighter than the NH_4^+ reactant, and the

subsequent NO_3^- product formed during the second step (Eq. 3) will be isotopically lighter than the NO_2^- reactant. However, during nitrification this is may not always be the case, because the first step of nitrification, oxidation of NH_4^+ to NO_2^- , is rate-determining (Högberg, 1997). During a series of reactions, the isotopic fraction during the rate limiting step will determine the net overall isotopic fractionation. Therefore, in nitrification the first step (Eq. 1 and 2) is the only expressed isotopic enrichment, and any isotopic enrichment during step two (Eq. 3) is not expressed. The absence of the expressed isotopic fraction in subsequent reaction is due to the lack of intermediate product, because it is completely consumed and thus the isotopic composition of that intermediate is completely transformed to the product. Consequently, in nitrification where no intermediate product forms $^{15}\epsilon_{\text{NO}_3^-/\text{NH}_4^+} = ^{15}\epsilon_{\text{NO}_2^-/\text{NH}_4^+}$, which ranges from -12 to -38‰ (Casciotti et al., 2003; Delwiche & Steyn, 1970b; Högberg, 1997; Nikolenko et al., 2018). This large range of $^{15}\epsilon$ values has been attributed to both various bacteria species, that have different isotopic selectivity, and environmental conditions (Casciotti et al., 2003; Mariotti et al., 1981). The $^{15}\epsilon_{\text{NO}_3^-/\text{NH}_4^+}$ usually causes the $\delta^{15}\text{N}$ values of the initial NO_3^- product to be lower relative to the NH_4^+ reactant. As the conversion of the ammonium pool goes to completion, the $\delta^{15}\text{N}$ values of the NO_3^- will continue to increase until the $\delta^{15}\text{N}$ of the NO_3^- pool equals the original $\delta^{15}\text{N}$ of ammonium (Feigin et al., 1974; Kendall & Aravena, 2000). This progressive change in $\delta^{15}\text{N}$ values of NO_3^- (and NH_4^+) can be predicted using a Rayleigh distillation model (Eq.4):

$$\delta^{15}\text{N}_f = \delta^{15}\text{N}_0 + ^{15}\epsilon_{\text{NO}_3^-/\text{NH}_4^+} \ln f(t) \quad \text{Eq. 4}$$

Where $\delta^{15}\text{N}_f$ is the $\delta^{15}\text{N}$ value of the remaining (final) NH_4^+ after some fraction has been lost to nitrification, $\delta^{15}\text{N}_0$ is the $\delta^{15}\text{N}$ value of the initial NH_4^+ , $^{15}\epsilon_{\text{NO}_3^-/\text{NH}_4^+}$ (‰) is the nitrification ^{15}N enrichment factor ($(\alpha-1)*1000$), and $f(t)$ is the fraction of the initial NH_4^+ remaining in the soil at

any time t . However, to apply this method the enrichment factor ($^{15}\epsilon_{\text{NO}_3^-/\text{NH}_4^+}$) must be known and constant. Thus, an understanding of $^{15}\epsilon_{\text{NO}_3^-/\text{NH}_4^+}$ is critical for proper modeling and understanding of isotopic data, such as the change in $\delta^{15}\text{N}$ of NH_4^+ or NO_3^- in agricultural soils (Chapter 4 in this dissertation).

The $\delta^{18}\text{O}$ value of nitrate generated by nitrification, regardless of whether the NH_4^+ is derived from soil N, manure, or ammonium fertilizer, will be similar because each undergoes the same oxidative pathway. The observed $\delta^{18}\text{O}$ value for nitrification depends on the source of the oxygen atoms added to NH_4^+ , during nitrification and their respective $\delta^{18}\text{O}$ values. As noted above the stoichiometry suggests that the two-steps of the nitrification process adds three oxygen atoms to NH_4^+ from either H_2O or O_2 (Eq. 1, 2, and 3) (Aleem et al., 1965; Andersson & Hooper, 1983; Hollocher, 1984; Kumar et al., 1983; Yoshinari & Wahlen, 1985a). From a stable oxygen isotope perspective, nitrate produced via nitrification should have an a $\delta^{18}\text{O}$ value that follows

$$\delta^{18}\text{O-NO}_3^- = f_{\text{H}_2\text{O}} * \delta^{18}\text{O-H}_2\text{O} + f_{\text{O}_2} * \delta^{18}\text{O-O}_2 + {}^{18}\epsilon_{\text{nit}} \quad \text{Eq. 5}$$

Where f is the mole fraction of O atoms from each oxidant (O_2 and H_2O) incorporated into the final NO_3^- product and ${}^{18}\epsilon_{\text{nit}}$ is the sum of all enrichment factors from the three oxidative steps of nitrification (Eq.1-3). Based on the stoichiometry in Eq.1-3, the expected f values are $f_{\text{H}_2\text{O}} = 0.66$ and $f_{\text{O}_2} = 0.33$ and many studies have found this prediction to hold true (Aleem et al., 1965; Buchwald et al., 2012; Hollocher, 1984; Kumar et al., 1983; Yoshinari & Wahlen, 1985a). However, other studies have observed $f_{\text{H}_2\text{O}}$ values greater than 0.66 (Buchwald et al., 2012; Casciotti et al., 2007; Snider et al., 2009, 2010).

These larger $f_{\text{H}_2\text{O}}$ values have been attributed to oxygen isotopic exchange between H_2O and NO_2^- (Buchwald & Casciotti, 2010; Sigman et al., 2009; Snider et al., 2010). Isotopic exchange of ^{18}O between H_2O and NO_2^- is an equilibrium isotope effect (EIE) denoted by

$((^{18}\text{R}_1/^{18}\text{R}_2) - 1) * 1000$ (where $^{18}\text{R}_1$ and $^{18}\text{R}_2$ is the oxygen isotope ratio of the two compounds in isotope equilibrium) and for the exchange between H_2O and NO_2^- is:



Due to the large molar amount of H_2O relative to NO_2^- in a cell, complete isotope exchange would eliminate the $\delta^{18}\text{O}$ signal from O_2 that was initially incorporated into NH_2OH during NH_4^+ oxidation (equation 1). Therefore, oxygen isotope exchange between H_2O and NO_2^- would cause the $\delta^{18}\text{O}$ value of nitrate to be lower than that calculated using equation 4, since the initial O atom derived from O_2 ($\delta^{18}\text{O} = +23\%$) is lost. As a result, the $\delta^{18}\text{O}$ value of NO_2^- produced by AOB/AOA (Eq.1 and 2) would be

$$\delta^{18}\text{O-NO}_3^- = 2/3(\delta^{18}\text{O-H}_2\text{O} + ^{18}\epsilon_{\text{Ex}}) + 1/3 (\delta^{18}\text{O-H}_2\text{O} + ^{18}\epsilon_{\text{H}_2\text{O-2}}) \quad \text{Eq. 7}$$

Where, $^{18}\epsilon_{\text{H}_2\text{O-2}}$ is the enrichment factor of H_2O by NOB during NO_2^- oxidation and the $^{18}\epsilon_{\text{NO}_2\text{-H}_2\text{O}}$ is EIE (where we have defined $^{18}\epsilon_{\text{NO}_2\text{-H}_2\text{O}} = ^{18}\text{R}_{\text{NO}_2^-} / ^{18}\text{R}_{\text{H}_2\text{O}}$), which has been measured at $\sim +14\%$ at 21°C (Casciotti et al., 2007). The $\delta^{18}\text{O}$ value of H_2O used during soil nitrification will reflect the $\delta^{18}\text{O}$ value of precipitation, which in the United States typically spans -24 to 0% and rarely exceeds $+5\%$ (Vachon et al., 2010). This suggests that in soil nitrate found in the United States should have a $\delta^{18}\text{O}$ values that range between -10 and $+14\%$ (assuming complete isotope equilibration with H_2O).

Oxygen EIE has been observed in culture, marine, and soil environments. In an experiment using cultures of marine nitrifiers. Casciotti (2010) observed NO_2^- - H_2O exchanged between 1 to 25%, while Buchwald and Casciotti (2010) observed less than 3% during nitrite oxidation. Sigman et al. (2009) evaluated the $\delta^{18}\text{O-NO}_3^-$ in the ocean using a multi-box model and suggested O exchange of at least 50%. In acidic forest soil incubations Mayer et al, (2001) observed no exchange of $\text{H}_2\text{O}^{18}\text{O}$ in NO_3^- and even observed $f_{\text{H}_2\text{O}}$ below the expected 0.66 value.

In contrast, an incubation study using agricultural and temperate forest soils by Snider et al. (2010) determined that between 37 to 88% of the O atoms in nitrate had equilibrated with water. Thus, there remains considerable debate about the degree and causality of the NO_2^- - H_2O oxygen isotope exchange in soil and aquatic systems.

Thus, this study has two goals, first to investigate the $^{15}\epsilon_{\text{NO}_3^-/\text{NH}_4^+}$ during nitrification occurring within an agricultural soil typical of the Midwestern United States. The $^{15}\epsilon_{\text{NO}_3^-/\text{NH}_4^+}$ may cause error in the source appointment of nitrate from nitrification, particular in environments where large amounts of NH_4^+ are added such as agricultural soils. Second, to determine the source of oxygen atoms in nitrate formed via nitrification and test the hypothesis based on the biogeochemical steps of nitrification that $\frac{2}{3}$ of oxygen are derived from H_2O and $\frac{1}{3}$ from O_2 .

3.3 Materials and Methods

3.3.1 Nitrification Incubations

Table 3-1 Experiment conditions used throughout incubations

Incubation #	Growth Solution	Shaken	NH_4^+ Concentration (M)	NH_4^+ Concentration ($\mu\text{Mol/g}$ soil)	$\delta^{18}\text{O-H}_2\text{O}$
1-8**	Yes	Yes	0.001 to 0.0027	66.67 to 180.0	Millipore (-7.10‰)
9-16	Yes	Yes	0.001	66.67	Light (-29.52‰)
17-20	Yes	Yes	0.001	66.67	Heavy (16.14‰)
21	Yes	No	0.001	66.67	Light (-29.52‰)
22	Yes	No	0.001	66.67	Millipore (-7.10‰)
23	No	No	0.00	0.00	Millipore (-7.10‰)
24	No	No	0.00	0.00	Light (-29.52‰)
25-26	No	Yes	0.00	0.00	Millipore (-7.10‰)
27-28	No	Yes	0.00	0.00	Light (-29.52‰)
29-30	No	Yes	0.00	0.00	Heavy (16.14‰)

**concentrations increased due to addition of nutrient solution after sampling

Soil was collected during the summer of 2014 from the Purdue Agronomy Center for Research and Education (ACRE) Farm (GPS coordinates 40.470453, -86.992614). The soil at this location is classified as Dummer series (USDA 2017) and was cropped with maize. The top portion of the soil (0-10 cm) was collected and oven dried at 30°C for seven days, the soil was then homogenized with a mortar and pestle and sieved to 2mm. The pH of soils collected from this location range from 6.0 to 6.5 (USDA, 2016).

30 incubations (Table 3-1) were performed to determine the $^{15}\epsilon_{\text{NO}_3^-/\text{NH}_4^+}$ and the origin of the oxidant used during nitrification. The $^{15}\epsilon_{\text{NO}_3^-/\text{NH}_4^+}$ was evaluated by adding NH_4^+ in excess and measuring the $\delta^{15}\text{N}$ of the NO_3^- product (see equation 8 below). The source of oxygen atoms in the final NO_3^- product were determined by using three isotopically different waters (light, Millipore, and heavy), each with a distinct $\delta^{18}\text{O}$ values and measuring the $\delta^{18}\text{O}$ of the NO_3^- product (Table 3-2). Sampling was performed at various times throughout the experiment and will be referred to as t_x , where x is the time (hours) after beginning the incubation.

1.3.2 Determination of nitrification rate and incubation length

Initial time trial incubations were performed to determine the amount of time required to generate enough NO_3^- for isotope analysis and for new nitrification NO_3^- to exceed the initial NO_3^- present in the soil. An aqueous nutrient solution was prepared by adding 0.410g KH_2PO_4 , 0.216g K_2HPO_4 , and 0.535g NH_4Cl into 1L of Millipore H_2O to give final concentrations of 0.004M PO_4^{3-} and 0.010M NH_4^+ . Then $15.1 \pm 0.12\text{g}$ of soil was then weighed and added into an Erlenmeyer flask (250mL) followed by $100 \text{ mL} \pm 0.05$ of Millipore H_2O . The soil and water mixtures were then place on a wrist shaker (Burrell Model 75) at 30 rpm. After 10 minutes a t_0 sample ($10\text{mL} \pm 0.05$) was withdrawn from each flask using a glass pipette and vacuumed filtered (0.45 μm mixed ester cellulose filter (MilliporeSigma)). The 10mL removed from the t_0

sample was then replaced with 10mL of the nutrient solution. After each of other sampling times the removed volumes were replaced by 10mL of nutrient solution. Incubations samples were collected at t_{24} , t_{48} , t_{72} , and t_{144} and analyzed by ion chromatography (IC) analysis to determine the NO_3^- concentration as a function of time. From this it was determined that after 72 hours there was sufficient NO_3^- for concentration and isotope analysis and for NO_3^- from nitrification to exceeds initial NO_3^- in the soils. By t_{72} NO_3^- from nitrification made up at least 87% of NO_3^- . Therefore, in the subsequent incubations (trails 9-24) samples were only drawn at t_0 and t_{72} . Control samples (trails 25-30) were also ran during these trails and they did not receive any nutrient solution to evaluate the contribution of NO_3^- by mineralization and nitrification of organic N.

1.3.3 Experiments to determine the $^{15}\epsilon_{\text{NO}_3^-/\text{NH}_4^+}$ and oxidant used during nitrification

Identical nutrient solutions were prepared using two isotopically different waters, light and heavy (Table 3-2). Incubation experiments were run using all three nutrient solutions and followed the same procedure as above, but samples were only drawn at t_0 and t_{72} . Control samples were also ran which consisted of samples that received either no nutrients or were not shaken (trails 23-24), These controls were designed to measure the rate of mineralization and subsequent nitrification in aerobic soils, and the non-shaken incubations with nutrient solutions (trails 21 -22) to examine the effect of nitrification in anaerobic soils.

The $\delta^{18}\text{O}$ values of H_2O used in the incubations were measured using a Los Gatos Research, Inc. (LGR) Liquid Water Isotope Analyzer (LWIA) at the Purdue Stable Isotope (PSI) Lab (Berman et al., 2013; Wassenaar et al., 2016). The $\delta^{15}\text{N}$ and $\delta^{18}\text{O}$ values of NO_3^- were measured at the PSI lab using the bacteria denitrifying method interfaced to a Thermo Delta V

isotope ratio mass spectrometer (IRMS) (Casciotti et al., 2002) (precision = $\pm 0.5\%$ for $\delta^{15}\text{N}$ and 0.7% for $\delta^{18}\text{O}$). The $\delta^{15}\text{N}$ of NH_4^+ from NH_4Cl was determined using standard methods on a Sercon 20-22 IRMS paired to a Sercon EA-CN 1 elemental analyzer (precision = $\pm 0.3\%$ for $\delta^{15}\text{N}$). Ion concentrations were determined by a Dionex DX-500 ion chromatography at the PSI lab. The NO_3^- per gram of soil was calculated by Eq 8.

$$\mu\text{g of N} - \text{NO}_3 \text{ g soil}^{-1} = \frac{\text{concentration of mg N L}^{-1} * \text{volume L} * 1000 \frac{\mu\text{g}}{\text{mg}}}{\text{grams of soil}} \quad \text{Eq. 8}$$

Where $\text{mg NO}_3^- \text{ L}^{-1}$ is the concentration of NO_3^- measured by the IC, volume L is the total amount of liquid added to the soil incubations (0.1L), and grams of soil is the total amount of soil used in each incubation (15g).

Table 3-2 $\delta^{18}\text{O}$ Values of various H_2O and O_2 used in Experiments

		$\delta^{18}\text{O}\text{-H}_2\text{O}$	
Sample		t_0	t_{72}
Millipore Water		-7.10‰	-7.06‰
Millipore Water with Growth Solution		-6.90‰	-6.98‰
Heavy Water with Growth Solution		16.14‰	N/A
Light Water with Growth Solution		-29.52‰	-30.27‰
		$\delta^{18}\text{O}\text{-O}_2$	
Sample		t_0	
Atmospheric Air		23.5‰	

$\delta^{18}\text{O}\text{-H}_2\text{O}$ of heavy water was not measured at t_{72}

3.4 Results

The nitrate concentration increased exponentially from $2.2 \pm 0.5 \mu\text{g N g soil}^{-1}$ at t_0 to $16.1 \pm 1.3 \mu\text{g N g soil}^{-1}$ by t_{72} (Figure 3-1). The total nitrification rate between t_0 and t_{72} was $0.19 \mu\text{g N g soil}^{-1} \text{ h}^{-1}$, and a first order nitrification rate constant of 0.029 hr^{-1} . Control experiments showed that the mineralization of soil N and subsequent nitrification could generate nitrate concentrations as great as $10.0 \pm 1.6 \mu\text{g N g soil}^{-1}$. The NO_3^- concentration after each sampling period was used to calculate the fraction of NH_4^+ that was oxidized, assuming all NO_3^- was

derived from the NH_4^+ amendment. Only 0.1% of NH_4^+ was converted to NO_3^- by t_{24} , 0.2% by t_{48} , and 0.5% at t_{72} in trails 1-8, and 1.9% at t_{72} in trials 9-22. No nitrite was detected within any of the samples. The NO_3^- $\delta^{15}\text{N}$ values ($\delta^{15}\text{N-NO}_3^-$) at t_0 , $3.34\text{‰} \pm 13.56$, had a large standard deviation and low NO_3^- concentrations ($2.2 \pm 0.5 \mu\text{g N g soil}^{-1}$). As nitrate concentrations increased over time, the $\delta^{15}\text{N-NO}_3^-$ values decreased to a value of $-25.5\text{‰} \pm 1.92$ at t_{72} . After t_{72} the $\delta^{15}\text{N-NO}_3^-$ values no longer decreased regardless of increasing NO_3^- concentrations (Figure 3-2). Based on the consistent $\delta^{15}\text{N}$ of NO_3^- throughout all incubations using various $\delta^{18}\text{O H}_2\text{O}$, the $\delta^{18}\text{O}$ value of H_2O ($\delta^{18}\text{O-H}_2\text{O}$) had no observable effect on the $\delta^{15}\text{N-NO}_3^-$ value. Similar to the initial $\delta^{15}\text{N-NO}_3^-$ values, the t_0 initial $\delta^{18}\text{O}$ values of NO_3^- ($\delta^{18}\text{O-NO}_3^-$) were highly variable at $13.80\text{‰} \pm 11.72$. However, unlike $\delta^{15}\text{N}$ the final $\delta^{18}\text{O-NO}_3^-$ at t_{72} had a strong dependence on the $\delta^{18}\text{O-H}_2\text{O}$: $-10.76\text{‰} \pm 2.5$ for Millipore H_2O ($\delta^{18}\text{O-H}_2\text{O} = -7.1\text{‰}$), $-29.23\text{‰} \pm 2.00$ for light H_2O ($\delta^{18}\text{O-H}_2\text{O} = -29.5\text{‰}$), and $9.06\text{‰} \pm 3.18$ for heavy H_2O ($\delta^{18}\text{O-H}_2\text{O} = 16.1\text{‰}$).

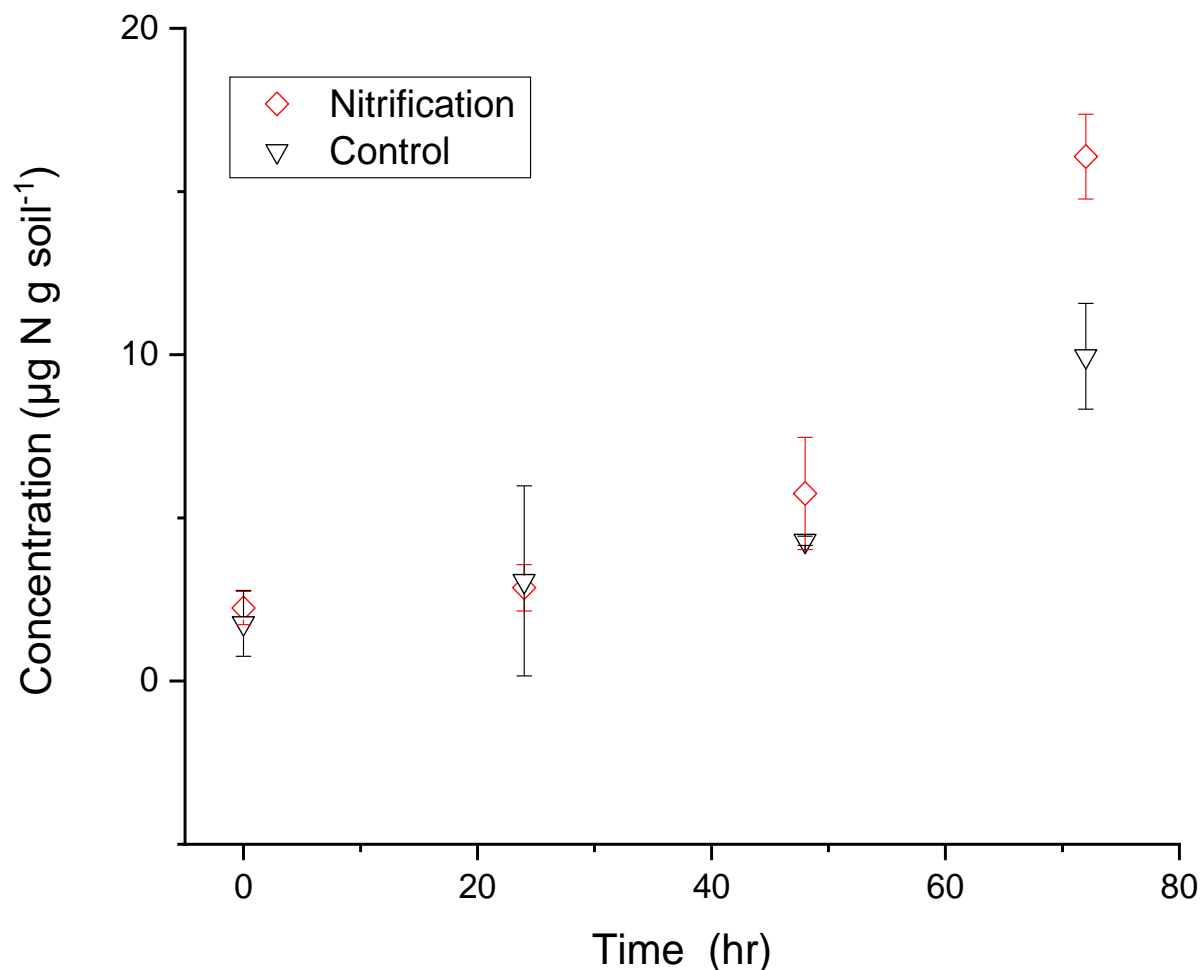


Figure 3-1 NO_3^- accumulation over time during nitrification and control incubations.

3.5 Discussion

3.5.1 Nitrification Rates

Overall the linear regression of nitrate concentration with time gives a nitrification rate of $0.19 \mu\text{g N g soil}^{-1} \text{h}^{-1}$. This rate is in agreement with results by Snider et al., (2010) who measured a nitrification rate of $0.25 \mu\text{g N g soil}^{-1} \text{h}^{-1}$, but greater than results by Nicol & Prosser, (2010) who determined a rate of $0.032 \mu\text{g N g soil}^{-1} \text{h}^{-1}$. Nitrification often increases NO_3^- with time within soils following a sigmoidal curve (Ghaly & Ramakrishnan, 2013). This curve often begins with a delay period as the bacteria population increases then reaching a maximum rate followed by termination phase as NH_4^+ concentrations diminish (Sabey et al 1969; Addiscott 1983). Based

on the exponential increase in concentration and the short incubation time scales our incubations were in the delay period throughout incubations. Nitrification has often been described and modeled by both zero and first order kinetics. In biological reactions the discrepancy between zero order and first order reactions rates can often be explained by Michaelis-Menten kinetics Eq. 9 that changes reaction order depending on substrate and enzyme concentrations (Charley et al., 1979; Hagopian & Riley, 1998).

$$V = V_{\max} * (S/K_m + S) \quad \text{Eq. 9}$$

Where V is the rate of the reaction, V_{\max} is the maximum rate of the reaction, S is the substrate, and K_m is the saturation constant equal to the substrates concentration at $0.5 V_{\max}$. In short when substrate concentrations are high the $V = V_{\max}$ and follows a zero-order kinetics and when substrate concentration are low $V = V_{\max} * (S/K_m)$ resulting in a first order kinetics with respect to the substrate.

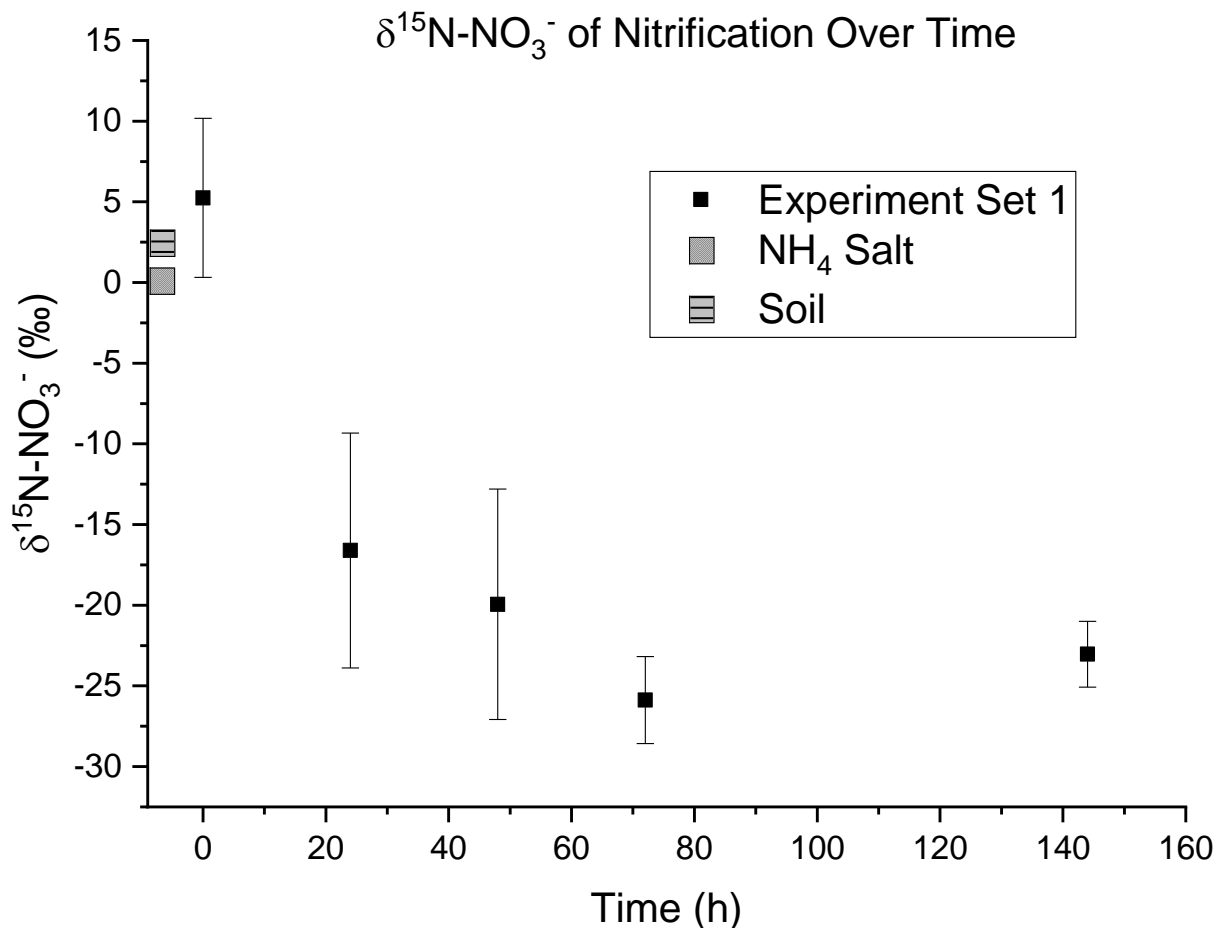


Figure 3-2 The change in $\delta^{15}\text{N}$ in incubations over time as NO_3^- from nitrification becomes a greater fraction of the total nitrate.

3.5.2 ^{15}N Enrichment Factor of Nitrification

The exponential decrease in the $\delta^{15}\text{N}$ value of NO_3^- over incubation time indicates that nitrification discriminated against $^{15}\text{NH}_4^+$. This agrees with other studies that found nitrification proceeds through a normal KIE, where the lower mass isotope preferentially reacts producing an isotopically lighter product (NO_3^-) relative to the reactant (NH_4^+) (Kendall & Aravena, 2000; Mariotti et al., 1981). The dynamics of the KIE can usually be reproduced using a standard Rayleigh distillation model, which is a function of the $^{15}\epsilon_{\text{NO}_3^-/\text{NH}_4^+}$ value and can be determined using Eq. 4.

Where $\delta^{15}\text{N}_f$ is the final $\delta^{15}\text{N}$ values of NH_4^+ at t_f , $\delta^{15}\text{N}_0$ is the initial $\delta^{15}\text{N}$ value of NH_4^+ at t_0 , f is the fraction reactant remaining at t_f , and $^{15}\epsilon_{\text{NO}_3^-/\text{NH}_4^+}$ is the isotope enrichment factor. Usually the $^{15}\epsilon_{\text{NO}_3^-/\text{NH}_4^+}$ value would be determined by the slope of the linear relationship of $\delta^{15}\text{N}$ vs. the natural logarithm of the fraction of remaining total reactant (Mariotti et al., 1981). However, here excess NH_4^+ with a known $\delta^{15}\text{N}$ value was added. Measuring the $\delta^{15}\text{N}$ of the instantaneous NO_3^- product at time t (Eq. 10)

$$\delta^{15}\text{NO}_3^-(t) = \delta^{15}\text{NH}_4^+ - ^{15}\epsilon_{\text{NO}_3^-/\text{NH}_4^+} \frac{f(t)\ln[f(t)]}{1-f(t)} \quad \text{Eq. 10}$$

Where $^{15}\epsilon_{\text{NO}_3^-/\text{NH}_4^+}$ is the nitrification enrichment factor, $f(t)$ is the fraction of substrate remaining at time t , $\delta^{15}\text{NH}_4^+$ is the $\delta^{15}\text{N}$ of the substrate, and $\delta^{15}\text{NO}_3^-$ is the $\delta^{15}\text{N}$ of the product. In a system where the substrate is “unlimited” the isotopic enrichment in the reactant does not occur as the reactant is converted to the product. Thus, if f is close to 1 than Eq. 10 is reduced to Eq. 11

$$^{15}\epsilon_{\text{NO}_3^-/\text{NH}_4^+} = \delta^{15}\text{NH}_4^+ - \delta^{15}\text{NO}_3^-(t) \quad \text{Eq. 11}$$

In these incubations $f(t)$ values were lower than 0.02 (or 2% of NH_4^+ was used, therefore the $^{15}\epsilon_{\text{NO}_3^-/\text{NH}_4^+}$ was determine using Eq. 11 and the measured $\delta^{15}\text{N}$ values of the initial NH_4^+ and final NO_3^- .

The $^{15}\epsilon_{\text{NO}_3^-/\text{NH}_4^+}$ value was determined to be $-25.46\% \pm 1.92$, which falls within the middle range of values previously observed in soil studies that range from -35 to -5‰. Delwiche & Steyn (1970) measured between -29 and -12‰, Yun et al., (2011) measured between -35 and -15‰, Yun & Ro, (2014) measured -31 to -25‰, and Mariotti et al (1981) observed values between -35 to -5‰ in soils. Bacteria cultures studies have found $^{15}\epsilon_{\text{NO}_3^-/\text{NH}_4^+}$ values that range from -38 to -10‰, as Yoshida (1988) found values of -32 to -25‰, Casciotti et al, (2003) measured values between -38 to -14‰, and Santoro & Casciotti, (2011) measured values

between -37 to -10‰. This wide range of fractionation values has been attributed to several causes including high N₂O yields (Yoshida, 1988), accumulation of intermediates (Casciotti et al., 2003; Yoshida, 1988), concentration of electron donors (Bryan et al., 1983), biodiversity (Casciotti et al., 2003) and environmental conditions (Mariotti 1981).

Control samples demonstrated that mineralization and subsequent nitrification could potentially contribute up to 80% of NO₃⁻ in some incubations. However, this is unlikely since mineralization rates decrease when excess N is available (Hart et al., 1994; Luxhøi et al., 2008). If all NO₃⁻ produced in incubations did indeed come from mineralization it would only alter the observed δ¹⁵N by less than 2‰. The δ¹⁵N of the soil differed from the δ¹⁵N of the applied NH₄⁺ salts by 1.8‰ (Table 3-3). The process of mineralization (organic N → NH₄⁺) has an ¹⁵ε_{NH₄⁺/organic N that is <1‰, therefore the δ¹⁵N of NH₄⁺ from mineralization is expected to be equivalent to the δ¹⁵N of the soil N at 1.54 ± 0.3‰ (Högberg, 1997; Kendall et al., 2000). Thus, while unlikely, mineralization could cause the observed ¹⁵ε_{NO₃⁻/NH₄⁺ to be lower by 2‰ and likely contributes to some of the observed standard deviation in ¹⁵ε_{NO₃⁻/NH₄⁺.}}}

To determine the influence from initial δ¹⁵N-NO₃⁻ values on the final δ¹⁵N-NO₃⁻ values a mixing model was performed between initial NO₃⁻ concentrations and final NO₃⁻ concentrations at t₇₂. Mixing models, are used to determine the degree of mixing or fraction composition of various sources in a mixed pool and in our system can be defined by Eq. 12

$$\delta^{15}\text{N}(\text{NO}_3^-) = f(t) \delta^{15}\text{N}(t) + f_{(t=0)} \delta^{15}\text{N}_{(t=0)} \quad \text{Eq. 12}$$

Where δ¹⁵N(NO₃⁻) is the observed δ¹⁵N of NO₃⁻, f(t) is the fraction of nitrate from nitrification at some time (t = 72hr), and δ¹⁵N_t is the δ¹⁵N value of NO₃⁻ and time t. This approach requires that each isotopic end-member (source) value is known, distinct, and acts conservatively. Initial NO₃⁻ concentrations were 2.2 ± 0.5 μg N g soil⁻¹ and final NO₃⁻ concentrations measured 16.1 ± 1.3 μg

N g soil^{-1} . The initial NO_3^- concentration could influence the final observed $\delta^{15}\text{N}(\text{NO}_3^-)$ value, since $f_{(t=0)}$ was as high as 0.13. If the average measured initial $\delta^{15}\text{N}(\text{NO}_3^-)$ value of 3.34‰ is used, which falls in the upper range of soil N $\delta^{15}\text{N}$ values of -5 to 5‰ (Kendall & Aravena, 2000), we find that initial nitrate can account for up to $\pm 2.8\%$ of the variability in incubations. Thus, the variability in $^{15}\epsilon_{\text{NO}_3^-/\text{NH}_4^+} \pm 1.92\%$ was most likely caused by the presence of initial NO_3^- , and from NO_3^- from mineralization and subsequent nitrification.

Table 3-3 NH_4^+ and initial and final NO_3^- $\delta^{15}\text{N}$ values of nitrification experiments

Initial $\delta^{15}\text{N}-\text{NO}_3^-$	$3.34 \pm 13.6\%$ [†]
$\delta^{15}\text{N}$ of Soil	$1.54 \pm 0.3\%$
$\delta^{15}\text{N}-\text{NH}_4^+$	$-0.32 \pm 0.09\%$
Final $\delta^{15}\text{N}-\text{NO}_3^-$	$-25.46 \pm 1.92\%$
$^{15}\epsilon_{\text{NO}_3^-/\text{NH}_4^+}$	$-25.14 \pm 2.01\%$

[†]Initial $\delta^{15}\text{N}-\text{NO}_3^-$ values have a large range of values due to low initial NO_3^- concentrations

3.5.3 Sources of ^{18}O incorporated into NO_3^- during nitrification

The $\delta^{18}\text{O}$ of NO_3^- ($\delta^{18}\text{O}-\text{NO}_3^-$) from nitrification at the end of incubations was strongly correlated ($R^2 > 0.999$) with the $\delta^{18}\text{O}$ of H_2O ($\delta^{18}\text{O}-\text{H}_2\text{O}$). This indicates that oxygen atoms from H_2O was a major source of oxygen in NO_3^- produced via nitrification. The fraction of oxygen contributed by H_2O to NO_3^- was related to the slope of the linear regression plot of $\delta^{18}\text{O}-\text{H}_2\text{O}$ vs $\delta^{18}\text{O}-\text{NO}_3^-$ (Fig. 3-3). The fraction of oxygen in NO_3^- derived from water averaged 0.82 (Figure 3-3 black squares). These fractions are greater than the fraction of 0.67 predicted by Andersson & Hooper, (1983) and Kumar et al., (1983) (Figure 3-3 red circles).

Fractions of oxygen derived from H_2O that are greater than 0.67 in microbial NO_3^- have been attributed to oxygen EIE between NO_2^- and H_2O (Granger & Wankel, 2016; Kool et al., 2010; Kool, Wrage, et al., 2007; Snider et al., 2010). Studies have shown that EIE of oxygen can occur during either nitrification or denitrification when the NO_2^- intermediate is produced (Casciotti et al., 2010; Granger et al., 2008; Kool, Wrage, et al., 2007) and has been shown to

occur in both marine and terrestrial environments (Granger & Wankel, 2016; Mayer et al., 2001; Sigman et al., 2009; Snider et al., 2010). Exchange in marine environments has been measured to range from 0 to 50%, while exchange in soils have range from 0 to 88% (Granger & Wankel, 2016; Mayer et al., 2001; Sigman et al., 2009; Snider et al., 2010).

The degree of exchange depends on the rate of isotope exchange and the lifetime of NO_2^- . The lifetime of NO_2^- is considered to be the time from when it is formed by AOB or AOA to the time when it is oxidized by NOB. Snider et al (2010) found an inverse relation between net nitrification rates and NO_2^- - H_2O oxygen isotope exchange, suggesting the longer the life time of NO_2^- the greater the amount of EIE. It is difficult to put a constraint on the life time of NO_2^- because it was below the limits of detection throughout incubations, however because of this its oxidation by NOB had to be faster than the oxidation rate of NH_4^+ by AOB or AOA, which was measured at $0.19 \mu\text{g N g soil}^{-1} \text{h}^{-1}$. Due to this rapid rate of NO_2^- oxidation, the rate of isotope exchange must have been faster than the rate of nitrite consumption by NOB to explain the observed EIE of 48%.

Oxygen isotope exchange rate is a pH dependent process occurring most rapidly at low pH's. Studies have found that over 21 days oxygen EIE between H_2O and NO_2^- increases from 0.5% at pH 12 to 5% at pH 10 to as high as 30% at a pH 6 (Casciotti & McIlvin, 2007). The estimated pH of our soils, calculated using NH_4^+ molarity, was 6.12 but could be as high as 7.8, because the pH of Drummer series soils can range from 6.6 to 7.8, so the rate of oxygen isotope exchange should have been slow relative to incubation times. Indeed, Casciotti et al., (2007) found that at these pHs only 10 to 30% of the NO_2^- oxygen had exchanged with water after three weeks. Using this calculated pH with the data from Casciotti et al (2007) the EIE rate would be $0.06\% \text{ hr}^{-1}$, therefore we would expect approximately 1.5% exchange in the nitrification

incubations over three days. But this was an inorganic NO_2^- - H_2O isotope exchange without any enzyme activity. It has been suggested that NO_2^- - H_2O isotope exchange could occur within the bacteria, either before the NO_2^- is expelled by AOB/AOA or before it is oxidized after uptake by NOB (Granger & Wankel, 2016; Kool, Wrage, et al., 2011; Snider et al., 2010). The process of nitrification is an acid producing process and Snider et al., (2010) suggested the intra-cellular pH maybe much lower providing the environment necessary for rapid exchange.

Nitrification (Eq. 1-4) can have an isotope enrichment factor associated each step that incorporates an oxygen onto NO_3^- . This includes the incorporation oxygen from of O_2 ($^{18}\epsilon_{\text{O}_2}$) and H_2O ($^{18}\epsilon_{\text{H}_2\text{O}-1}$) by AOA/AOB and H_2O ($^{18}\epsilon_{\text{H}_2\text{O}-2}$) by NOB. If these ϵ values are known, the $\delta^{18}\text{O}$ - NO_3^- value can be predicted by Eq. 13.

$$\delta^{18}\text{O}-\text{NO}_3^- = 1/3(\delta^{18}\text{O}-\text{O}_2 + ^{18}\epsilon_{\text{O}_2}) + 1/3 (\delta^{18}\text{O}-\text{H}_2\text{O} + ^{18}\epsilon_{\text{H}_2\text{O}-1}) + 1/3 (\delta^{18}\text{O}-\text{H}_2\text{O} + ^{18}\epsilon_{\text{H}_2\text{O}-2}) \quad \text{Eq. 13}$$

However, when the oxygen EIE ($^{18}\epsilon_{\text{Ex}}$) occurs the signal from the first two equations (first step) (Eq. 1 and 2) is partial or completely lost, depending on the amount of EIE. Thus, if the amount of exchange is known the new $\delta^{18}\text{O}-\text{NO}_3^-$ can be calculated by Eq. 14;

$$\delta^{18}\text{O}-\text{NO}_3^- = 1/3(1-f_{\text{exchange}}) (\delta^{18}\text{O}-\text{O}_2 + ^{18}\epsilon_{\text{O}_2}) + 1/3(1-f_{\text{exchange}}) (\delta^{18}\text{O}-\text{H}_2\text{O} + ^{18}\epsilon_{\text{H}_2\text{O}-1}) + f_{\text{exchange}} (\delta^{18}\text{O}-\text{H}_2\text{O} + ^{18}\epsilon_{\text{Ex}}) + 1/3 (\delta^{18}\text{O}-\text{H}_2\text{O} + ^{18}\epsilon_{\text{H}_2\text{O}-2}) \quad \text{Eq. 14}$$

and if the isotope exchange is 100% equation 14 reduces each step to.

$$\delta^{18}\text{O}-\text{NO}_3^- = 2/3(\delta^{18}\text{O}-\text{H}_2\text{O} + ^{18}\epsilon_{\text{Ex}}) + 1/3 (\delta^{18}\text{O}-\text{H}_2\text{O} + ^{18}\epsilon_{\text{H}_2\text{O}-2}) \quad \text{Eq. 15}$$

The intercept of the linear regression of $\delta^{18}\text{O}-\text{H}_2\text{O}$ vs $\delta^{18}\text{O}-\text{NO}_3^-$ (-4) is a function of several factors that include $^{18}\epsilon_{\text{O}_2}$, $^{18}\epsilon_{\text{H}_2\text{O}-1}$, $^{18}\epsilon_{\text{H}_2\text{O}-2}$, and $^{18}\epsilon_{\text{Ex}}$. Due to these many factors and the absences of measurements for them, little can be extracted from our experimental intercept value of -4‰ (Figure 3-3).

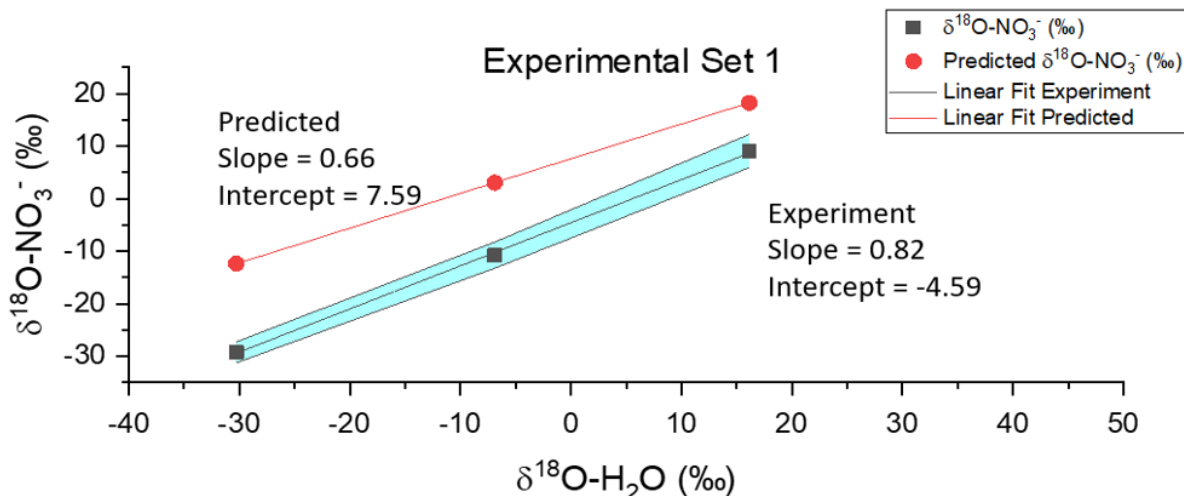


Figure 3-3 The slope of $\delta^{18}\text{O-NO}_3^-$ to $\delta^{18}\text{O-H}_2\text{O}$ of experiment is shown in the black squares/line. The theoretical slope of $\delta^{18}\text{O-NO}_3^-$ to $\delta^{18}\text{O-H}_2\text{O}$ based on the biochemical steps ($f_{\text{H}_2\text{O}} = 0.66$, $f_{\text{O}_2} = 0.33$) is shown in the red dots/line. The blue area represents the standard deviations of experimental measurements.

3.6 Conclusion

It was shown here that the value of $^{15}\epsilon_{\text{NO}_3^-/\text{NH}_4^+}$ is large and can affect the observed $\delta^{15}\text{N}$ of NO_3^- in soils. This is particularly important in soil systems where ammonium is the primary source of N, such as intensively managed landscapes. Additionally, these experiments indicate equilibrium isotopic exchange of oxygen between NO_2^- and H_2O during nitrite oxidation can be up to 48%, occurs during the process of nitrification altering the $\delta^{18}\text{O}$ signal of microbial NO_3^- . As a result, this research recommends that the use of dual isotopes ($\delta^{15}\text{N}$ and $\delta^{18}\text{O}$) of NO_3^- to assess or identify microbial processes and sources must be used cautiously. Because the $^{15}\epsilon_{\text{NO}_3^-/\text{NH}_4^+}$ and oxygen exchange during nitrification may cause incorrect end member assumptions resulting in incorrect source apportionment. For example, the $^{15}\epsilon_{\text{NO}_3^-/\text{NH}_4^+}$ could result in enriched $\delta^{15}\text{N}$ from manure being mistaken as soil or fertilizers N, while oxygen EIE could cause an underestimation of the contribution of atmospheric or anthropogenic fertilizer nitrate in measured in soils. Furthermore, isotopic enrichment of $\delta^{15}\text{N}$ and $\delta^{18}\text{O}$ of NO_3^- caused by

denitrification may be misrepresented or underestimated as the assumed isotopic increase ratio of 2:1 of $\delta^{15}\text{N}$ to $\delta^{18}\text{O}$ may be altered. Thus, research attempting to source nitrate or assess denitrification by dual isotopes where nitrification is a source of NO_3^- should consider and monitor $^{15}\epsilon_{\text{NO}_3^-/\text{NH}_4^+}$ and oxygen exchange and its implications on the observed $\delta^{15}\text{N}$ and $\delta^{18}\text{O}$ values of NO_3^- . Future experiments should investigate the $^{15}\epsilon_{\text{NO}_3^-/\text{NH}_4^+}$ and amount of oxygen exchange that occurs during nitrification in different soils and under different environmental soil conditions, as well as investigate the isotopic exchange that occurs during denitrification of NO_3^- since NO_2^- is an intermediate of denitrification.

CHAPTER 4. DETERMINATION OF THE ¹⁵N ENRICHMENT OF NITRATE AND NITRITE REDUCTION DURING DENITRIFICATION BY EXPERIMENTAL AND KINETIC MODELS

4.1 Abstract

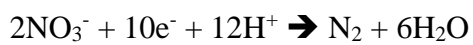
Nitrogen stable isotopes are often used to delineate between different sources of nitrate and nitrite in soils and marine environments. In isotope mixing models the nitrogen isotope ratios in nitrate and nitrite from different sources are often assumed to be constant and conservative. However, a process such as denitrification can cause substantial changes in the nitrogen stable isotope ratios, causing error in nitrate and nitrite source apportionment when using isotope mixing models. Because nitrate and nitrite are reduced by different enzymes they have different degrees of isotope enrichment and studies have demonstrated the overall rate can vary due to environmental conditions. Here we report the nitrogen isotope enrichment factor for both nitrate and nitrite reduction in a Midwestern intensively managed landscape (IML) soil. Enrichment values were determined by performing denitrification incubations using IML soils and measuring the change in nitrite and nitrate concentrations and their nitrogen isotope ratios as a function of time. Data was then modeled using a kinetic compiler, *kinetcus*, to determine the nitrate and nitrite isotope enrichment values using first order, zero order, and Michaelis-Menten models.

4.2 Introduction

Nitrate is a required nutrient for plant growth but can also have adverse impacts on the environment when nitrate concentrations are elevated. Nitrate is readily leachable and excessive nitrate loading in coastal waters, estuaries, lakes, and riverine systems can lead to eutrophication, causing hypoxia and ultimately resulting in loss of aquatic life and biodiversity (Yang et al., 2008). Furthermore, leached nitrate can penetrate aquifers degrading drinking water (Spalding &

Exner, 1993). Nitrate consumption has been linked to harmful health effects, such as cancer and methemoglobinemia, in both humans and livestock, and has led to the regulation and monitoring of drinking water by the US EPA (Environmental Protection Agency., 2018). Nitrate pollution of drinking water within the US has been estimated to cost \$19 billion annually, while its impact to freshwater ecosystems is estimated at \$78 billion (Sobota et al., 2015). Furthermore, nitrate pollution has harmful effects in the urban atmosphere, where it is a component of acid rain and respirable particulate matter (Adams et al., 1999; Fairley, 1999; Lynch et al., 2000; Samet et al., 2000; Seinfeld & Pandis, 2012; Wright & Schindler, 1995). Overall, it is estimated that the potential health and environmental damages of anthropogenic N in the US range from \$81 to \$441 billion yr⁻¹ (Sobota et al., 2015).

How much nitrate is present in an environment at any given time is a balance between nitrate sources and sinks. The main nitrate source is nitrification, a process that refers to the oxidation of ammonium into nitrate, mainly by bacteria, but also Archaea and fungi (Ward, 2011). The source of the ammonium used during nitrification is either from the degradation of organic matter via mineralization or from ammonia fertilizers applied during agricultural practices. The second largest nitrate source is synthetic nitrate fertilizers such as ammonium nitrate and urea ammonium nitrate or UAN (Galloway et al., 2004, 2008). The last major input of nitrate is from the atmosphere where it is formed by the oxidation of nitrogen oxides that are produced by lightening, fossil fuel combustion, and incomplete nitrification/denitrification (Finlayson-Pitts & Pitts Jr, 1999; Seinfeld & Pandis, 2006). The main permanent sink of nitrate is denitrification. Denitrification is a multi-step anaerobic process that ultimately reduces NO₃⁻ to N₂ (Eq.1).



Eq. 1

The anaerobic conditions required for denitrification occur primarily in saturated soils, where bacteria use NO_3^- as an electron acceptor in place of oxygen (Golterman & Chalamet, 2013). The rate of denitrification is controlled by a variety of environmental factors, such as temperature, soil moisture, organic carbon content, pH, and oxygen availability, all of which often have a high degree of spatial and temporal variability (Hofstra & Bouwman, 2005; Woo & Kumar, 2017). Due to this variability, accurate estimates of the amount of NO_3^- lost to denitrification is difficult to determine at both local and global scales.

Globally, soil N loss via denitrification is estimated to range from 22 to 185 Tg N yr^{-1} , while local scale loss can range from 8 to 51 kg N $\text{ha}^{-1} \text{yr}^{-1}$ (Bouwman et al., 2013; Hofstra & Bouwman, 2005; Tiedje, 1988). Some of this variability can be attributed to “hot spots” and “hot moments” of denitrification caused by the nitrate concentration, % water filled pore space, temperature, fertilizer application, crop type, and other factors that can fluctuate dramatically in space and time at the field scale (Harms & Grimm, 2008; Hofstra & Bouwman, 2005; Pilegaard, 2013; Weier et al., 1984). Hofstra & Bouwman, (2005) found that much of this variability may also be driven by differences in the various techniques used to determine denitrification and suggested that denitrification estimates can vary by more than 50% depending on the method used. Therefore, the ability to quantify denitrification loss is important for understating the N cycle on both a local and global scales.

One approach to quantifying denitrification is by using stable isotope systematics. Changes in isotope ratios are reported in delta units δ (‰) = $[\text{R}_{\text{sample}}/\text{R}_{\text{reference}} - 1] * 1000$ (Kendall & Aravena, 2000). Where R is the ratio of the minor to major isotope abundance in either a sample or the reference. For nitrogen, the $^{15}\text{N}/^{14}\text{N}$ is referenced with respect to atmospheric N_2 (Bohlke & Coplen, 1995). Denitrification induces a kinetic isotope effect (KIE),

where the denitrifying bacteria use the lighter isotope preferentially over the heavy isotope (Mariotti et al., 1981). Quantitatively, $KIE = \alpha = k_H/k_L$ where the k 's are the denitrification rate constants for the heavy (H) and light (L) isotopes and α is called the isotope fractionation factor (Mariotti et al., 1981). The isotope fractionation factor (α) is often converted into permil (parts per thousand) notation and is referred to as the isotope enrichment factor (ϵ) Eq. 2.

$$\epsilon (\text{‰}) = (\alpha - 1) * 1000 \quad \text{Eq. 2}$$

The denitrification KIE usually causes an increase in $\delta^{15}\text{N}$ value of the residual nitrate as a function of the fraction of nitrate lost by denitrification because the value of ϵ for denitrification is negative (Granger et al., 2004; Knöller et al., 2011; Mariotti, 1982; Osaka et al., 2018; Sigman et al., 2009). The $^{15}\epsilon_{\text{NO}_3^-}$ value can be calculated using the observed change in $\delta^{15}\text{N}$ values as denitrification progresses and a Rayleigh distillation model (Eq. 3).

$$^{15}\epsilon_{\text{NO}_3^-} = (\delta^{15}\text{N}_f - \delta^{15}\text{N}_0) / \ln f \quad \text{Eq. 3}$$

Where $\delta^{15}\text{N}_f$ is the $\delta^{15}\text{N}$ value of the final (remaining) nitrate after some fraction has been lost to denitrification, $\delta^{15}\text{N}_0$ is the $\delta^{15}\text{N}$ value of the initial nitrate, f is the fraction of the initial NO_3^- remaining, and $^{15}\epsilon_{\text{NO}_3^-}$ (‰) is the denitrification ^{15}N enrichment factor for denitrification. If the $^{15}\epsilon$ value for denitrification in a soil is well defined, the Rayleigh model (Eq.3) can then be used to quantify f , the fraction of the initial NO_3^- remaining, which is a measure of the amount of denitrification that has occurred. The object of this paper is to determine the $^{15}\epsilon$ value for denitrification occurring in an agricultural soil collected from the Midwestern United States so that it can be used in future work to determine field scale denitrification (Chapter 5).

4.3 Materials and Methods

4.3.1 Denitrification Incubations

Controlled denitrification incubation experiments were conducted using a Midwestern US soil and reagents that were isotopically well characterized. In 2014, soil was collected from a plot growing corn at the Purdue Agronomy Center for Research and Education (ARCE) (GPS coordinates 40.470453, -86.992614). Soil was a silty clay loam classified as Dummer (USDA, 2017). Soil was collected from the top (0 - 10cm) portion of the plot and placed in a 5-gallon bucket where it was transported back to Purdue University and laid in stainless steel pans to dry for seven days at 30°C. Before use, soil was homogenized by mortar and pestle and sieved to 2.0 mm diameter. For each trial, 3.000 ± 0.001 g of soil was added to a 15 mL polypropylene centrifuge tube. A nitrate nutrient solution was prepared using NaNO_3 with known $\delta^{15}\text{N}$ and $\delta^{18}\text{O}$ values. The solution was prepared using high purity Millipore water mixed with nitrate and glucose to yield concentrations of 11 mM and 89 mM, respectively, resulting in a C/N ratio of 96 without considering the C or N present in the soil. The NaNO_3 was a Hoffman brand fertilizer imported from Chile and had $\delta^{15}\text{N} = 0.5\text{‰}$ and a high $\delta^{18}\text{O} = 54.1\text{‰}$, typical of Chilean nitrates (Michalski et al., 2015). For each incubation trial, 0.900 ± 0.002 mL of the nutrient solution (10 μmol of NO_3^-) was pipetted into the tube containing the soil, resulting in 46.6 μg N/g soil. This volume of water to soil gave a water filled pore space of $94\% \pm 3$ (see supplemental information for complete method). Control samples were prepared using soil and Millipore water only. Immediately after adding the nutrient solution to the soil, the centrifuge tubes were capped with a septum lid and flushed with N_2 to induce anaerobic conditions and soil/solution was mixed by shaking. The soil were allow to incubations in under these denitrifying conditions for 6 different periods of time (0, 12, 15, 18, 21, and 24 hours). These various sampling times will be referred to as t_x , where x is the time (hours) after beginning the incubation. After each time interval, nitrate

in the soil was double extracted by adding 5.00 ± 0.01 mL of deionized water to the vial, which was shook vigorously for 2.5 minutes, centrifuged for 30 minutes, and vacuum filtered (0.45 μm mixed ester cellulose filter, MilliporeSigma). The extraction process yielded roughly 8.5 mL of a clear solution. The extracted solution was frozen and stored until analysis.

All samples were analyzed for anions by ion chromatography Ion Chromatography (IC) (Metrohm 940 Professional). The mobile phase was a 3.2 mM Na_2CO_3 and 1.0 mM NaHCO_3 carbonate buffer and the column was a Metrosep A supp 5 -150.4.0 (at 30°C) and 8.94 MPa, at a flow rate of 0.700 mL/min. Samples were run for concentrations of Cl^- , SO_4^{2-} , NO_2^- , and NO_3^- (precision = $\pm 2\%$ for all ions), with a detection limit of 200 ppb for all analytes. The $\text{NO}_{2/3}$ ($\text{NO}_2^- + \text{NO}_3^-$) per gram of soil was calculated by Eq 4.

$$\mu\text{g of } \text{NO}_{2/3} \text{ g soil}^{-1} = \frac{\text{concentration of mg } \text{NO}_{2/3} \text{ L}^{-1} * 0.011 \text{ L} * 1000 \frac{\mu\text{g}}{\text{mg}}}{\text{grams of soil}} \quad \text{Eq. 4}$$

Where concentration of $\text{mg } \text{NO}_{2/3} \text{ L}^{-1}$ is the concentration of $\text{NO}_2^- + \text{NO}_3^-$ measured by the IC, 0.011 L is the total volume of liquid added to the soil for incubations and extraction, and grams of soil is the total amount of soil used in each incubation (3 g).

The combined $\delta^{15}\text{N}$ values of NO_3^- and NO_2^- were measured at the PSI lab using the bacteria denitrifying method (Casciotti et al., 2002) using a Thermo Delta V isotope ratio mass spectrometer (IRMS) (precision = $\pm 0.5\text{‰}$ for $\delta^{15}\text{N}$ and 0.7‰ for $\delta^{18}\text{O}$). The bacteria method does not distinguish between NO_3^- and NO_2^- but rather converts both compounds to N_2O . In hindsight, it would have been informative to remove nitrite by sulfamic acid or ascorbic acid (Granger et al., 2006) or separation of the two compounds by ion chromatography (Knöller et al., 2011). However, this was not done and therefore the reported $\delta^{15}\text{N}$ values are for N_2O produced from both NO_2^- and NO_3^- which will be referred to as $\delta^{15}\text{N}$ value of $\text{NO}_{3/2}$ throughout this paper. The $\delta^{15}\text{N}$ of soil and soil C/N ratios were determined using standard methods on a Sercon 20-22

IRMS paired to a Sercon EA-CN 1 elemental analyzer (precision = $\pm 0.3\text{‰}$ for $\delta^{15}\text{N}$). The data was analyzed using a computer program *Kintecus* that numerically solves ordinary differential equations and is commonly used to model chemical kinetic processes (Ianni., 2003)

4.4 Results

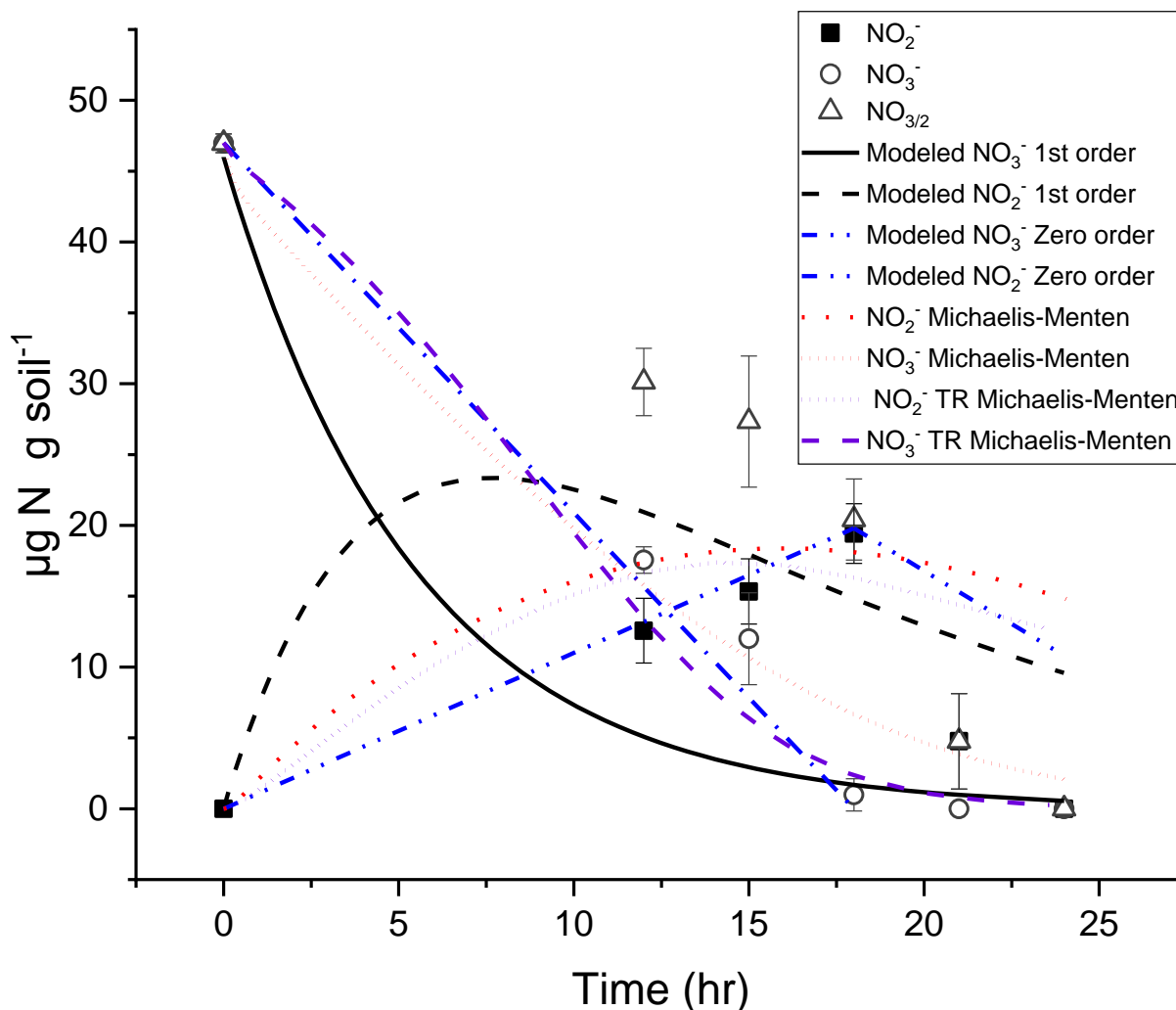


Figure 4-1 Concentrations of NO_2^- , NO_3^- , and $\text{NO}_{3/2}$, throughout the 24-hour denitrification incubations. The concentrations predicted by the first (black lines) and zero (blue lines) order, Michaelis-Menten (red lines), and Transient Coupled Michaelis-Menten (purple lines) kinetic models.

All nitrate was consumed within the 24-hour incubation period, decreasing from an initial $47.0 \mu\text{g N g soil}^{-1} \pm 0.6$ to below the limit of detection by the end of the incubation (Figure 4-1). The disappearance of nitrate occurred in a linear fashion and concentrations were below the detection limit by t_{21} . As the nitrate concentration decreased, the nitrite increased, also in a linear fashion, peaking at t_{18} at a concentration of $21 \mu\text{g N/g soil}$. Nitrate and nitrite concentrations

became nearly equal at $\sim t_{15}$ at a concentration of $\sim 15 \mu\text{g N/g soil}$. After t_{18} , nitrite decreased linearly with a slope that was steeper than the slope during the nitrite build up between t_0 and t_{18} . The total N loss rate was $2.6 \mu\text{g N g soil}^{-1} \text{ h}^{-1}$. Blank samples had a t_0 nitrate concentration of $1.17 \mu\text{g N/g soil}$, which was only 2.5% of the initial N added in non-control incubations and decreased below the IC detection limit by t_{12} . The measured $\delta^{15}\text{N}$ values of $\text{NO}_{3/2}$ increased exponentially from an initial (t_0) value of $1.3\text{‰} \pm 1.0$ to a final average $\delta^{15}\text{N}$ value of $31\text{‰} \pm 6.4$ at t_{21} , with $\delta^{15}\text{N}$ maximum of 40.4‰ (Figure 4-2). The $\delta^{15}\text{N}$ values of $\text{NO}_{3/2}$ of control samples could not be determined due to low $\text{NO}_{3/2}$ concentrations.

4.5 Discussion

The measured rate of denitrification in the saturated soils ($2.6 \mu\text{g N g soil}^{-1} \text{ h}^{-1}$) was within the range of 1.14 and $3.21 \mu\text{g N g soil}^{-1} \text{ h}^{-1}$ reported in the literature (Blackmer & Bremner, 1977; Limmer & Steele, 1982; Osaka et al., 2018; Smith et al., 1979; Smith & Tiedje, 1978; Walters & Power, 1991). The results were only compared to denitrification incubations that used soils with similar NO_3^- concentrations, C/N ratios, and moisture content because all of these factors influence the rate of denitrification (Ge et al., 2012; Glass & Sliverstein, 1998; Golterman & Chalamet, 2013; Her & Huang, 1995; Hu et al., 2011). For example, Osaka observed denitrification rates decrease from $1.15 \mu\text{g N g soil}^{-1} \text{ h}^{-1}$ at 25°C , temperatures similar to our incubations, to rates lower than $0.4 \mu\text{g N g soil}^{-1} \text{ h}^{-1}$ at 10°C .

4.5.1 Accumulation of Nitrite in Denitrification Incubations

Nitrite buildup during incubations was interesting, considering that nitrite accumulation in soil is uncommon (Burns et al., 1996; Paul & Clark, 1989). This NO_2^- buildup is important for two reasons. First, the bacteria denitrifier method reduces both NO_3^- and NO_2^- , therefore the

measured $\delta^{15}\text{N}$ is $\text{NO}_{3/2}$, not solely the residual NO_3^- . Second, isotopic fractionation can occur during the reaction pathways of NO_3^- to NO_2^- (Bryan et al., 1983; Mariotti et al., 1981) and NO_2^- to N gas (Blackmer & Bremner, 1977; Osaka et al., 2018) which is discussed below. The lack of NO_2^- build up in natural systems has been attributed to the two dominant microbial processes, nitrification and denitrification. In soils, both of these processes can remove NO_2^- faster than its production. Nitrification removes NO_2^- by re-oxidation back to NO_3^- under aerobic conditions (R_2), and denitrification removes it by reduction to NO, N_2O and N_2 under anaerobic conditions (R_3). NO_3^- in the control incubations decreased rather than increased, indicating that limited nitrite oxidation occurred in our incubations. Thus, for nitrite to accumulate in our experiments, the rate of reduction of nitrate by nitrate reductase (R_1) must be greater than reduction of nitrite by nitrite reductase (R_3) and oxidation of nitrite by nitrite oxidoreductase (R_2) (Eq. 4).



Each step of denitrification uses a different reductase, each having different optimal conditions, thus environmental conditions can play a vital role on whether denitrification goes to completion or is partial, resulting in NO_2^- accumulation. The incubations in this study had glucose added as a carbon source to act as an electron donor. Which organic compound is used as an electron donor can greatly affect the accumulation of NO_2^- generated during denitrification (Akunna et al., 2008; Her & Huang, 1995; Wilderer et al., 2000). The increase in NO_2^- is caused by the difficulty bacteria have in using glucose, which creates competition for electrons between nitrite reductase and nitrate reductase, and ultimately causes the accumulation of NO_2^- (Ge et al., 2012; Glass & Sliverstein, 1998; Her & Huang, 1995; Hu et al., 2011). For example, Ge et al., (2012), found that NO_2^- accumulation rate was 30% higher when glucose was used as an electron donor compared to acetate or methanol. Similar conclusions about nitrite accumulation and

glucose have been reached by others (Akunna et al., 2008; Her & Huang, 1995; Wilderer et al., 2000).

4.5.2 Modeling Denitrification Concentration by Zero, First, and Michealis-Menten Kinetics

In order to interpret the concentration and isotope data we explored several kinetic models of denitrification. There is considerable debate about which kinetic schemes best capture the microbial process of denitrification (Glass & Sliverstein, 1998; Kanwar et al., 1982; Mariotti et al., 1981; Osaka et al., 2018) and its corresponding kinetic isotope effect (Maggi & Riley, 2009, 2015; Vavilin & Rytov, 2015). Laboratory studies often suggest denitrification follows first order kinetics, because these models account for the exponential decrease in nitrate often seen during denitrification experiments (Blackburn et al., 1994; Corey et al., 1967; Kanwar et al., 1982; Kirda et al., 1974; Mariotti et al., 1981; Osaka et al., 2018; Starr & Parlange, 1975). However, other studies have found zero order kinetics best reproduce experimental denitrification results (Glass & Sliverstein, 1998; Kanwar et al., 1980; Reddy et al., 1978; Starr & Parlange, 1976). Furthermore, studies suggest that conditions within the soil may control whether denitrification follows first or zero order kinetics. For example, Doner et al., (1974) concluded that denitrification initially followed zero order until a low nitrate concentration was reached after which it transitioned to a first order loss. Reddy et al., (1978) found that the diffusion of nitrate in flooded soils could alter the denitrification kinetic rate order. Furthermore, Maggi & Riley, (2009) found that a Michaelis-Menten approach (discussed below) can account for a change in rate order. The Michaelis-Menten-Monod model also accounts for increases in bacteria biomass and uses enzyme dynamics, which is more representative of a bacterial process, such as denitrification. Such models have recently been used to determine the denitrification $^{15}\epsilon$ values (Maggi & Riley, 2009, 2015; Vavilin & Rytov, 2015) to better understand the mechanism

of the KIE during denitrification. But these models must also accurately reproduce NO_2^- and NO_3^- experimental concentration data. Therefore, we modeled soil denitrification and the associated isotope effects using first order, zero order, and two different Michealis-Menten kinetics models.

The nitrate and nitrite concentration data were first interpreted assuming denitrification rates followed first order kinetics. Here a simple kinetics scheme for denitrification that consisted of three ordinary differential equations was tested.

$$d\text{NO}_3^-/dt = k_1[\text{NO}_3^-]^x \quad \text{Eq. 6}$$

$$d\text{NO}_2^-/dt = k_1[\text{NO}_3^-]^x - k_2[\text{NO}_2^-]^y \quad \text{Eq. 7}$$

$$d\text{NO}_g/dt = k_2[\text{NO}_2^-]^y \quad \text{Eq. 8}$$

Where the concentration power coefficients (x and y) were set equal to 1 for first order reactions and $d\text{NO}_g/dt$ is the total loss of N via denitrification into gaseous N, which could be NO, N_2O or N_2 . The rate constant k_1 was determined by plotting the natural logarithm $[\text{NO}_3^-]$ versus time and using the slope, yielding a k_1 equal to 3.0 hr^{-1} . Nitrite was simultaneously produced and consumed at the beginning of the incubation, therefore k_2 was determined between t_{18} and t_{21} , when nitrate was below the detection limit, thus the NO_2^- production term in Eq.7 was assumed to be zero. Over this interval the slope of the natural logarithm $[\text{NO}_2^-]$ versus time yielded a k_2 of 2.9 hr^{-1} . The *Kintecus* simulation (Table 4-2) was run for a 24-hour period using an initial NO_3^- concentration of $47 \text{ } \mu\text{g N/g soil}$ (average t_0 measurement), to predict NO_3^- and NO_2^- concentrations with time (figure 4-1).

The first order model predicted $\text{NO}_{3/2}$ concentrations that are similar to the experimental data, but poorly described the trends in the NO_3^- and NO_2^- concentrations (figure 4-1). Comparing the modeled $\text{NO}_{3/2}$ concentration to the experimental data yielded a R^2 correlation

coefficient of 0.833, suggesting total N loss could be explained by first order kinetics. This is similar to others who found that the N_2O produced and NO_3^- loss by denitrification followed first order kinetics (Blackburn et al., 1994; Corey et al., 1967; Kanwar et al., 1982; Kirda et al., 1974; Mariotti et al., 1981; Osaka et al., 2018; Starr & Parlange, 1975). The modeled NO_3^- concentrations decayed exponentially, as expected for a first order loss process, but compared to the experimental data, the correlation was weaker ($R^2 = 0.69$) than that of total N loss, suggesting that NO_3^- reduction to NO_2^- was not well explained by first order kinetics. The simulated NO_2^- concentration increased parabolically during the first 7 hours, then decreased roughly linearly thereafter. Similar to the change in NO_3^- , a comparison between experimental and modeled NO_2^- concentrations were not well explained by first order kinetics ($R^2 = 0.57$).

Because of the failure of this first order model to accurately reproduce the NO_2^- and NO_3^- concentration data, we adopted the zero-order model detailed in Glass and Silverstein (1998) (figure 4-1). A zero order denitrification rate can be used when denitrification is not limited by nitrate concentration (Glass & Silverstein, 1998; Moore & Schroeder, 1971). In short, this change can be summarized from our previous model by setting the x and y exponents in equations 6 through 8 to 0. The rate for zero order loss of N will be linear therefore, the rate constants (k) were determined using the observed linear slopes of nitrate and nitrite loss. The soil NO_3^- decreased by $47 \mu\text{g N g soil}^{-1}$ between t_0 and t_{18} yielding a zero order rate constant of $2.6 \mu\text{g N g soil}^{-1} \text{ h}^{-1}$, which was used for k_1 . The nitrite loss rate constant (k_2) was determined by the change in NO_2^- concentration ($21 \mu\text{g N g soil}^{-1}$) between t_0 and t_{18} and using k_1 in Eq. 6 and solving for $k_2 = 1.5 \mu\text{g N g soil}^{-1} \text{ h}^{-1}$ (Eq. 7). Compared to the experimental data, the zero order kinetics accurately predicted $\text{NO}_{3/2}$ loss ($R^2 = 0.89$), similar to the first order model correlation. Zero order kinetics also explained NO_3^- loss better than first order kinetics, yielding a R^2 of 0.99.

Similarly, the zero order model of NO_2^- loss better reproduced the experimental data (R^2 of 0.66), signifying that the loss of NO_2^- can be better explained by zero order rather than first order. In general, the zero-order model more accurately predicts the change in $\text{NO}_{3/2}$, NO_3^- , and NO_2^- concentrations from t_0 to t_{18} relative to the first order model (figure 4-1), but under predicted the rate loss of NO_2^- and $\text{NO}_{3/2}$ between t_{18} to t_{24} .

The failure of first and zero order kinetics to predict $\text{NO}_3^-/\text{NO}_2^-$ consumption or N_2O production by denitrification has been attributed to not accounting for enzyme kinetics that would be expected during denitrification (Bowman & Focht, 1974; Maggi & Riley, 2009; Vavilin & Rytov, 2015). Michaelis-Menten kinetics are commonly used to model biochemical reactions involving enzymes, such as denitrification. To account for the role of the enzymes, Michaelis-Menten equations for both denitrification loss of nitrate and nitrite were used (Eq. 9 and 10).



Where E is the nitrate reductase and F is the nitrite reductase enzyme. NO_3^- binds with the enzyme (k_1) to form the $\text{NO}_3^- \text{-E}$ complex, that can then break apart to reform NO_3^- (k_2) or the enzyme-substrate complex can progress forward reducing $\text{NO}_3^- \text{-E}$, to NO_2^- (k_3). The complex is assumed to be at quasi equilibrium (Laidler, 1955; Maggi & Riley, 2009; Vavilin & Rytov, 2015). This same mechanism occurs between NO_2^- and its reducing enzyme F. The nitrate and nitrite concentration data were interpreted using Michaelis-Menten kinetics at quasi equilibrium. Here the kinetics scheme can be defined by Eq. 11 and 12.

$$d\text{NO}_3^-/dt = k_3[\text{E}] * ([\text{NO}_3^-]/(k_2+k_3/k_1)+[\text{NO}_3^-]) \quad \text{Eq. 11}$$

$$d\text{NO}_2^-/dt = k_3[\text{E}] * ([\text{NO}_3^-]/(k_2+k_3/k_1)+[\text{NO}_3^-]) - k_6[\text{F}] * ([\text{NO}_2^-]/(k_5+k_6/k_4)+[\text{NO}_2^-]) \quad \text{Eq. 12}$$

The initial rate constants for the Michaelis-Menten model for k_1 - k_6 where based rate constant values used for the first order model k_1 and k_2 . Rate constant values were then adjusted iteratively until the model best fit experimental concentration data.

At the limits, the Michaelis-Menten model can change its apparent reaction order, depending on the amount of enzyme relative to the substrate. At high substrate concentrations, $\text{NO}_3^- \gg (k_2+k_3/k_1)$, Eq. 11 reduces to $d\text{NO}_3^-/dt = k_3[\text{E}]$ and the reaction order is zero with respect to $[\text{NO}_3^-]$. But when substrate concentrations are low Eq.11 reduces to $d\text{NO}_3^-/dt = k_3[\text{E}] * [\text{NO}_3^-] / (k_2+k_3/k_1)$, resulting in a first order rate law with respect to $[\text{NO}_3^-]$. This could be an interpretation of our NO_3^- concentration data, where zero is occurring between t_0 to t_{15} , then switching to first order thereafter (figure 4-1). This approach has been used in several studies to improve kinetic modeling on denitrification and nutrient uptake (Betlach & Tiedje, 1981; Blum et al., 2009; Garcia-Ruiz et al., 1998; Hoering & Ford, 1960; Wanek, 2008). For example, Garcia-Ruiz et al., (1998) used a Michaelis-Menten curve to explain the denitrification rate in sediments containing added nitrate. Betlach & Tiedje, (1981) used a two term Michaelis-Menten equation to describe substrate consumption and used two one-term Michaelis-Menten equation models for the appearance of denitrified products.

The Michaelis-Menten kinetics model, like the zero-order model, accurately modeled $\text{NO}_{3/2}$, and NO_3^- concentrations (figure 4-1) but poorly modeled NO_2^- concentrations. The model predicted the linear decrease in NO_3^- from t_0 to t_{18} and $\text{NO}_{3/2}$ concentrations aligned well with experimental data, producing a R^2 correlation coefficients of 0.96 and 0.91 respectively. However, the Michaelis-Menten model poorly predicted NO_2^- concentrations, compared to experimental ($R^2 = 0.36$).

A second Michaelis-Menten model was based on that of Maggi & Riley, (2009) called the Transient Coupled Michaelis-Menten (TRMM). This approach uses Monod kinetics that accounts for bacterial growth and death in addition to enzyme kinetics (Monod, 1949). This simply consisted of adding two additional variables (Eq.13 and 14) to the Michaelis-Menten model above (Eq. 11 and 12) to account for enzyme growth and decay, Eq. 15 and 16(Maggi & Riley, 2009; Monod, 1949).

$$B(t) = E(t) + ES(t) \quad \text{Eq. 13}$$

$$dB/dt = Y(dp/dt) - \beta B \quad \text{Eq. 14}$$

$$dNO_3/dt = k_3[E] * ([NO_3^-]YB/(k_2+k_3/k_1)+[NO_3^-]) \quad \text{Eq. 15}$$

$$dNO_2/dt = k_3[E] * ([NO_3^-]YB/(k_2+k_3/k_1)+[NO_3^-]) - \beta B - k_6[F] * ([NO_2^-]YB/(k_2+k_3/k_1)+[NO_2^-]) - \beta B \quad \text{Eq. 16}$$

Where B is the total enzyme concentration, Y is a total enzyme coefficient expressing an increase in enzyme concentration due to bacteria growth and β is the bacteria death rate or removal of enzyme. In *kintecus* this was achieved by adding enzyme growth and loss to denitrification equations and coefficients adjusted iteratively to best match experimental data (table 4-2). The TRMM rate constants used were based on the k_1 - k_6 used in the Michaelis-Menten model but were adjust to best fit experimental data. The rate of enzyme growth and decay was modified two ways. First, by adjusting enzyme production and loss coefficients with the completion of each reaction and second, by the addition of k_7 which was adjusted iteratively until the model best fit experimental data. Table 4-2 lists all the reaction rate constants used for both Michaelis-Menten models.

The TRMM model, like the Michaelis-Menten model, accurately modeled NO_3^- and $NO_{3/2}$ concentrations (figure 4-1). The modeled $NO_{3/2}$ concentrations aligned well with

experimental data producing an overall R^2 correlation coefficient of 0.93. Similarly, the TRMM model very accurately predicted the linear decrease in NO_3^- from t_0 to t_{18} with an R^2 of 0.98. The TRMM model more accurately predicted the change in NO_3^- and $\text{NO}_{3/2}$ because it accounts for enzyme growth. Compared to the Michaelis-Menten model the initial rate of NO_3^- decrease is slower, however as enzyme concentrations increase so does the rate of NO_3^- loss. This adjustable rate of loss caused by changing enzyme concentrations allows this model to more accurately predict changes in NO_3^- concentrations. However, like the Michaelis-Menten and first order model the TRMM model did not predicted the change in NO_2^- concentration well. When compared to experimental data the modeled NO_2^- data had a R^2 value of 0.50.

Among the models used to predict the concentration change of NO_2^- , NO_3^- , and $\text{NO}_{3/2}$ during denitrification the zero order, Michaelis-Menten, and TRMM models all predicted the loss in $\text{NO}_{3/2}$ and NO_3^- reasonably well. All models poorly predicted the change in NO_2^- concentration, but the zero order best reproduced this change. The poor predictions of NO_2^- can be primarily attributed to the decrease in NO_2^- that occurs after t_{18} , when NO_3^- concentrations are below detection. All models failed to predict this rapid rate of NO_2^- loss (Figure 4-1). Previous studies have also shown significant discrepancy between modeled and observed NO_2^- concentrations after NO_3^- consumptions in denitrification incubations (Betlach & Tiedje, 1981; Glass & Sliverstein, 1998; Wilderer et al., 2000). A first order Rayleigh distillation is often used for modeling the change in $\delta^{15}\text{N}$ with loss of N during denitrification. Due to the zero order, Michaelis-Menten, TRMM models better models concentrations of NO_2^- , NO_3^- , and $\text{NO}_{3/2}$ than the first order, these models were also used to model the change in the $\delta^{15}\text{N}$ with fraction of N loss.

4.5.3 The $\delta^{15}\text{N}$ of $\text{NO}_{3/2}$ During Denitrification Incubations

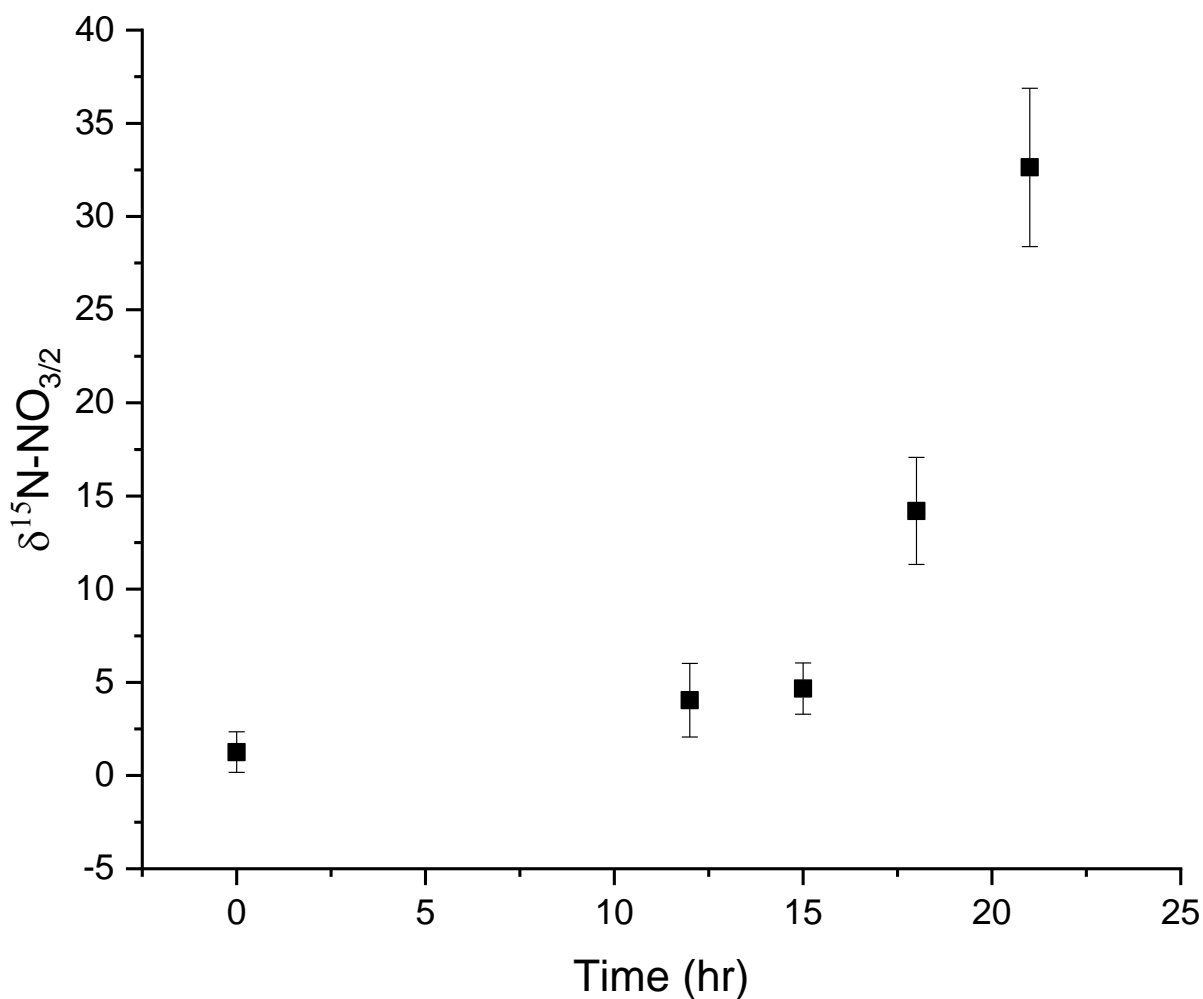


Figure 4-2. The average $\delta^{15}\text{N}$ value of $\text{NO}_{3/2}$ throughout the 24-hours denitrification incubations of all 5 incubation trials. The increase in standard deviation of samples with time is due to higher isotope and concentration standard deviations at low concentrations of $\text{NO}_{3/2}$.

The exponential increase in $\delta^{15}\text{N-NO}_{3/2}$ values over time (figure 4-2), indicates that denitrifying bacteria discriminated against ^{15}N and consistent with Rayleigh distillation. This agrees with other studies that have shown that denitrification causes an increase in $\delta^{15}\text{N}$ values of residual NO_3^- (Böttcher et al., 1990; Kendall & McDonnell, 1998; Knöller et al., 2011; Mariotti et al., 1981; Osaka et al., 2018). The $\text{NO}_{3/2}$ kinetic isotope enrichment factor, for the simultaneous reduction of both NO_3^- and NO_2^- , was determined using Eq. 3. Plotting the $\delta^{15}\text{N}$ values against

the natural logarithm of the fraction of $\text{NO}_{3/2}$ remaining resulted in a linear relationship ($R^2 > 0.92$ for all trials) that yielded $^{15}\epsilon_{\text{NO}_{3/2}} = -12.0\text{‰} \pm 2.7$ for total denitrification ($\text{NO}_{3/2}$) (Figure 4-3, Table 4-3). These values fall within the $^{15}\epsilon_{\text{NO}_3^-}$ values in studies of denitrification in agricultural soils, which range from -11.0 to -29.4‰ (Blackmer & Bremner, 1977; Mariotti et al., 1981; Osaka et al., 2018). This wide range of denitrification $^{15}\epsilon_{\text{NO}_3^-}$ values in soils has been associated with changes in temperature (Mariotti et al., 1981), denitrification rates (Mariotti et al., 1981), and differences in soil type (Blackmer & Bremner, 1977). In other environments, such as marine sediments, ocean water, and bacteria culture studies, a difference in $^{15}\epsilon_{\text{NO}_3^-}$ values has been attributed to other factors including substrate composition, concentration, and availability of electron donors, and bacteria strains (Böttcher et al., 1990; Bryan et al., 1983; Knöller et al., 2011; Macko, 1987). Studies that used clayey soils and were under intensive agricultural management, similar to our soil, had $^{15}\epsilon_{\text{NO}_3^-}$ values between -11.0 and -17.0‰ (Blackmer & Bremner, 1977; Osaka et al., 2018) which agree well with our $^{15}\epsilon_{\text{NO}_{3/2}}$ values of $-12.0\text{‰} \pm 2.7$.

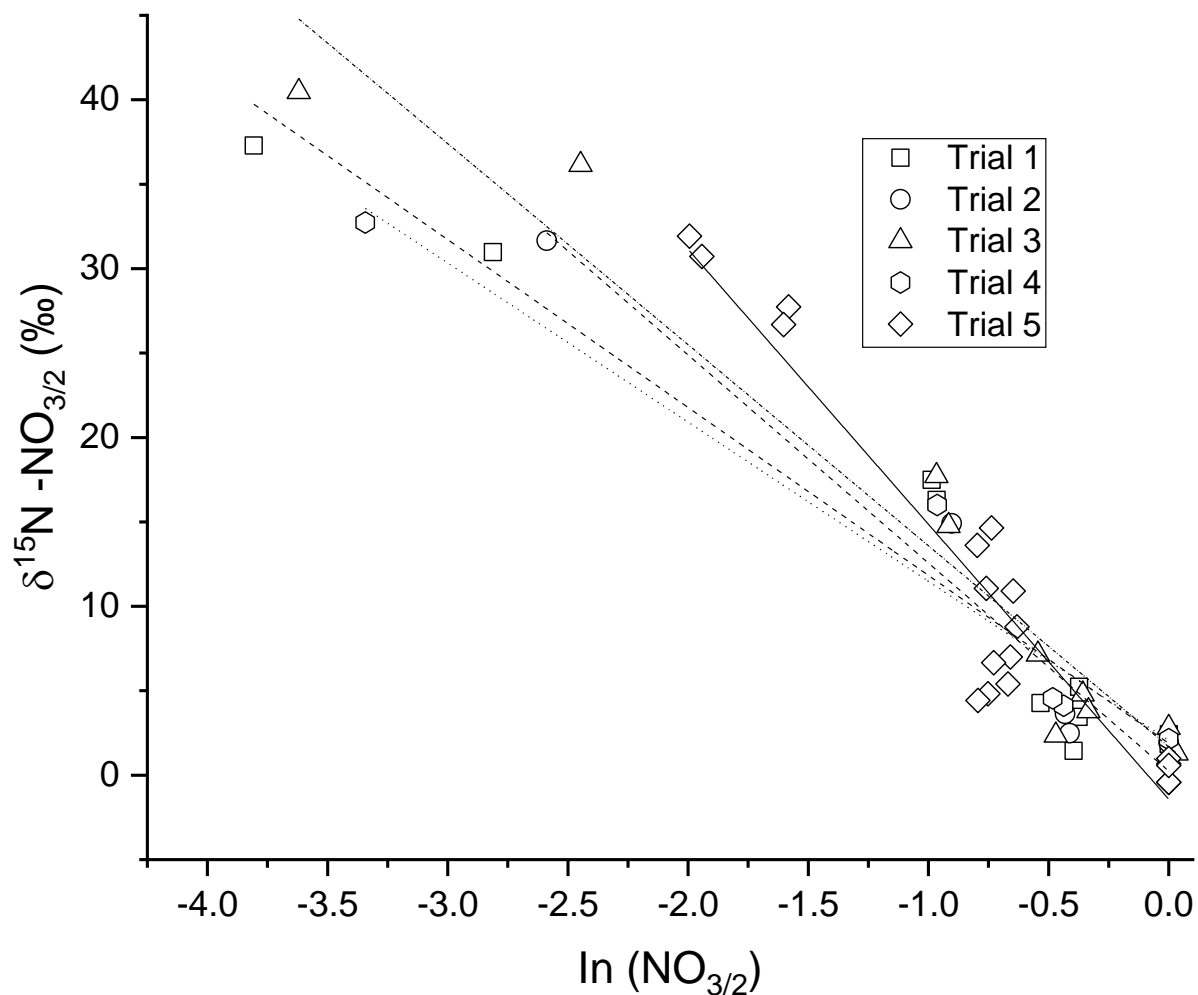


Figure 4-3 The enrichment factors were determined by plotting the measured $\delta^{15}\text{N}$ values of $\text{NO}_{3/2}$ ($\text{NO}_2^- + \text{NO}_3^-$) against the natural logarithm of the fraction of remaining $\text{NO}_{3/2}$. This was performed for each incubation trial and the slope ($^{15}\epsilon_{\text{NO}_{3/2}}$) is recorded in table 4-3.

Table 4-1: The experimental $^{15}\epsilon_{\text{NO}_{3/2}}$ and $^{15}\epsilon_{\text{NO}_2^-}$ values determined using measured $\delta^{15}\text{N}$ values with fraction of $\text{NO}_{3/2}$ remaining.

Experimental Values from Incubations					
Plot	Trial 1 (‰)	Trial 2 (‰)	Trial 3 (‰)	Trial 4 (‰)	Trial 5 (‰)
Intercept	1.89	0.24	1.68	2.05	-1.43
Slope ($^{15}\epsilon_{\text{NO}_{3/2}}$)	-9.94	-12.3	-11.9	-9.43	-16.3
($^{15}\epsilon_{\text{NO}_{3/2}}$) R^2	0.94	0.95	0.94	0.95	0.91
Slope ($^{15}\epsilon_{\text{NO}_2^-}$)	-7.8	-11.4	-9.94	-7.028	*

*The $^{15}\epsilon_{\text{NO}_2^-}$ of trail 5 could not be determined as NO_3^- was present at t_{18} .

In many studies that measure the denitrification of NO_3^- , it is often approximated that NO_3^- is directly reduced into gaseous N because there is no accumulation of NO_2^- . This is because NO_3^- reduction to NO_2^- is often assumed to be the rate limiting step of denitrification (Granger et al., 2008; Högberg, 1997). In contrast, we observe the accumulation of nitrite, which can have large implications with respect to the isotope results because isotope fractionation can occur during both NO_3^- reduction and NO_2^- reduction (Blackmer & Bremner, 1977; Granger et al., 2008). For example, Blackmer and Bremer (1978) found an $^{15}\epsilon_{\text{NO}_3/2}$ value that ranges from -14 to -23‰ but concluded that both $^{15}\epsilon_{\text{NO}_3^-}$ and $^{15}\epsilon_{\text{NO}_2^-}$ controlled the $\delta^{15}\text{N}$ value of $\text{NO}_{3/2}$ and determined that the $^{15}\epsilon_{\text{NO}_3^-}$ value ranged from -11 to -17‰. Subsequent studies have shown that the denitrification $^{15}\epsilon_{\text{NO}_2^-}$ in soils ranges from -6.9 to -19.4‰ (Bryan et al., 1983; Mariotti et al., 1981) and $^{15}\epsilon_{\text{NO}_3^-}$ from -11.8 to -29.4‰ in soils (Mariotti et al., 1981; Osaka et al., 2018). The $^{15}\epsilon_{\text{NO}_2^-}$ values in this study were directly determined using difference in $\delta^{15}\text{N}$ values of NO_2^- between t_{18} and t_{21} , $f = [\text{NO}_2^-]_{t_{18}}/[\text{NO}_2^-]_{t_{21}}$ (when only NO_2^- was present) and using Eq. 3. From this a $^{15}\epsilon_{\text{NO}_2^-}$ value of $-9.1\text{‰} \pm 1.9\text{‰}$ was determined, which falls on the lower range of $^{15}\epsilon_{\text{NO}_2^-}$ values in soils of -6.9 to -19.4‰ (Bryan et al., 1983; Mariotti et al., 1981). The $^{15}\epsilon_{\text{NO}_3}$ could not be directly determined in the same manner as $^{15}\epsilon_{\text{NO}_2^-}$ (or $^{15}\epsilon_{\text{NO}_3/2}$) because, except at t_0 , at no time was NO_3^- present without NO_2^- . In order to evaluate the value of $^{15}\epsilon_{\text{NO}_3^-}$ the experimentally determined $^{15}\epsilon_{\text{NO}_2^-}$ value was used in a first order, zero order, and two Michaelis-Menten kinetic models with isotope reactions by best fitting the models to the data.

Table 4-2 The reactions and rate constants for all denitrification isotope enrichment models. The α value represents the fractionation factor or the relative reaction rate of the heavier isotope to the lighter isotope. The reaction rate for the heavier isotope was determined by multiplying the rate of the light isotope by the α value. Though arbitrary, the initial concentrations were set to best represent the initial NO_3^- concentration in our incubations. The critical part in this model is that the $^{15}\text{N}/^{14}\text{N}$ ratios are equal to the $\delta^{15}\text{N}$ of NO_3^- added to our soils. Therefore, initial ratios of $^{15}\text{N}/^{14}\text{N}$ here were set to equal 0.5‰, the $\delta^{15}\text{N}$ value of the NaNO_3 added to soil during incubations.

	Reaction	k	α	Initial Concentration of Reactant	
First Order (1/s)					
$^{14}\text{k}_1$	$^{14}\text{NO}_3^- \rightarrow ^{14}\text{NO}_2^-$	$1.02 \cdot 10^{-4}$	1.000	$1.000 \cdot 10^{-6}$	
$^{15}\text{k}_1$	$^{15}\text{NO}_3^- \rightarrow ^{15}\text{NO}_2^-$	$1.01 \cdot 10^{-4}$	0.990	$3.069 \cdot 10^{-9}$	
$^{14}\text{k}_2$	$^{14}\text{NO}_2^- \rightarrow ^{14}\text{NO}$	$4.90 \cdot 10^{-5}$	1.000	0	
$^{15}\text{k}_2$	$^{15}\text{NO}_2^- \rightarrow ^{15}\text{NO}$	$4.85 \cdot 10^{-5}$	0.989	0	
Zero Order (molecules N/L h)					
$^{14}\text{k}_1$	$^{14}\text{NO}_3^- \rightarrow ^{14}\text{NO}_2^-$	$1.50 \cdot 10^{18}$	1.000	$2.49 \cdot 10^{19}$ Molecules	
$^{15}\text{k}_1$	$^{15}\text{NO}_3^- \rightarrow ^{15}\text{NO}_2^-$	$5.51 \cdot 10^{15}$	0.995	$9.19 \cdot 10^{16}$ Molecules	
$^{14}\text{k}_2$	$^{14}\text{NO}_2^- \rightarrow ^{14}\text{NO}$	$9.03 \cdot 10^{17}$	1.000	0	
$^{15}\text{k}_2$	$^{15}\text{NO}_2^- \rightarrow ^{15}\text{NO}$	$3.31 \cdot 10^{15}$	0.992	0	
Michaelis-Menten (1/s)					
$^{14}\text{k}_1$	$^{14}\text{NO}_3^- + \text{E} \rightarrow \text{E}^{14}\text{NO}_3^-$	$2.10 \cdot 10^{-5}$	1.000	$^{14}\text{NO}_3^- = 47$	E = 4
$^{14}\text{k}_3$	$\text{E}^{14}\text{NO}_3^- \rightarrow \text{E} + ^{14}\text{NO}_2^-$	$2.40 \cdot 10^{-4}$	1.000	0	
$^{14}\text{k}_2$	$\text{E}^{14}\text{NO}_3^- \rightarrow \text{E} + ^{14}\text{NO}_3^-$	$5.16 \cdot 10^{-5}$	1.000	0	
$^{15}\text{k}_1$	$^{15}\text{NO}_3^- + \text{E} \rightarrow \text{E}^{15}\text{NO}_3^-$	$2.06 \cdot 10^{-5}$	0.983	$^{15}\text{NO}_3^- = 0.141$	E = 4
$^{15}\text{k}_3$	$\text{E}^{15}\text{NO}_3^- \rightarrow \text{E} + ^{15}\text{NO}_2^-$	$2.36 \cdot 10^{-4}$	1.000	0	
$^{15}\text{k}_2$	$\text{E}^{15}\text{NO}_3^- \rightarrow \text{E} + ^{15}\text{NO}_3^-$	$5.16 \cdot 10^{-5}$	1.000	0	
$^{14}\text{k}_4$	$^{14}\text{NO}_2^- + \text{F} \rightarrow \text{F}^{14}\text{NO}_2^-$	$3.00 \cdot 10^{-5}$	1.000	$^{14}\text{NO}_2^- = 0$	F = 1
$^{14}\text{k}_6$	$\text{F}^{14}\text{NO}_2^- \rightarrow \text{F} + ^{14}\text{NO}$	$1.50 \cdot 10^{-3}$	1.000	0	
$^{14}\text{k}_5$	$\text{F}^{14}\text{NO}_2^- \rightarrow \text{F} + ^{14}\text{NO}_2^-$	$5.16 \cdot 10^{-6}$	1.000	0	
$^{15}\text{k}_4$	$^{15}\text{NO}_2^- + \text{F} \rightarrow \text{F}^{15}\text{NO}_2^-$	$2.97 \cdot 10^{-5}$	0.989	$^{15}\text{NO}_2^- = 0$	F = 1
$^{15}\text{k}_6$	$\text{F}^{15}\text{NO}_2^- \rightarrow \text{F} + ^{15}\text{NO}$	$1.50 \cdot 10^{-3}$	1.000	0	
$^{15}\text{k}_5$	$\text{F}^{15}\text{NO}_2^- \rightarrow \text{F} + ^{15}\text{NO}_2^-$	$5.16 \cdot 10^{-6}$	1.000	0	
TR Michaelis-Menten (1/s)					
$^{14}\text{k}_1$	$^{14}\text{NO}_3^- + \text{E} \rightarrow \text{E}^{14}\text{NO}_3^-$	$1.40 \cdot 10^{-5}$	1.000	$^{14}\text{NO}_3^- = 47$	E = 2
$^{14}\text{k}_3$	$\text{E}^{14}\text{NO}_3^- \rightarrow 1.15\text{E} + 0.22\text{F} + ^{14}\text{NO}_2^-$	$4.00 \cdot 10^{-4}$	1.000	0	
$^{14}\text{k}_2$	$\text{E}^{14}\text{NO}_3^- \rightarrow \text{E} + ^{14}\text{NO}_3^-$	$3.44 \cdot 10^{-5}$	1.000	0	
$^{15}\text{k}_1$	$^{15}\text{NO}_3^- + \text{E} \rightarrow \text{E}^{15}\text{NO}_3^-$	$1.38 \cdot 10^{-5}$	0.983	$^{15}\text{NO}_3^- = 0.141$	E = 2
$^{15}\text{k}_3$	$\text{E}^{15}\text{NO}_3^- \rightarrow \text{E} + ^{15}\text{NO}_2^-$	$4.00 \cdot 10^{-5}$	1.000	0	

Table 4-2 Continued

¹⁵ k ₂	$E^{15}\text{NO}_3^- \rightarrow 1.05E + {}^{15}\text{NO}_3^-$	$3.44 \cdot 10^{-4}$	1.000	0	
¹⁴ k ₄	${}^{14}\text{NO}_2^- + F \rightarrow F^{14}\text{NO}_2^-$	$4.00 \cdot 10^{-5}$	1.000	0	
¹⁴ k ₆	$F^{14}\text{NO}_2^- \rightarrow F + {}^{14}\text{NO}$	$2.00 \cdot 10^{-2}$	1.000	0	
¹⁴ k ₅	$F^{14}\text{NO}_2^- \rightarrow 1.05F + {}^{14}\text{NO}_2$	$2.24 \cdot 10^{-3}$	1.000	0	
¹⁵ k ₄	${}^{15}\text{NO}_2^- + F \rightarrow F^{15}\text{NO}_2^-$	$3.96 \cdot 10^{-5}$	0.989	${}^{14}\text{NO}_2^- = 0$	$F = 1.00 \cdot 10^{-5}$
¹⁵ k ₆	$F^{15}\text{NO}_2^- \rightarrow F + {}^{15}\text{NO}$	$1.98 \cdot 10^{-2}$	1.000	0	
¹⁵ k ₅	$F^{15}\text{NO}_2^- \rightarrow 1.05F + {}^{15}\text{NO}_2$	$2.24 \cdot 10^{-3}$	1.000	0	
k ₇	$\text{N}_2 \rightarrow F$	$1.40 \cdot 10^{-6}$	1.000	0	

Kinetic models for the ¹⁵N isotopologues of NO₂⁻ and NO₃⁻ were derived to mirror the ¹⁴N reactions in each of the kinetic models discussed above. The rate constant for each of these ¹⁵N reactions was determined by multiplying the rate constant of the ¹⁴N isotopologue with an α value (${}^{15}k = {}^{14}k * \alpha$), where α is the isotope fractionation factor (see Eq. 2). For all models, the ${}^{15}\epsilon_{\text{NO}_2} = -9.1\text{‰} \pm 1.9$ determined experimentally was converted to the ${}^{15}\alpha_{\text{NO}_2} = 0.991 \pm 0.002$ using Eq. 2. The initial ${}^{15}\alpha_{\text{NO}_3}$ was set to 0.986 based on the range of values from 0.989 to 0.983 determined in other studies (Blackmer & Bremner, 1977; Osaka et al., 2018). The ${}^{15}\alpha_{\text{NO}_3}$ was then adjusted iteratively by ± 0.001 until the model best fit the $\delta^{15}\text{N}$ of NO_{3/2} data. The final rate constants used in the models can be found in table 4-2.

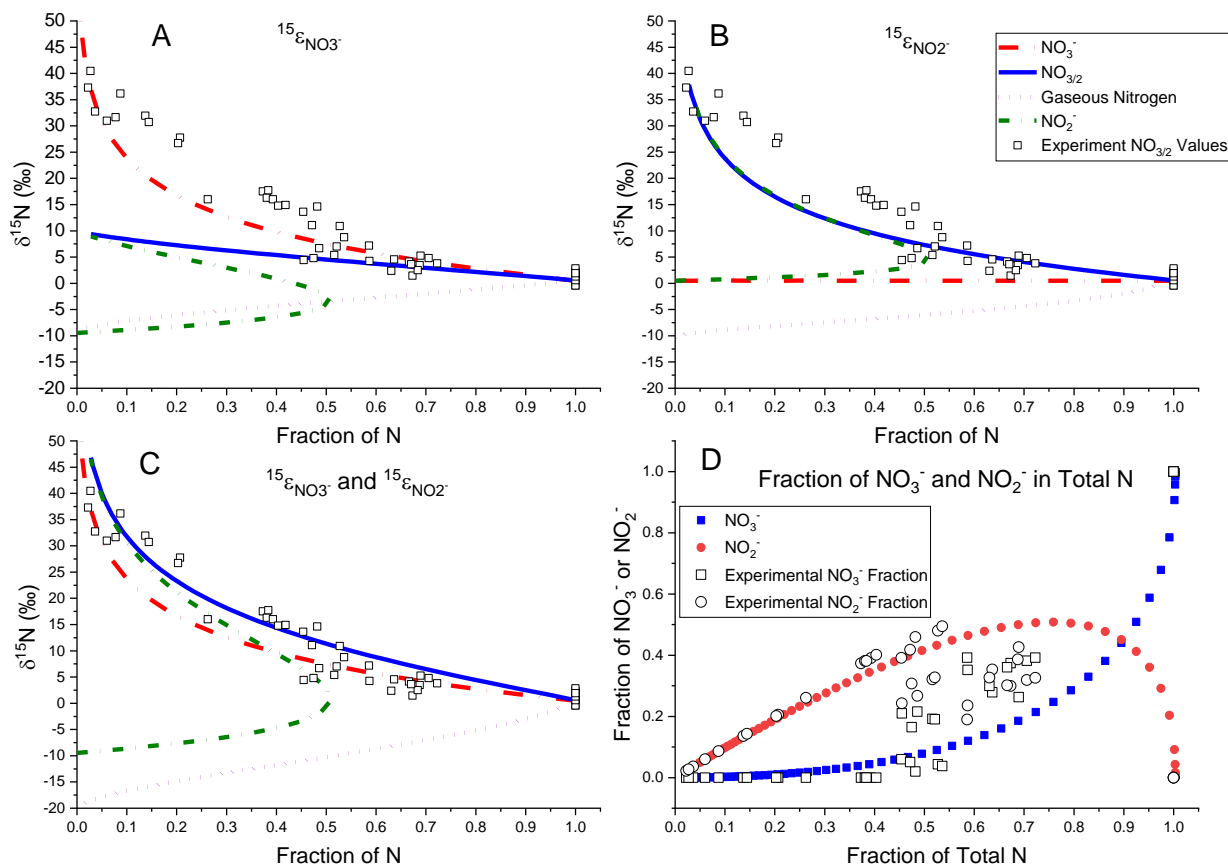


Figure 4-4 Three first order *Kintecus* models were used, one with only enrichment during NO_3^- reduction (A), one with only enrichment during NO_2^- reduction (B), and another with enrichment during the reduction of both NO_2^- and NO_3^- (C). The NO_3^- line predicts the change in $\delta^{15}\text{N}$ of NO_3^- throughout the incubations, NO_2^- predicted the change in the $\delta^{15}\text{N}$ of NO_2^- throughout incubations, the $\text{NO}_{3/2}$ is the $\delta^{15}\text{N}$ that would be measured if both NO_2^- and NO_3^- molecules are not separated during the bacteria method, and the gaseous nitrogen is the $\delta^{15}\text{N}$ of the final gaseous nitrogen products produced at the end of denitrification. The fraction of NO_3^- and NO_2^- in total N graph (D) demonstrates the importance of accurate modeling of NO_2^- and NO_3^- fractions, because data points that do not fall along this predicted fraction are poorly modeled by the first order model. Results show that if only one of the enrichments is considered predicted $\delta^{15}\text{N}$ values of $\text{NO}_{3/2}$ are too low. The model best predicted experimental results when enrichment by both NO_2^- and NO_3^- was considered. During all models after all NO_3^- and NO_2^- has been consumed the $\delta^{15}\text{N}$ of gaseous N all returned to 0.5‰ indicating conservation of all N to gaseous N.

The first order kinetic isotope model was initially run under three assumptions, the first was that only $^{15}\epsilon_{\text{NO}_3^-}$ enrichment was active (figure 4-4A), the second, assumed only $^{15}\epsilon_{\text{NO}_2^-}$ was active (figure 4-4B), and the third was assuming that both $^{15}\epsilon_{\text{NO}_2^-}$ and $^{15}\epsilon_{\text{NO}_3^-}$ were active (figure 4-4C). From these model comparisons, the relevance of the enrichment factors can easily be observed (figure 4-4). When only $^{15}\epsilon_{\text{NO}_3^-}$ was active, the predicted $\delta^{15}\text{N}$ value of $\text{NO}_{3/2}$ (blue line figure 4-4A) was low compared to the experimental values and the predicted $\delta^{15}\text{N}$ $\text{NO}_{3/2}$ values only reached 10‰ after 99% of the NO_3^- had been denitrified, four times lower than the maximum 40‰ measured in incubations. Likewise, if only $^{15}\epsilon_{\text{NO}_2^-}$ was active the predicted $\delta^{15}\text{N}$ of $\text{NO}_{3/2}$ values were much lower compared to the experimental values (figure 4-4B). Its only when both $^{15}\epsilon_{\text{NO}_3^-}$ and $^{15}\epsilon_{\text{NO}_2^-}$ are active in the model that the simulated $\text{NO}_{3/2}$ $\delta^{15}\text{N}$ values accurately match the experimental $\text{NO}_{3/2}$ $\delta^{15}\text{N}$ values ($R^2 = 0.93$) (figure 4-4C).

The first order kinetic model with isotope reactions found that a $^{15}\epsilon_{\text{NO}_3^-}$ of -10‰ and a $^{15}\epsilon_{\text{NO}_2^-}$ of -11‰ best fit our experiment $\delta^{15}\text{N}$ of $\text{NO}_{3/2}$ data (figure 4-4). The best fit $^{15}\epsilon_{\text{NO}_2^-}$ value of -11‰ is the average experimental value (9.1‰) plus the max standard deviation (1.9‰). This value falls within the reported $^{15}\epsilon_{\text{NO}_2^-}$ values of -6.9 to -19.4‰ for soil denitrification (Bryan et al., 1983; Mariotti et al., 1981). The best fit for $^{15}\epsilon_{\text{NO}_3^-}$ was determined to be -10‰ which is slightly lower than the $^{15}\epsilon_{\text{NO}_3^-}$ found in other soil denitrification experiments, which range from -11.0 and -17.0‰ (Blackmer & Bremner, 1977; Osaka et al., 2018) and much lower than the value of -29‰ determined by Marriotti (1988). This may be because Marriotti (1981) measured the N_2O product and assumed no isotopic fractionation between it and other intermediate N gases, particularly NO. In contrast Osaka et al., (2018) and Blackmer & Bremner, (1977) measured isotopes of the residual NO_3^- and NO_2^- , similar to our experiment. Additionally, our modeled $^{15}\epsilon_{\text{NO}_2^-}$ and $^{15}\epsilon_{\text{NO}_3^-}$ values match those used by, Granger & Wankel, (2016), who modeled the

$\delta^{15}\text{N}$ values of nitrate and nitrite in marine environments and found that a $^{15}\epsilon_{\text{NO}_3^-}$ of $-10\text{‰} \pm 1.3$ and a $^{15}\epsilon_{\text{NO}_2^-}$ of $-10.9\text{‰} \pm 4.4$ allowed them to best fit the observations.

This first order model best predicted the $\delta^{15}\text{N}$ values of $\text{NO}_{3/2}$ when the fraction of N remaining was between 0.45 and 0 (R^2 of 0.94). This was because at this point, the first order model predicts that the $f_{\text{remaining}}$ is around 1, i.e. $\text{NO}_{3/2} = \text{NO}_2^-$ (figure 4-4D). However, between the fraction of N remaining of 0.75 to 0.45 this model poorly predicted the experimental $\delta^{15}\text{N}$ of $\text{NO}_{3/2}$ values ($R^2 = 0.26$). This is due to the first order model incorrectly predicting the NO_2^- and NO_3^- molar ratios (figure 4-4D). The isotopic enrichment of both NO_3^- and NO_2^- reduction by denitrification proceeds in a Rayleigh distillation fashion. Figure 4-4 shows that if the modeled molar fractions of NO_2^- and NO_3^- are incorrectly predicted then the first order calculated $\delta^{15}\text{N}$ value of $\text{NO}_{3/2}$ will also be incorrect. In the first order model, between fractions of N remaining of 0.75 to 0.45, the molar fractions of NO_3^- was under predicted and the fraction of NO_2^- was over predicted. This ultimately caused the first order model to over calculate the $\delta^{15}\text{N}$ values of $\text{NO}_{3/2}$ by 5 to 10‰ and highlights the importance of accurate modeling of concentrations of NO_3^- and NO_2^- when attempting to determine the $\delta^{15}\text{N}$ of $\text{NO}_{3/2}$ of denitrification. Still despite the poor modeling of the fraction of N loss between 0.75 and 0.45, the first order model accurately predicted the experimental $\delta^{15}\text{N}$ value of $\text{NO}_{3/2}$ ($R^2 = 0.93$).

Because concentrations of NO_2^- , NO_3^- , and $\text{NO}_{3/2}$ were better modeled using zero-order kinetics, a zero-order kinetic isotope model was also tested. Here, the rate units used were molecules of N $\text{L}^{-1} \text{h}^{-1}$, different from the 1st order, Michaelis-Menten, and TRMM models units of s^{-1} . Experimental rate constants were transformed to account for differences in natural abundances (4-2). Because the rate of a zero order reaction is independent of concentration, the rate constant k (molecules of N $\text{L}^{-1} \text{h}^{-1}$) was set to $k = {}^{14}k + {}^{15}k$, where ${}^{14}k$ is the rate for ${}^{14}\text{N}$ loss

and ^{15}k is the rate of ^{15}N loss. The ratios of ^{14}k and ^{15}k were equal the isotopic abundance of the initial nitrate. By setting these rates there is no isotopic fractionation for the zero order reaction. From this it was determined ^{14}k is equal to 0.997 and ^{15}k is equal to 0.003. The ^{15}k was then adjust by ± 0.001 while the ^{14}k was kept constant. From this model is was calculated that $^{15}\epsilon_{\text{NO}_3^-} = -5\text{‰}$ and a $^{15}\epsilon_{\text{NO}_2^-} = -8\text{‰}$ (figure 4-5). The values of both $^{15}\epsilon_{\text{NO}_3^-}$ and $^{15}\epsilon_{\text{NO}_2^-}$ were lower than the values determined by the first order kinetic isotope model, which was -10‰ for $^{15}\epsilon_{\text{NO}_3^-}$ and -11‰ for $^{15}\epsilon_{\text{NO}_2^-}$. The zero order model weakly predicted the $\delta^{15}\text{N}$ of $\text{NO}_{3/2}$ generating an overall R^2 of 0.58. The poor correlation is due to this model increasing the predicted $\delta^{15}\text{N}$ of $\text{NO}_{3/2}$ exponentially after a fraction of N remaining of 0.15. If these points are removed the zero order model predicts the $\delta^{15}\text{N}$ values of $\text{NO}_{3/2}$ well, generating an R^2 of 0.87. The zero order model was better able to account for the experimental $\delta^{15}\text{N}$ values of $\text{NO}_{3/2}$ when fractions were between 0.7 and 0.45 than the first order model failed to encompass, generating an R^2 of 0.29 compared to 0.26 in the first order model. Despite a strong correlation ($R^2 = 0.91$) at fractions of total N remaining from 0 to 0.45, the zero order model under predicts $\delta^{15}\text{N}$ values of $\text{NO}_{3/2}$ from 0.42 to 0.3 by 5‰ and then over predicts the $\delta^{15}\text{N}$ values from fractions 0.3 to 0 by over 20‰ (fig 4-5).

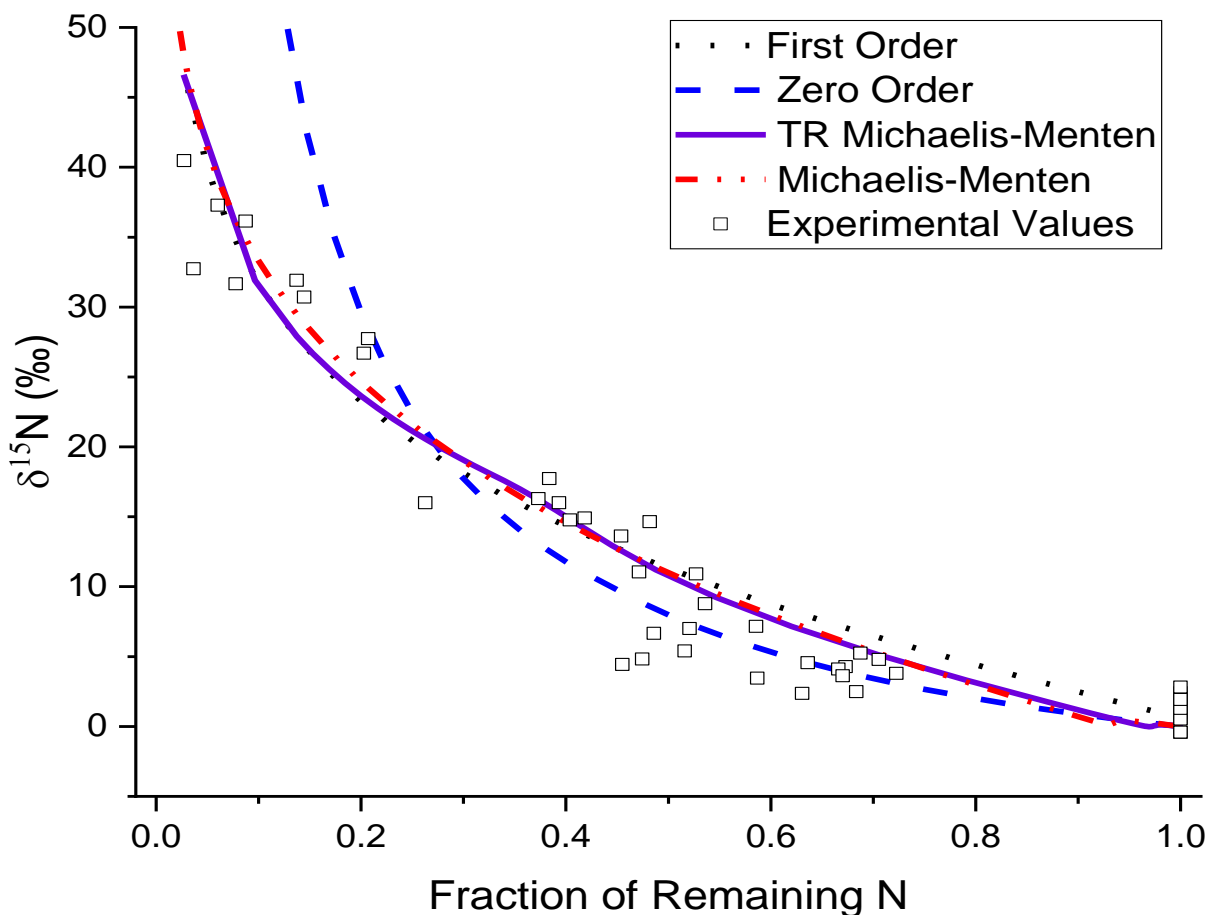


Figure 4-5 The change of $\delta^{15}\text{N}$ of NO_3/NO_2 with decreasing fraction of remaining N of experimental denitrification incubation and computational models. The fraction of remaining N consisted of both the remaining amount of NO_2^- and NO_3^- compared to the initial amount of N added. Hollow squares are experiment values and the dash, dot, and solid lines are values generated by computational models. Models consisted of zero order (blue dash line), first order (black dot line), Michaelis-Menten (red dot dash line), and Transient Coupled Michaelis-Menten (purple solid line). R^2 values can be found in figure 4-6.

The Michaelis-Menten isotope model produced an isotope enrichment trend similar to the first order model, but the enrichment values differed (Figure 4-5, Table 4-2). The Michaelis-Menten, unlike the zero and first order kinetic models had three reactions for both $^{15}\epsilon_{\text{NO}_3^-}$ (Eq. 9) and $^{15}\epsilon_{\text{NO}_2^-}$ (Eq. 10). These reactions consist of the binding of NO_3^- or NO_2^- to the enzyme (k_1 and k_4) followed by either the reverse reaction and release of NO_2^- or NO_3^- from the enzyme (k_2 and k_5) or forward reaction and the reduction of NO_3^- to NO_2^- or NO_2^- to N_2 (k_3 or k_6) by the enzyme. Each of these reactions could have a corresponding isotope enrichment factor. The enrichment values used for reaction pathway in this model can be found on table 4-2. In the Michaelis-Menten model the delay in isotope enrichment that occurs from 1.0 to 0.95 of fraction of N remaining (figure 4-5) is due to increase in intermediate products (E- NO_3^- and F- NO_2^-). This is best observed in figure 4-7 where despite the loss of NO_3^- the NO_2^- product does not begin to increase until 0.95, suggesting N is being stored in the enzyme substrate complex, whereas in the first order model NO_2^- begins to increase instantly with NO_3^- loss. While a combination of different enrichment factors on k_1 through k_6 could be used to produce the Michaelis-Menten enrichment curve in Figure 4-5, here for simplicity only one of the forward reactions for NO_3^- and NO_2^- reduction (k_1 and k_4) were assigned an enrichment factor. This allows an easier comparison of enrichment factors from our first order model as well as other literature values that used first order kinetics. Using the values in table (4-2), the Michaelis-Menten model produced a better R^2 correlation of 0.95 compared to the zero and first order kinetic models. Though only marginally better, this improved correlation can be attributed to the Michaelis-Menten model's more accurate prediction of NO_3^- and NO_2^- (figure 4-7). Like the first order model, the Michaelis-Menten model very accurately predicted the change in $\delta^{15}\text{N}$ of NO_3^-

after a fraction of N remaining below 0.45 because the fraction of NO_2^- approaches 1.0 as predicted by the Michaelis-Menten model (Figure 4-7).

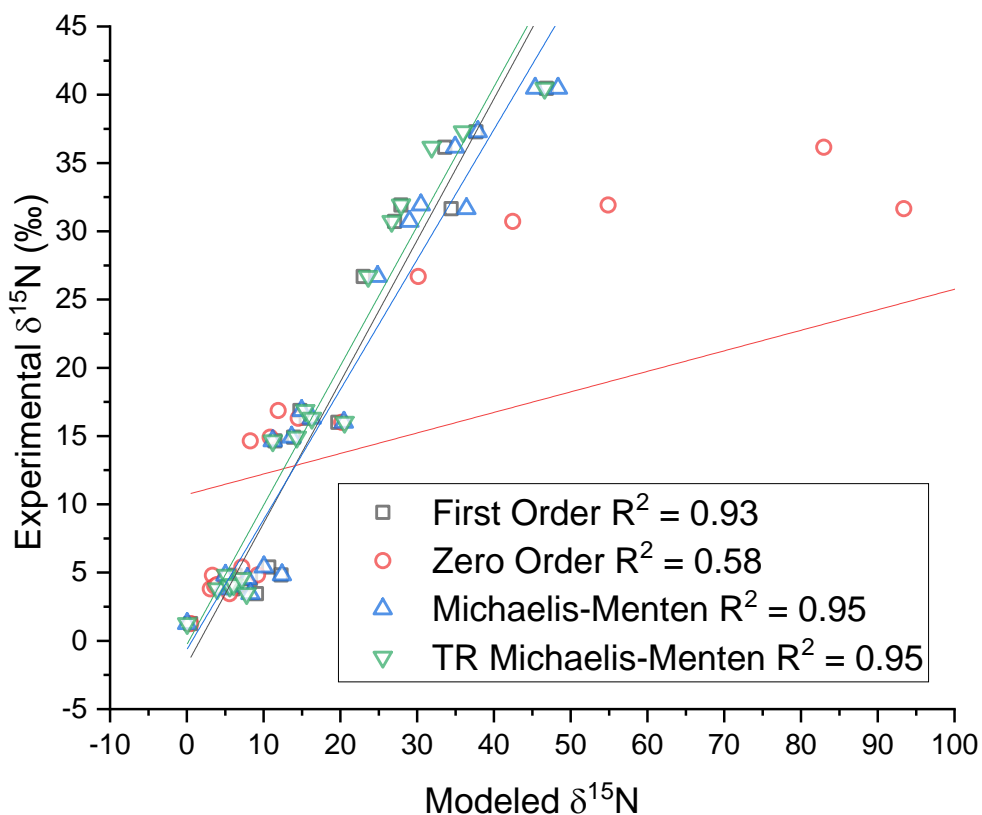


Figure 4-6 Experimental $\delta^{15}\text{N}$ of $\text{NO}_{3/2}$ versus modeled $\delta^{15}\text{N}$ of $\text{NO}_{3/2}$. Experimental values are the measured $\delta^{15}\text{N}$ values of $\text{NO}_{3/2}$ from different fractions of N remaining measured from denitrification incubations sampled at 6 different incubation times. Modeled values are the computational calculated $\delta^{15}\text{N}$ values of $\text{NO}_{3/2}$ at the measured fractions of N remaining during denitrification incubations. Models performed were zero order (red circles), first order (black squares), Michaelis-Menten (blue triangles), and Transient Coupled Michaelis-Menten (green upside down triangle).

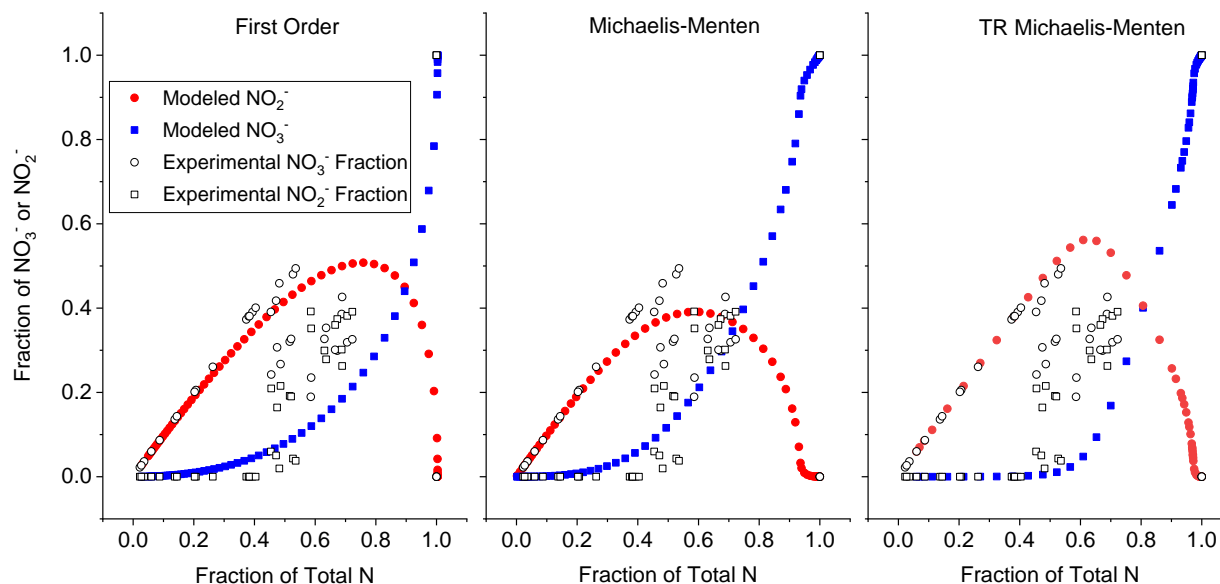


Figure 4-7 Fractions of NO₃⁻ and NO₂⁻ in fraction of total N (NO_{3/2}) remaining during denitrification of the first order, Michaelis-Menten and TRMM kinetic models compared to experimental results. The Michaelis-Menten model best predicts the fractions of NO₂⁻ and NO₃⁻ at fraction of total N remaining at 0.7. The TRMM model more accurately predicts fractions of NO₂⁻ and NO₃⁻ at fraction of total N remaining at 0.5 to 0. Proper modeling of molar fraction of NO₃⁻ and NO₂⁻ of NO_{3/2} is critical for accurate modeling of $\delta^{15}\text{N}$ values of NO_{3/2}.

The TRMM isotope model, produced a similar isotope enrichment trend compared to the Michaelis-Menten model but had slightly different calculated $\delta^{15}\text{N}$ values of NO_{3/2} despite using the same isotope enrichment values for both k_1 and k_4 . This difference is caused by both different reaction rates and the reduce initial amount of enzyme (E) of 2 moles present in the TRMM model compared to the initial amount of 4 moles in Michaelis-Menten model. Furthermore, as the TRMM model progresses more enzyme is produced, and the amount of E reaches 9 moles by the end. The less initial amount of E causes the initial isotopic increase to be observed sooner in the TRMM model, at a fraction of N remaining of 0.98 compared to 0.95 in the Michaelis-Menten model (figure 4-5 and 4-7). Like the Michaelis-Menten model, the TRMM model better predicts the change in $\delta^{15}\text{N}$ of NO_{3/2} than the first order model producing an $R^2 = 0.95$. This

improved R^2 , like the Michaelis-Menten model, can be attributed a more accurate modeling of the ratio of NO_3^- and NO_2^- in $\text{NO}_{3/2}$ (figure 4-7).

4.6 Conclusion

The findings of this chapter suggest Michaelis-Menten kinetic models for calculating changes in concentration of NO_3^- and NO_2^- are more accurate than a simple first order approach. Furthermore, the addition of Monod kinetics taking enzyme growth and death into account further improved the modeling of concentration data in the TRMM model. The reaction rates for reactions k_1 through k_6 were different between the Michaelis-Menten and TRMM model in order to best model experimental data, similar to the findings by (Maggi & Riley, 2009). The advantage of more accurate concentrations modeling resulted in more accurate modeling of $\delta^{15}\text{N}$ value of $\text{NO}_{2/3}$ during denitrification, particularly when both NO_2^- and NO_3^- were present in detectable concentrations. Only the forward reactions, k_1 for NO_3^- reduction, and k_4 for NO_2^- reduction, were given enrichments factors in the Michaelis-Menten and TRMM models and were assigned the same enrichment values in both Michaelis-Menten and TRMM models. The enrichment value of 17‰ used in $k_1 = {}^{15}\epsilon_{\text{NO}_3^-}$ of the Michaelis-Menten and TRMM model was greater than the 10‰ determined by the first order Rayleigh. However, this 17‰ value is similar to the value of 17‰ measured by Blackmer & Bremner, (1977) and just above the high values of 15‰ measured by Osaka et al., (2018). The enrichment value of 11‰ for $k_4 = {}^{15}\epsilon_{\text{NO}_2^-}$ of the Michaelis-Menten and TRMM models were within our experiment results of $9.1‰ \pm 1.9$ and matched both our first order value of 11‰ and the average values of 11‰ determined by Bryan et al., (1983). Overall the Michaelis-Menten and TRMM models not only provided more accurate modeling of concentration and $\delta^{15}\text{N}$ values but also produced enrichment values that better match the literature values. Furthermore, the inability of the zero order to accurately model

the change in $\delta^{15}\text{N}$ of $\text{NO}_{3/2}$, particularly when fractions of N remaining were low, suggest that the enzyme substrate denitrification reactions are not strictly zero order.

A full understanding of isotope kinetics can only be achieved by accounting for isotopologue speciation and fractions by transient Michaelis-Menten Monod kinetics as stated by Maggi & Riley, (2009). However, results demonstrate a first order kinetic approach is suitable for estimating the $\delta^{15}\text{N}$ of NO_3^- or NO_2^- if the fraction of NO_2^- or NO_3^- is much greater than the other. For example, Casciotti & McIlvin, (2007), were able to ignore the presence of nitrite when measuring the $^{15}\epsilon_{\text{NO}_3^-}$ of marine waters because the molar ratio of nitrate to nitrite was extremely large and any influence from $^{15}\epsilon_{\text{NO}_2^-}$ on the measure $\delta^{15}\text{N}$ was trivial. However as demonstrated in our denitrification incubation and theoretical findings, significant isotopic enrichment occurs during NO_2^- reduction and must be considered when present. Thus, if both NO_3^- and NO_2^- are present than a Michaelis-Menten kinetic approach should be taken.

Scenarios and environments where a Michaelis-Menten kinetic approach would be most applicable is in those where both NO_2^- and NO_3^- present in measurable concentrations. These include nitrification and denitrification incubations studies of cultures, marines, and soils, as well as in environments like sewage treatment centers where high NO_3^- and NO_2^- concentrations can simultaneously occur. However, results within this study show that in environments where concentration or fractions of NO_2^- or NO_3^- greatly out number the other, such as in marine and agricultural soils the $\delta^{15}\text{N}$ of $\text{NO}_{3/2}$ can be accurately model by first order kinetics.

Overall the experimental data collected and multiple models performed in this study are limited and do not represent all $^{15}\epsilon_{\text{NO}_3^-}$ and $^{15}\epsilon_{\text{NO}_2^-}$ of soils but they do help confirm that midwestern agricultural soils have enrichment factors that are just below or within range of other soils. The implications of our research demonstrate that when both NO_2^- and NO_3^- are present in

considerable concentrations they must be separated and measured individually for isotopic analysis to accurately measure the $^{15}\epsilon_{\text{NO}_2^-}$ and $^{15}\epsilon_{\text{NO}_3^-}$. However, our computational models show that even if not separated, isotopic results can be accurately modeled by Michaelis-Menten and TRMM kinetics. Future research efforts should be made to apply the Michaelis-Menten and TRMM models to environments where high NO_2^- and NO_3^- concentration are observed to test this approach as well as improve our understanding of isotope kinetics and microbial processes within these environments.

CHAPTER 5. QUANTIFICATION OF FIELD-SCALE DENITRIFICATION BY STABLE ISOTOPE ANALYSIS OF NITRATE AND WATER FROM TILE DRAIN DISCHARGE

A version of the following chapter has been submitted to Water Resources Research (WRR) for publication.

(Benjamin P. Wilkins, Dong kook Woo, Praveen Kumar, Donald A. Keefer, Laura L. Keefer, Mark Fisher, Jianghanyang Li, Timothy Hodson, Lisa Welp, Greg Michalski Quantification of Field-Scale Denitrification by Stable Isotope Analysis of Nitrate and Water from Tile Drain Discharge)

¹Department of Chemistry, Purdue University, West Lafayette, IN

²Lawrence Berkeley National Laboratory, Berkeley, CA

³Civil and Environmental Engineering, University of Illinois at Urbana-Champaign, Urbana, IL

⁴Illinois State Geological Survey, Prairie Research Institute, University of Illinois at Urbana-Champaign, Urbana, IL

⁵Illinois State Water Survey, Prairie Research Institute, University of Illinois at Urbana-Champaign, Urbana, IL

⁶Department of Earth, Atmosphere, and Planetary Sciences, Purdue University, West Lafayette, IN

Corresponding author: Benjamin Wilkins (wilkin40@purdue.edu)

Key Points:

- $\delta^{15}\text{N}$ and $\delta^{18}\text{O}$ values of nitrate in tile drainage increase from Spring to early Fall
- The amount of N denitrified over the growing season was quantified by stable isotopes of $\delta^{15}\text{N}$ of NO_3^- and found to be 7.6 kg N ha^{-1}
- Denitrification rates are highest during the Summer months

5.1 Abstract

Denitrification is a microbial process that occurs in anaerobic conditions reducing NO_3^- / NO_2^- in solution to N_2 and N_2O gases, resulting in the undesired loss of N from intensively managed landscapes (IML). Quantifying the amount of N loss by denitrification within IMLs is difficult. Current chamber, tracer, and open-path optical methods can be time-consuming and limited in spatial and temporal resolution. Here we present an isotopic approach to quantify denitrification that is able to account for spatial and temporal variability by integrating across the field scale. Tile drain discharge was collected at an IML site between May and November and was analyzed for ion concentrations (NO_3^-) and isotopic composition of H_2O ($\delta^2\text{H}$ and $\delta^{18}\text{O}$) and NO_3^- ($\delta^{15}\text{N}$ and $\delta^{18}\text{O}$). The $\delta^{15}\text{N}$ and $\delta^{18}\text{O}$ values of nitrate increased from an average of 2.8‰ and 1.4‰, respectively, in the Spring to an average greater than 6.2‰ for $\delta^{15}\text{N}$ and 6.4‰ for $\delta^{18}\text{O}$ during the remainder of the study period. This isotope increase was then paired with an isotopic Rayleigh distillation model to determine the fraction of nitrogen loss by denitrification. The fraction loss was then paired with nitrate concentration data to quantify the amount of nitrogen loss via denitrification. In total the amount of NO_3^- leached from the beginning of May to the end of October was 31 kg N ha^{-1} , while denitrification was 7.6 kg N ha^{-1} . Seasonal estimates of denitrification N loss were 2.0, 4.7, and 0.9 kg N ha^{-1} for Spring, Summer, and Fall respectively.

5.2 Introduction

Nitrogen loss from Intensively Managed Landscapes (IMLs) has been a major focus of government and environmental agencies over the last few decades. This is of particular interest in the midwestern United States where IMLs are key to food and energy security and overall quality of life. Midwestern IMLs have an estimated market value of over \$80 billion per year,

making the Midwest critically important to the United States' economy and for worldwide meat and grain production (USDA, 2009). Corn production dominates Midwestern agribusiness with over 20.3 million hectares in corn production followed by soybean at 14.2 million hectares, producing roughly 40% of the world's corn and soybean (USDA, 2009). This corn supply is also important for ethanol production, and recently mandated US biofuel regulations will only increase future demand for corn in the US (Duffield, 2015). This demand will require more nitrogen (N) fertilizer application in the coming decades (Bundy, 1985; Gericke, 1992). However, much of the N added to an IML does not end up in the crop, but is lost through leaching, volatilization, and denitrification. Among these N loss pathways, the most difficult to quantify is denitrification.

Denitrification is difficult to quantify because it depends on a variety of environmental factors, which have a high degree of spatial and temporal variability. Denitrification transforms NO_3^- into N_2 and N_2O , a greenhouse gas, under anaerobic conditions. Denitrification rates are controlled by transient soil conditions, such as temperature, moisture, pH, and oxygen availability, which are often functions of soil topography (Hofstra & Bouwman, 2005; Woo & Kumar, 2017). Variability of these environmental factors leads to a range of global denitrification estimates, from 22 to 185 Tg N yr⁻¹ (Bouwman et al., 2013; Hofstra & Bouwman, 2005; Tiedje, 1988). This large uncertainty makes understanding the global nitrogen cycle challenging (Bouwman et al., 2013; Boyer et al., 2018; Castellano et al., 2012; Galloway et al., 2004). Similarly, denitrification measured in different plots within the same field also show large variability, ranging from 8 to 51 kg N ha⁻¹ (Hofstra & Bouwman, 2005). Much of this variation may be due to different methods used to measure denitrification rates. For example, Hofstra & Bouwman (2005) compared four different methods, and found that the estimated denitrification

rates could vary by more than 50%. Some of these differences were attributed to denitrification “hot spots” and “hot moments” that depend on nitrate concentrations, water filled pore space, temperature, fertilizer application, crop type, and other factors that can fluctuate dramatically at the field scale (Harms & Grimm, 2008; Hofstra & Bouwman, 2005; Pilegaard, 2013; Weier et al., 1984). These ambiguities demonstrate that there are important challenges in determining field-scale denitrification when using methods that have limited spatial and temporal scope. Thus, an approach that can quantify denitrification by integrating the heterogeneity at the field scale would be desirable.

Natural abundance stable isotopes have been used to better understand the nitrogen cycle, including denitrification (Böhlke & Denver, 1995; Kaushal et al., 2011; Kendall & McDonnell, 1998; Nikolenko et al., 2018; Robinson, 2001; Walters et al., 2015). Changes in isotope abundances are small and are normally reported as δ (delta) in parts per thousand (‰):

$$\delta_{sample}(\text{‰}) = \frac{R_{Sample} - R_{Reference}}{R_{Reference}} \times 1000 \quad \text{Eq. 1}$$

Where the R 's refer to the ratio of the rare to common isotope in a sample or an international reference material. The international reference for nitrogen isotope $^{15}\text{N}/^{14}\text{N}$ ratios is atmospheric N_2 and for oxygen isotope $^{18}\text{O}/^{16}\text{O}$ ratios it is Vienna Standard Mean Ocean Water (VSMOW). Many nitrate sources have distinctive $\delta^{15}\text{N}$ values and can be used for source apportionment. For example, the $\delta^{15}\text{N}$ value of nitrate in manure ranges from +10‰ to +20‰ whereas synthetic N fertilizers values range from -5‰ to +5‰. Hence, it is possible to distinguish between manure and synthetic nitrate in tile discharge (Kendall & McDonnell, 1998). Stable isotope abundances can also be used to quantify kinetic processes, such as denitrification. Denitrifying bacteria's preferential use of $^{14}\text{NO}_3^-$ over the heavier $^{15}\text{NO}_3^-$ is known as a kinetic isotope effect (KIE). The KIE is defined here as $\alpha = k^{15}/k^{14}$, where k are the rate constants of the minor and major isotopes

and α is referred to as the isotope fractionation factor. Monitoring changes in $\text{NO}_3^- \delta^{15}\text{N}$ values over time has been used successfully to assess and evaluate denitrification in rivers (Böhlke et al., 2004; Chen et al., 2009; Fukada et al., 2003; Sebiló et al., 2006), oceans (Cline & Kaplan, 1975; Sigman et al., 2009) and groundwater aquifers (Aravena & Robertson, 2005; Böttcher et al., 1990; Fukada et al., 2003; Mariotti et al., 1988). However, the $\delta^{15}\text{N}$ approach for assessing denitrification can be ambiguous because changes in $\delta^{15}\text{N}$ can simply be due to mixing of nitrate from different sources that have different $\delta^{15}\text{N}$ values (Kellman, 2005; Kellman & Hillaire-Marcel, 2003; Kendall & McDonnell, 1998; Ostrom et al., 1998).

The “dual isotope approach”, the simultaneous measurement of $\text{NO}_3^- \delta^{15}\text{N}$ and $\delta^{18}\text{O}$ values, is particularly useful when two sources of nitrate have indistinguishable $\delta^{15}\text{N}$ values or to assess if denitrification has occurred. For example, nitrate in atmospheric deposition and synthetic fertilizer (Figure 5-2) have overlapping $\delta^{15}\text{N}$ values and cannot be distinguished using $\delta^{15}\text{N}$, but can be using their unique $\delta^{18}\text{O}$ values (Kendall & McDonnell, 1998). The dual isotope approach has also been shown to be useful for understanding microbial processes such as denitrification (Einsiedl et al., 2005; Knöller et al., 2011; Liu et al., 2013; Mariotti et al., 1981; Nikolenko et al., 2018). A simultaneous increase in nitrate $\delta^{15}\text{N}$ and $\delta^{18}\text{O}$ values and decrease in nitrate concentration would be difficult to attribute to source mixing (Kendall & McDonnell, 1998). However, the KIE in denitrification is selective in both isotopes of N and O, causing a simultaneous increase in both isotopes of residual NO_3^- (Granger et al., 2008; Knöller et al., 2011; Mariotti et al., 1981). While changes in $\delta^{15}\text{N}$ and $\delta^{18}\text{O}$ values have been used in systems to qualitatively assess denitrification, to our knowledge, using nitrate $\delta^{15}\text{N}$ and $\delta^{18}\text{O}$ values to *quantify* denitrification that has occurred in an agricultural landscape has never been successfully demonstrated (Kellman, 2005; Kellman & Hillaire-Marcel, 2003; Ostrom et al., 1998). Increases

in $\delta^{15}\text{N}$ and $\delta^{18}\text{O}$ values in nitrate from tile drainages have been observed, but separating the denitrification effect from nitrate source mixing has proven challenging (Kellman, 2005; Kellman & Hillaire-Marcel, 2003; Ostrom et al., 1998). Most of these studies have concluded that changing $\delta^{15}\text{N}$ and $\delta^{18}\text{O}$ values are primarily due to mixing of different nitrates sources (Keller et al., 2008; Oelmann et al., 2007; Smith & Kellman, 2011). While, others have qualitatively attributed these changes in values to denitrification, but did not quantify the amount of denitrification (Kellman, 2005; Kellman & Hillaire-Marcel, 2003; Ostrom et al., 1998). Here we show that field scale denitrification can be quantified by measuring nitrate concentration and $\delta^{15}\text{N}$ and $\delta^{18}\text{O}$ values at a high temporal resolution in drainage tile waters discharged from a corn plot in the Midwestern United States.

5.3 Materials and Methods

5.3.1 Site description

The experimental plot used in this research is part of the Intensively Managed Landscapes-Critical Zone Observatory (IML-CZO) located in Monticello, IL (40.025611, -88.661167) (Kumar et al., 2018). See supplemental information for an aerial image of the plot. The soil is a mixture of Ipava silt loam and Sable silty clay loam and the topography is nearly flat (0 to 2% slope) (USDA, 2017). The study site is a 6.75 hectares drainage area within a field that is 53 hectares. The drainage infrastructure consists of 5 individual 4-inch diameter perforate pipes, tiles, spaced ~25 meters apart and located ~1 meter below the surface. These funnel into a 4-inch diameter main drain that discharges into an open drainage ditch. An automatic sampling system (ISCO 3700, Teledyne) collected discharge samples from the main tile drain, 10 meters upstream from the drainage ditch. Tile discharge samples were collected between May 1st and October 31st, 2016. A V-notch orifice weir was used to determine the main tile discharge rate.

The field receives no irrigation water, so the only water input at the study site was precipitation. Fertilizer was added during two periods. In the Fall of 2015, 179 kg N ha⁻¹ of anhydrous ammonium was applied, and in the Spring of 2016, 50 kg N ha⁻¹ of urea ammonium nitrate (UAN) was applied. The annual crop rotation employed at this site is corn, corn, soybean, and it was the second year of corn in 2016, which was planted in early May and harvested in late September. The tillage practiced at the study site was no till.

5.3.2 Meteorological and Soil Data

Meteorological and soil data at the site were collected between 5/1/16 and 10/31/16 at the study site. This included precipitation amounts using a rain gauge (Campbell Instruments, TR525I), atmospheric temperature, and humidity using a weather station (Decagon, VP-3) and 2D wind speed using a sonic anemometer (Campbell Instruments, 05103-L) located 120 cm above ground. Tile discharge, specific conductance, water temperature and level were measured using two CTD-10 sensors (Decagon) located immediately up- and down-stream of the V-notched weir. See supplemental information for how discharge rates were determined using pressure data. The NO₃⁻ and NH₄⁺ wet deposition rates were determined using precipitation concentration data from the National Deposition Atmospheric Program (NADP) network (NADP Program Office, 2012) for Bondville, Illinois located 20 km away from the study site, multiplied by the on-site precipitation amounts. Dry deposition of nitrate (HNO₃ and NO₃⁻) and NH₄⁺ were estimated using the EPA CASTNET (USEPA, 2018) model (Bondville, IL site). Three soil probes (Decagon, 5 TE) were used to measure soil moisture and temperature at depths 5 cm, 20 cm, and 60 cm below the surface. All field data were stored on data loggers (Decagon, EM50G and Campbell Scientific, CR1000) and uploaded hourly to the University of Illinois CLOWDER open source database (<http://data.imlczo.org/clowder/>).

5.3.3 Sample Collection and Storage

Tile drain water samples were collected between 5/1/16 and 10/31/2016 during tile flow. Initially, the ISCO was programmed to collect samples every 3 hours if the tile was flowing. On 8/3/2016 the ISCO was reprogrammed to collect samples every 15 minutes during the storm events and every 12 hours during baseflow. Tile water samples were retrieved from the ISCO before the 24-bottle carousel filled. After collection, the samples were filtered using a Nalgene 0.45 μm polypropylene filter, stored in pre-washed 125mL Nalgene bottles, and frozen until analysis.

Geochemical and isotopic analysis was conducted on all tile discharge samples. All water samples were thawed at room temperature and a 5.0 mL aliquot of each sample was placed into a 15 mL centrifuge tube and diluted to 10.0 mL using high-purity Millipore water. Anion concentrations were analyzed on an Alltech Ion chromatography (IC) instrument using 3.5 mM NaHCO_3 + 1.0 mM Na_2CO_3 eluent and a conductivity detector. Standard error for this analysis was determined to be $\pm 3\%$ based on replicate standard analysis. The $\delta^{18}\text{O}$ values of tile drainage water were measured using a Los Gatos Research, Inc. (LGR) Liquid Water Isotope Analyzer (LWIA) at the Purdue Stable Isotope (PSI) Lab (Berman et al., 2013; Wassenaar et al., 2016). Frozen samples were thawed and again filtered (Nalgene 0.45 μm polypropylene filter), to remove any newly precipitated material, and 1.0 mL of sample was pipetted into a 1.5mL autosampler vial and capped. Ten injections of each sample were introduced to the LWIA. The first four are ignored, and the last six values are averaged. Three in-house water standards were used for calibration, and these were assigned values using USGS45, USGS46, and USGS47. The standard deviation for $\delta^{18}\text{O}\text{-H}_2\text{O}$ was $\pm 0.40\text{‰}$. The $\delta^{15}\text{N}$ and $\delta^{18}\text{O}$ values of NO_3^- were measured at the PSI lab using the bacteria denitrifying method (Casciotti et al., 2002). This method required approximately 500 nmol of NO_3^- injected into a 12-mL airtight He-flushed vial, containing 1 mL of denitrifying bacteria (*P. aureofaciens*) and allowed to sit for 8 hours, at

room temperature (~ 20 °C), converting the NO_3^- into N_2O . The N_2O in the vial's headspace was extracted, concentrated, and purified using a custom-built automated extraction and gas chromatography system and then introduced into a Thermo Delta V continuous-flow isotope ratio mass spectrometer (CF-IRMS). Isotopic compositions were calibrated using 5 internal standards that were compared to NIST isotope reference nitrate USGS34 and USGS35 (Böhlke et al., 2003; Michalski et al., 2002). The standard deviations of our analysis are $\pm 0.50\text{‰}$ for $\delta^{15}\text{N}$ and $\pm 0.70\text{‰}$ for $\delta^{18}\text{O}$.

In the winter of 2018, a soil core was collected and analyzed. The core was collected using two soil core samplers (length = 0 to 25cm and 25 to 50cm, outer diameter = 2.54 cm), at two different depths, 0 to 25 cm and 25 to 50 cm from the surface. The intact soils were dried at 50 °C in a drying oven for 5 days. After drying, the 25 cm cores were separated into 10-cm increments. The bulk soil $\delta^{15}\text{N}$, total carbon (%) and total nitrogen (%) were determined using a Sercon 20-22 isotope ratio mass spectrometer (IRMS) paired to a Sercon EA-CN 1 elemental analyzer and mass-corrected using three in-house soil standards which were calibrated relative to three reference materials from National Institute of Standards and Technology (NIST) (Apple Leaves 1515, USGS 40, Cystine 143d).

5.4 Results

5.4.1 Hydrology and Chemistry of Discharge Overview

Increases in tile discharge generally corresponded with rain events (Fig 5-1A and B). However, increases in tile flow were not always proportional to the amount of precipitation, due to antecedent soil moisture conditions. For example, on 8/12 2.5 mm of precipitation produced a maximum flow rate of $0.010 \text{ m}^3/\text{s}$, while on 7/28 15 mm of precipitation, 6 times the amount on 8/12, produced the same flow rate. Over the entire sampling period there were three periods

when no tile flow was recorded. Between 5/28 to 6/3, no discharge data was recorded due to transducer malfunction, but the chemographs suggested that flow was occurring. During 6/15 to 7/28, and 8/3 to 8/15 no tile flow occurred despite significant rainfall.

During the entire study period, anion concentrations and isotope values in tile discharge varied considerably. Nitrate concentrations ($n=506$, where n is the total number of measurements made) ranged from 3 mg N/L to 32 mg N/L, with an average value of 18 ± 8 mg N/L. There was a clear reduction in the NO_3^- concentrations between Spring and Fall, decreasing by ~ 21 mg N/L (Figure 5-1B). Both $\delta^{15}\text{N}$ and $\delta^{18}\text{O}$ values ($n=309$) of NO_3^- had lower values in early Spring and transitioned to higher values over the growing season and into the Fall (Fig 5-2). Overall $\delta^{15}\text{N}$ values average $5.2\text{‰} \pm 2.3$ with a minimum of 0.1‰ and maximum of 13.5‰ . While $\delta^{18}\text{O}-\text{NO}_3^-$ values average $4.7\text{‰} \pm 2.7$ with a minimum of -1.1‰ and a maximum of 11.4‰ . The concentration and isotope data show that there are four distinctive periods throughout the study (Fig 5-1A and B), that we will define as Spring (5/1 to 6/15), Transition (6/16 to 7/28), Summer (7/28 to 9/15), and Fall (9/15 to 10/31).

The concentrations of nitrate ($n=269$) during the Spring were generally steady, with some variations. Nitrate concentrations averaged 25 ± 4 mg N/L with a maximum of 32 mg N/L and minimum of 5 mg N/L (Fig 5-1B). The $\delta^{15}\text{N}$ and $\delta^{18}\text{O}$ values of nitrate ($n=110$) during the Spring period were generally steady with minor variations (Fig 5-1A). $\delta^{15}\text{N}$ values averaged $2.8\text{‰} \pm 1.2$ with a maximum of 6.0‰ and minimum of 0.10‰ . $\delta^{18}\text{O}$ values averaged $1.4\text{‰} \pm 0.8$ with a maximum of 3.8‰ and minimum of -1.13‰ . The correlation between $\delta^{15}\text{N}$ and $\delta^{18}\text{O}$ was weak ($R^2=0.27$) with a slope of -0.40 .

Tile flow was absent during the Transition period, despite the occurrence of 12 precipitation events (Fig 5-1A and B). These events produced a total of 186 mm of precipitation

with an average of $15.5\text{mm} \pm 13.6$. The largest of these events was on 7/24 when 46.5 mm of rainfall occurred. The absence of discharge recorded by the weir's pressure transducers, the lack of samples collected by the ISCO autosampler, and no observed tile discharge during field visits during some of these events suggest this was not instrument malfunction but simply the absence of tile flow during this period. This type of behavior is known to occur in IML systems during months of peak crop growth when evapotranspiration rates are very high (David et al., 1997; Gentry et al., 1998; Keller et al., 2008; Kladvik et al., 1991). Evapotranspiration and plant transpiration rate in corn fields is greatest 70 to 100 days after planting, at the end of the vegetative stage and the beginning of the reproductive stage, with transpiration rates up to 8.1-10.1 mm of water per day (Kimball et al., 2016; Licht & Archontoulis, 2017; R. L. B. Nielsen, 2000). In the Midwestern US, this period occurs between the end of June to the beginning of August, which corresponds to the period of no flow at our IML site (Borah et al., 2003; Gentry et al., 2009; Lavaire et al., 2017).

The nitrate concentration and isotope data show a dramatic shift in the Summer and Fall periods relative to the Spring. The concentrations of nitrate ($n=152$) during the Summer period were not steady and had large variations compared to Spring. Nitrate concentrations in summer were much lower compared to Spring, averaging $10\text{ mg N/L} \pm 3$ with a maximum of 16 mg N/L and minimum of 2 mg N/L (Fig 5-1B). The $\delta^{15}\text{N}$ and $\delta^{18}\text{O}$ values ($n=138$) during the Summer were not steady and had large variations compared to the Spring (Fig 5-1A). Summer nitrate $\delta^{15}\text{N}$ values were higher relative to Spring, averaging $6.7\text{‰} \pm 1.4$ with a maximum of 13.5‰ and minimum of 4.4‰ (Fig 5-1A). Summer nitrate $\delta^{18}\text{O}$ values were also high relative to the Spring, averaging $6.4\text{‰} \pm 1.4$ with a maximum of 11.4‰ and minimum of 3.7‰ . There were three large discharge events in the Summer period and the evolution of $\delta^{15}\text{N}$ and $\delta^{18}\text{O}$ values during each of

these events are unique. This behavior is discussed later. The correlation of $\delta^{15}\text{N}$ and $\delta^{18}\text{O}$ was found to be weak with an $R^2=0.31$, and a positive slope of 0.55. The nitrate concentrations ($n=85$) during the Fall period, similar to the Spring, had little variation (Fig 5-1B), averaged 11 ± 1 mg N/L, less than half the average concentration observed during the Spring, and had a maximum of 14 mg N/L and minimum of 5 mg N/L. During this period tile discharge occurs continuously with only minor increases in discharge corresponding to precipitation. The $\delta^{15}\text{N}$ and $\delta^{18}\text{O}$ values ($n=61$) during the Fall, like the Spring, were generally steady (Fig 5-1A). $\delta^{15}\text{N}$ values averaged $6.2\% \pm 1.08$ with a maximum of 9.1% and minimum of 4.3%. $\delta^{18}\text{O}$ values averaged $6.8\% \pm 1.0$ with a maximum of 8.7% and minimum of 4.2%. Similar to the Summer period, the Fall $\delta^{15}\text{N}$ and $\delta^{18}\text{O}$ values were higher than Spring values. Unlike Spring and Summer there was no correlation between NO_3^- $\delta^{15}\text{N}$ and $\delta^{18}\text{O}$ values ($R^2=0.009$). The most noticeable feature in the Fall is the increased shift of $\delta^{15}\text{N}$ and $\delta^{18}\text{O}$ values relative to the Spring. A dual isotope plot (Fig. 5-2) of tile nitrate shows that the Spring $\delta^{15}\text{N}$ and $\delta^{18}\text{O}$ values group differently compared to the Summer and Fall periods. The $\delta^{15}\text{N}$ and $\delta^{18}\text{O}$ values increased from an average of 2.8% and 1.4%, respectively, in the Spring to an average greater than 6.2% for $\delta^{15}\text{N}$ and 6.4% for $\delta^{18}\text{O}$ during the remainder of the study period. The slope of $\delta^{15}\text{N}$ vs. $\delta^{18}\text{O}$ values in all our samples is 0.82 (Fig 5-2) a slope that we hypothesize represents a denitrification line.

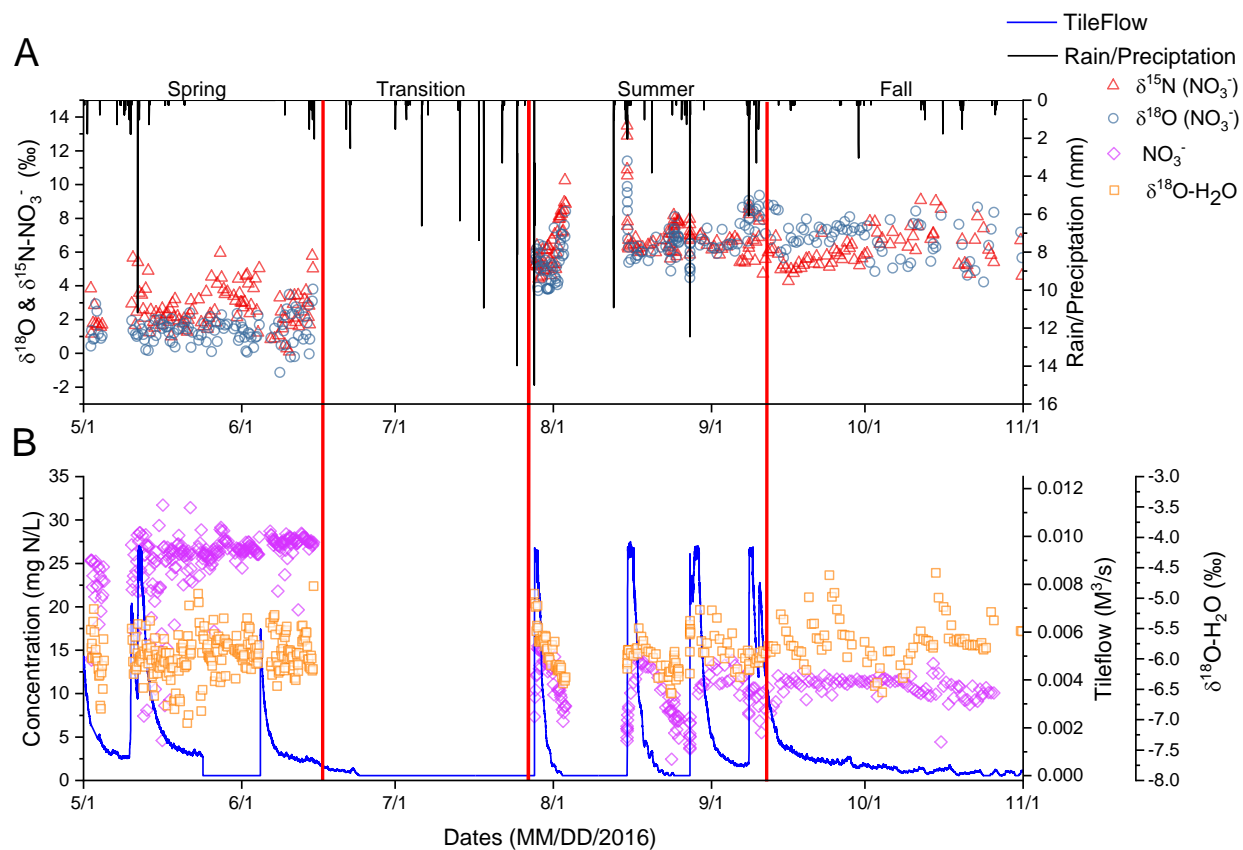


Figure 5-1 (A) $\delta^{15}\text{N}-\text{NO}_3^-$ (red triangles) and $\delta^{18}\text{O}-\text{NO}_3^-$ values (blue circles) and precipitations amounts (black lines). (B) nitrate concentrations as N (purple diamonds), $\delta^{18}\text{O}-\text{H}_2\text{O}$ (orange squares), and tile flow (blue lines) throughout the year. Red lines separate each of the four periods (Spring, Transition, Summer, and Fall).

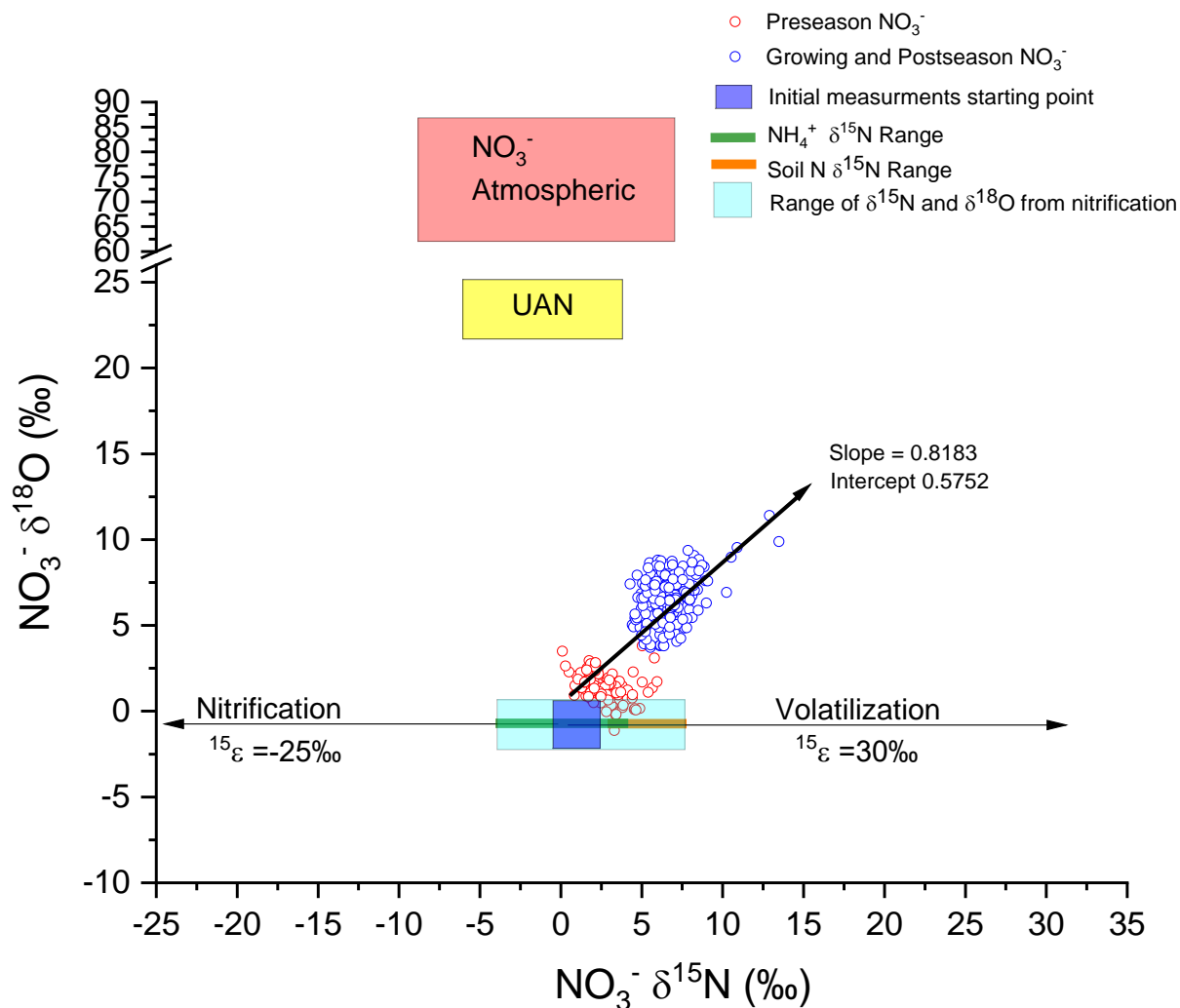


Figure 5-2 A dual isotope plot of tile drain nitrate and all potential sources of nitrogen within the experimental plot. Sources of nitrogen added directly to the land as NO_3^- include atmospheric deposition (red box) and UAN (yellow box). The green and orange line are sources of reduced N added to the system that might be nitrified. The light blue box is the $\text{NO}_3^- \delta^{18}\text{O}$ values of nitrification assuming all oxygen in NO_3^- was derived from H_2O and the theorized $\delta^{15}\text{N}$ isotope values of nitrate formed by nitrification of urea, NH_4/NH_3 and soil N. The red hollow circles are tile drain $\text{NO}_3^- \delta^{15}\text{N}$ and $\delta^{18}\text{O}$ values in the Spring and the blue hollow circles are those in Summer and Fall. The solid blue square is the estimated starting value of $\delta^{15}\text{N}$ and $\delta^{18}\text{O}$ determined by mass balance of all inputs (see discussion). The solid black line with a slope of 0.82 is the increase of $\text{NO}_3^- \delta^{15}\text{N}$ relative to $\delta^{18}\text{O}$. The arrows labeled nitrification and volatilization are the potential enrichment in $\delta^{15}\text{N}$ that can occur by those processes.

5.5 Discussion

5.5.1 Qualitative Evidence of Denitrification

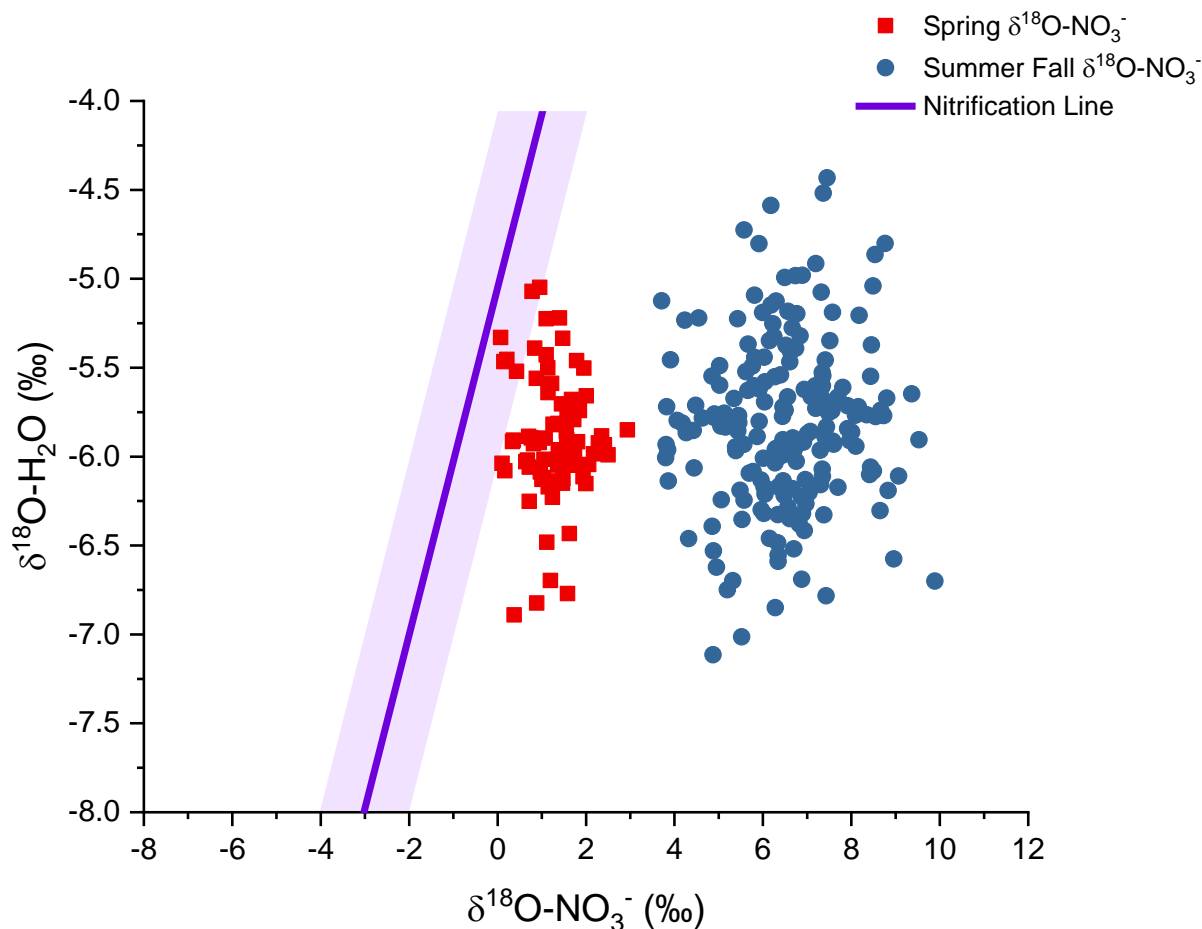


Figure 5-3 The $\delta^{18}\text{O-H}_2\text{O}$ vs. $\delta^{18}\text{O-NO}_3^-$ in tile discharge. Nitrification using tile water as the oxidant source would produce $\delta^{18}\text{O-NO}_3^-$ values that follow the predicted nitrification line. Changes in tile $\delta^{18}\text{O-H}_2\text{O}$ are caused by a combination of variations in precipitation $\delta^{18}\text{O}$ values and ^{18}O enrichment caused by evaporation. A shift to the right increases $\delta^{18}\text{O-NO}_3^-$, with no change in H_2O $\delta^{18}\text{O}$, suggesting denitrification.

A noticeable feature in the tile drain nitrate $\delta^{15}\text{N}$ and $\delta^{18}\text{O}$ plot (Figure 5-2) are the two distinct clusters of values, one in the Spring and the other Summer/Fall that we are interpreting as an isotopic shift caused by field scale denitrification over the growing season. The Summer and Fall nitrate have $\delta^{15}\text{N}$ and $\delta^{18}\text{O}$ values that are 4‰ and 6‰ higher, respectively, than nitrate in the Spring. Simultaneous increases in nitrate $\delta^{15}\text{N}$ and $\delta^{18}\text{O}$ values in IMLs have been attributed to both denitrification and source mixing (Keller et al., 2008; Kelley et al., 2013;

Kellman, 2005; Kellman & Hillaire-Marcel, 2003; Ostrom et al., 1998). In this discussion, we will use isotope and concentration mass balance to show that nitrate source mixing cannot account for this observed simultaneous shift. Further, we demonstrate that using known isotope systematics that the initial nitrate $\delta^{15}\text{N}$ and $\delta^{18}\text{O}$ values can be reasonably constrained and the observed $\delta^{15}\text{N}$ can be used to quantify the amount of denitrification that occurred over the growing season.

The first evidence that the two $\delta^{15}\text{N}$ and $\delta^{18}\text{O}$ clusters were caused by a denitrification isotope effect is the relationship between $\delta^{18}\text{O}$ values of tile water and nitrate (Figure 5-3). Roughly 95% of nitrate within the field was produced from nitrification (see discussion below), and therefore nitrification controls the initial $\delta^{18}\text{O}$ value of nitrate in the IML. Thus, knowing the $\delta^{18}\text{O}$ of NO_3^- produced by nitrification is key for interpreting the tile NO_3^- $\delta^{18}\text{O}$ data. The nitrification $\delta^{18}\text{O}$ value will depend, in part, on the sources of oxygen used to oxidize NH_4^+ to NO_3^- during nitrification, which is from H_2O and O_2 . The fractions (f) of oxygen incorporated into NO_3^- during nitrification are commonly reported as $f_{\text{H}_2\text{O}} = 0.67$ and $f_{\text{O}_2} = 0.33$ (Aleem et al., 1965; Buchwald et al., 2012; Hollocher, 1984; Kumar et al., 1983; Yoshinari & Wahlen, 1985). However, this does not strictly hold, and $f_{\text{H}_2\text{O}}$ values ranging from 0.66 to 1.00 have also been inferred (Buchwald et al., 2012; Kool et al., 2011; Snider et al., 2010). The variability in $f_{\text{H}_2\text{O}}$ and f_{O_2} values in field studies is likely a consequence of microbial diversity and complexity within soils as opposed to conditions in single-culture lab experiments (Buchwald & Casciotti, 2010; Casciotti et al., 2010; Kool, Wrage, et al., 2011). The nitrification $\delta^{18}\text{O}$ value for this IML was determined experimentally (see supplemental information). Briefly, the experiment consisted of a series of incubations using an aerated IML soil amended with NH_4^+ to promote nitrification and using water with different $\delta^{18}\text{O}$ values. The nitrate concentration and its $\delta^{15}\text{N}$ and $\delta^{18}\text{O}$ were

monitored over the course of the experiment. The final $\delta^{18}\text{O-NO}_3^-$ was compared to the $\delta^{18}\text{O-H}_2\text{O}$ and $\delta^{18}\text{O-O}_2$ to determine the ratios of each source. The results showed that the $\delta^{18}\text{O-NO}_3^-$ produced from nitrification in this IML's soil were proportional (1:1) to the value of $\delta^{18}\text{O-H}_2\text{O}$ with an offset of +5‰. The 5‰ offset is likely a consequence of kinetic or equilibrium fractionation factors associated with the stepwise oxidation process (i.e., Granger & Wankel, 2016). These results are consistent with observation made by Snider et al., 2010, who measured $f_{\text{H}_2\text{O}}$ of 0.84 to 0.96 in NO_3^- from agricultural soils with offsets of +2.77 to +7.73‰. Therefore, the $\delta^{18}\text{O-NO}_3^-$ from nitrification within our IML was estimated by Eq. 2, which is shown in Figure 5-3 by a solid 1:1 line with an off set of 5‰.

$$\delta^{18}\text{O}_{\text{NO}_3} = \delta^{18}\text{O-H}_2\text{O} + 5\text{‰} \quad \text{Eq. 2}$$

In this equation, $\delta^{18}\text{O-H}_2\text{O}$ is the $\delta^{18}\text{O}$ value of the water used by nitrifying bacteria in the soil, which we have assumed is the water in the tile discharge.

The tile discharge water $\delta^{18}\text{O}$ values ranged from -7.3 to -4.5‰ during the study period (Figure 5-1B). Thus, the predicted $\delta^{18}\text{O-NO}_3^-$ values (from Eq. 2) should range from -2.3 to -1.5‰. This “nitrification only” trend is not observed in the data (Figure 5-3). The variability in the $\delta^{18}\text{O}$ values of soil H_2O is driven by seasonal and event-based variation in the $\delta^{18}\text{O}$ of precipitation, enrichment of soil water $\delta^{18}\text{O}$ by evaporation, or a combination of the two (Gat, 1998; Hsieh et al., 1998). However, since nitrification is using soil water (assumed to be identical to tile water), nitrification should still obey Eq. 2, since the tile water reflects both the input water $\delta^{18}\text{O}$ value and any evaporation effect. Any data points to the right of the predicted nitrification line will have elevated $\delta^{18}\text{O-NO}_3^-$ values with respect to nitrification. We hypothesize that this shift could be due to either the additions of NO_3^- from sources with elevated $\delta^{18}\text{O}$ values, i.e. atmospheric deposition and UAN, or by an $\delta^{18}\text{O}$ enrichment process affecting

soil NO_3^- .

To test the hypothesis that the shift of nitrate $\delta^{18}\text{O}$ values to the right of the nitrification prediction line (Figure 5-3) was caused by the addition of NO_3^- from atmospheric deposition or UAN, we used a simple three-component isotope mixing model (Eq. 3).

$$\delta^{18}\text{NO}_3^-(\text{O}) = f_{\text{atm}}\delta^{18}\text{O}_{\text{atm}} + f_{\text{UAN}}\delta^{18}\text{O}_{\text{UAN}} + f_{\text{N}}\delta^{18}\text{O}_{\text{N}} \quad \text{Eq. 3}$$

Where f_{atm} , f_{UAN} , and f_{N} are the mole fractions of NO_3^- from atmospheric deposition, UAN, and nitrification and the $\delta^{18}\text{O}$'s are the respective values of those sources. Atmospheric NO_3^- may have a significant effect on the overall $\delta^{18}\text{O}$ - NO_3^- value, even when it's a small fraction of total nitrate, because of its uniquely high $\delta^{18}\text{O}$ value. Atmospheric NO_3^- has $\delta^{18}\text{O}$ values ranging from 60 to 100‰, due to its formation by ozone oxidation of NO_x (Hastings et al., 2003; Michalski et al., 2002, 2012). Likewise, NO_3^- in UAN has a relatively high $\delta^{18}\text{O}$ value that could potentially impact the $\delta^{18}\text{O}$ value of tile NO_3^- even at small molar fractions. Nitrate contained in UAN has a $\delta^{18}\text{O}$ value of $23 \pm 3\%$ (Michalski et al., 2015), a result of oxidizing NH_3 to NO_3^- using atmospheric O_2 , which has a $\delta^{18}\text{O}$ value of 23.5‰ (Dole et al., 1954). Taking the upper bounds of $\delta^{18}\text{O}$ for these two NO_3^- sources and using Eq. 2, Eq. 3 becomes

$$\delta^{18}\text{NO}_3^-(\text{O}) = f_{\text{atm}}(100\%) + f_{\text{UAN}}(26\%) + f_{\text{N}}(\delta^{18}\text{O}_{\text{H}_2\text{O}} + 5\%) \quad \text{Eq. 4}$$

The total amount of NO_3^- added to the IML plot is needed in order to calculate the f values in Eq. 4, which was determined by known N inputs and outputs. The atmospheric NO_3^- inputs were calculated using weekly precipitation volumes multiplied by the nitrate concentrations (NAPD) to yield a weekly wet NO_3^- deposition rate of $0.03 \pm 0.03 \text{ kg N ha}^{-1}$ for a total of $0.85 \text{ kg N ha}^{-1}$ over the study period. The dry deposition of nitrate (HNO_3 and NO_3^-) averaged $0.02 \pm 0.01 \text{ kg N-HNO}_3 \text{ ha}^{-1} \text{ week}^{-1}$ and $0.001 \pm 0.001 \text{ kg N-NO}_3^- \text{ ha}^{-1}$ during the sampling period, for a total of $0.63 \text{ kg N ha}^{-1}$. UAN was added in May of 2016 as one a time application to the field of 117

liters ha⁻¹ of 32% UAN (32% wt. of solution as N). The density of 32% UAN is 1.33kg/L yielding 0.43kg/L of total N of which 25% is NO₃⁻, for a one time addition of UAN NO₃⁻ of 12.4 kg N ha⁻¹. The NO₃⁻ added by nitrification was estimated using nitrate concentration and tile flows, assuming nitrification greatly exceeded atmospheric and UAN NO₃⁻ and assuming a steady state over a short time frame (Eq. 5).

$$\frac{\Delta NO_3^- \text{ nitrification}}{\Delta t} = \text{Production} - \text{Loss} = 0 = \text{Nitrification} - \text{Leaching} -$$

Denitrification - Plant Uptake

Eq. 5

Also, between 5/3 to 6/12 changes in nitrate concentrations with time were small regardless of the tile discharge rate (Figure 5-1), thus the steady state condition ($dNO_3^-/dt = 0$) would appear valid during this interval. By setting denitrification and plant uptake loss to 0, equation 5 reduces to nitrification rate = leaching rate. These assumptions would predict the minimum nitrification rate. A total of 16.7 kg N ha⁻¹ (as NO₃⁻) were leached over a 28-day period, resulting in a minimum nitrification rate of 3.5 kg N ha⁻¹ week⁻¹, or 14 kg N ha⁻¹ of nitrate during the May-June period, and 98 kg N (NO₃⁻) ha⁻¹ for the entire study period. However, temperatures in early may were between 10 - 15°C, with temperatures increase to 25-30°C by the end of June, which can more than double the rate of nitrification (Sabey et al., 1956). Thus, the amount of N nitrification is likely closer to the amount of reduced N added (216 kg N (NH₃)) (Chalk et al., 1975). Therefore, each hectare will have nearly 230 kg N as NO₃⁻ (216 kg N + 14 kg NO₃⁻). Using this total amount of NO₃⁻, the f_{atm} , f_{UAN} , and f_{N} were determined and gauged for accuracy.

If the total atmospheric NO₃⁻ deposition was averaged over entire sampling period it would result in a $f_{\text{atm}} = 0.005$ at the IML. This could only move the nitrate $\delta^{18}\text{O}$ in Figure 5-3 to the right of the predicted nitrification line by maximum 0.5‰ (assuming atmospheric NO₃⁻ $\delta^{18}\text{O} = +100\text{‰}$), significantly less than the observed ~4‰ and ~8‰ shifts observed in Spring and

Summer. This estimate of atmospheric deposition's influence on nitrate $\delta^{18}\text{O}$ assumes a constant deposition rate when in fact wet deposition, the main deposition component, is driven by punctuated events. The most intense nitrate deposition occurred between 8/23 to 8/30 when approximately $0.09 \text{ kg N ha}^{-1} \text{ week}^{-1}$ was added via wet and dry deposition, 3 times the weekly average. The f_{atm} could be as high as 0.020 ($0.09/(0.09+3.5)$) during this week that could produce a $\text{NO}_3^- \delta^{18}\text{O}$ excursion of up to a maximum 1.5‰, still much less than the observed 8‰ shift. In addition, the actual influence of atmospheric deposition on $\delta^{18}\text{O}$ is likely significantly less for two reasons. First atmospheric $\delta^{18}\text{O}$ values are most often not 100‰, but average closer to 70‰ in the Midwest (Hastings et al., 2003; Rihn, 2013). Second, the actual nitrification rate must be greater than $3.5 \text{ kg N ha}^{-1} \text{ week}^{-1}$ since we are not accounting for loss by denitrification or plant uptake, resulting in a smaller f_{atm} . Regardless, the maximum 2.0‰ is a factor of 4 smaller than the observed nitrate $\delta^{18}\text{O}$ shift in Figure 5-3, and we conclude that atmospheric nitrate cannot account for the deviation from the predicted nitrification line.

If the total NO_3^- added by UAN was averaged over entire sampling period it would result in a $f_{\text{UAN}} = 0.05$ at the IML and could shift the $\text{NO}_3^- \delta^{18}\text{O}$ by 1.3‰. This, however, assumes that the f_{UAN} from the May UAN addition did not change over the study period, which would be highly unlikely given its high solubility and bioavailability. If we instead assume that any UAN NO_3^- would have been leached during May then $f_{\text{UAN}} = 0.47$ and $f_{\text{Nitr}} = 0.52$. This could have increased the tile $\text{NO}_3^- \delta^{18}\text{O}$ values by about 10‰. Such an increase was not observed in our May data (Figure 5-1) and suggests that either the nitrate from UAN leached slowly, was utilized by plant growth, was denitrified, or the rate of nitrification was greater than $3.5 \text{ kg N ha}^{-1} \text{ week}^{-1}$, or some combination of all these effects, which would result in a smaller f_{UAN} value. The latter option seems most probable. While UAN may account for some of the nitrate $\delta^{18}\text{O}$ shift (Figure

5-3) from the nitrification line in the Spring, its importance would have diminished over the course of the growing season since it was a one-time application. We therefore conclude that the UAN nitrate source cannot explain nitrate $\delta^{18}\text{O}$ shifts observed in the Summer and Fall.

A majority of NO_3^- observed in the field was from nitrification because of the 230 kg N ha^{-1} added, 216 kg N ha^{-1} N was added as urea (24.8) and $\text{NH}_3/\text{NH}_4^+$ (192 kg N ha^{-1}) that can easily undergo nitrification to NO_3^- . These sources, without considering organic N which would increase f_{nitri} , total to a $f_{\text{nitri}} = 0.95$ (95%) ($f_{\text{urea}} = 0.11$, $f_{\text{NH}_4} = 0.84$), therefore the observed $\delta^{18}\text{O}$ - NO_3^- should fall along on the predicted nitrification line. The initial observed Spring values are shifted right (isotopically heavy) from the predicted nitrification line and while $\pm 1.25\%$ of this variation can be contributed to the $\delta^{18}\text{O}$ - H_2O , the rest must be attributed to denitrification.

Since nitrate source mixing cannot adequately explain the shifts in nitrate $\delta^{18}\text{O}$ values in the Summer/Fall, biogeochemical processes within the soil must be causing it. Two of the major NO_3^- loss processes, leaching and plant uptake, do not change the remaining nitrate $\delta^{18}\text{O}$ or $\delta^{15}\text{N}$ values (Högberg, 1997). Denitrification, however, has a KIE occurring at the enzyme level (Granger et al., 2006, 2008) leading to ^{18}O and ^{15}N enrichment. Thus, we can qualitatively attribute the increase in NO_3^- $\delta^{18}\text{O}$ values in Summer and Fall to field-scale denitrification. The further right any data point lays from the predicted nitrification line indicates that particular sample underwent more relative denitrification. The data implies that, in general, the fraction of denitrification was higher in the Summer/Fall relative to the Spring, and that a significant shift in $\delta^{18}\text{O}$ occurred from denitrification after the extended period without tile flow. This demonstrates that a plot of NO_3^- and H_2O $\delta^{18}\text{O}$ values in tile discharge is good qualitative indicator of field-scale denitrification assuming the fractions and $\delta^{18}\text{O}$ values of other NO_3^- sources and the relationship between nitrification and to H_2O $\delta^{18}\text{O}$ values are well constrained.

The increase in $\delta^{15}\text{N}$ values of tile discharge NO_3^- also support this qualitative interpretation of field scale denitrification. During the study period, nitrate $\delta^{15}\text{N}$ values were greater in the Summer/Fall than in the Spring (Figure 5-2). Studies have shown that increases in $\delta^{15}\text{N}$ in soil can be due to denitrification (Knöller et al., 2011; Mariotti et al., 1981; Menyailo & Hungate, 2006). Others have cautiously come to similar conclusions (Kellman 2004; Ostrom, et al. 1998; Kellman & Hillaire-Marcel 2003) suggesting that elevated soil nitrate $\delta^{15}\text{N}$ values are indicators of denitrification. Ostrom et al. (1998) noted that N isotope data “can provide considerable insight into microbial processes in soil” and “it may be this line of research that will be most fruitful for researchers using this technique”. Meanwhile Kellman & Hillaire-Marcel (2003) concluded that “results also point to the potential for using NO_3^- N isotopes to examine other biogeochemical transformations processes such as denitrification”.

It is unlikely that the observed nitrate $\delta^{15}\text{N}$ increase in our IML is source related because of the concordant increase in the $\delta^{18}\text{O}$ values. Spring nitrate $\delta^{15}\text{N}$ values ($\sim 2\%$) fall within expected values for complete nitrification of anhydrous ammonium. The Summer and Fall $\delta^{15}\text{N}$ values ($\sim 6\%$), however, are similar to soil N $\delta^{15}\text{N}$ values. This change could be due to a shift from nitrification of NH_4^+ in the Spring to mineralization and nitrification of soil organic N in the Summer and Fall. However, nitrification would incorporate the same soil water regardless of whether the N source was NH_4^+ or organic N, and $\delta^{18}\text{O}$ - H_2O of tile flow suggest little change in soil water throughout the seasons. The only scenario that can explain the simultaneously movement of nitrate $\delta^{15}\text{N}$ and $\delta^{18}\text{O}$ to more positive values in the Summer and Spring is denitrification. Smith and Kellman (2011) observed a similar simultaneous increase in $\delta^{15}\text{N}$ and $\delta^{18}\text{O}$ in tile drained IML in Canada but attributed it to source mixing, not denitrification. This conclusion was based on their observed $\Delta\delta^{15}\text{N}:\Delta\delta^{18}\text{O}$ ratio of 2.2:1 that did not match the

commonly reported 2:1 ratio for denitrification (Bottcher et al., 1990; Aravena and Robertson, 1998; Kendall, 1998). However, subsequent studies have shown denitrification induces a broad range of $\Delta\delta^{15}\text{N}:\Delta\delta^{18}\text{O}$ ratios from 1:1 to 2.1:1 (Aravena & Robertson, 1998; Baily et al., 2011; Cey et al., 1999; Kendall & Aravena, 2000; Knöller et al., 2011; Mengis et al., 2005). This wide range of values maybe the result of various isotope selectivity of denitrifying bacteria populations (Granger et al., 2008; Lehmann & Schroth, 2002; Wang et al., 2018). Our observed a ratio of 1.2 is within this range and our constraints on source NO_3^- $\delta^{18}\text{O}$ values and fractions show it cannot be the result of mixing, so we attribute this $\Delta\delta^{15}\text{N}:\Delta\delta^{18}\text{O}$ to denitrification. While several IML studies have inferred denitrification using nitrate stable isotopes, to our knowledge none have utilized these measurements to quantify the denitrification, which we attempt using a simple Rayleigh model.

5.5.2 Rayleigh Distillation Model

A Rayleigh distillation model was used to predict partitioning of isotopologues as a function of the fraction of NO_3^- lost during denitrification. In an open denitrification system, where the product N_2 does not revert back to reactant NO_3^- , the final $\delta^{15}\text{N}$ value of NO_3^- is a function of the amount of denitrification, which can be determined by (Eq. 6).

$$\delta^{15}\text{N}_f = \delta^{15}\text{N}_0 + {}^{15}\epsilon_{\text{denitri}} \ln f_{\text{remain}} \quad \text{Eq. 6}$$

Where $\delta^{15}\text{N}_f$ is the $\delta^{15}\text{N}$ value of the remaining (final) nitrate after some fraction has been lost to denitrification, $\delta^{15}\text{N}_0$ is the $\delta^{15}\text{N}$ value of the initial nitrate, ${}^{15}\epsilon_{\text{denitri}}(\text{‰})$ is the denitrification ^{15}N enrichment factor ($(\alpha-1)*1000$), and f_{remain} is the fraction of the initial NO_3^- remaining in the soil. Equation 6 can be rearranged (Eq. 7) to determine the fraction of loss from denitrification.

$$f_{\text{Lost}} = 1 - f_{\text{remain}} = 1 - e^{\frac{\delta^{15}\text{N}_f - \delta^{15}\text{N}_0}{{}^{15}\epsilon_{\text{denitri}}}} \quad \text{Eq. 7}$$

This open Rayleigh model was used to estimate field scale denitrification by measuring the $\delta^{15}\text{N}$ values of nitrate in tile discharge over time ($\delta^{15}\text{N}_t$), determining the $^{15}\epsilon_{\text{denitri}}$ value of denitrification, and estimating the initial $\delta^{15}\text{N}_0$.

The denitrification enrichment factor ($^{15}\epsilon_{\text{denitri}}$) can have a wide range of values, from 0‰ to -34‰ (Vogel et al, 1981, Mariotti et al 1988; Bottcher et al 1990, Mengis et al 1999, Fukada, 2003, Wexler et al 2014, Ji et al. 2017, Osaka 2018, Brandes and Devol 1997, Blackmer and Bremner 1976). This range in enrichment values is attributed to the diversity of denitrifying bacteria in different systems, environmental conditions, and sediment matrixes (Knöller et al., 2011, Mariotti 1981). We carried out denitrification incubations experiments using our IML soil and determined a $^{15}\epsilon_{\text{denitri}} = -15\%$. (see supplementary). This enrichment factor falls within the $^{15}\epsilon_{\text{denitri}}$ values of most soil studies that range from -8‰ to -17‰ (Osaka, 2018 and Blackmer 1976; Wellman et al. 1968; Delwiche and Steyn 1970; Barford et al. 1999, Miyaka and Wada 1971; Blackmer and Bremner 1977; Mariotti et al. 1981). Therefore, we used $^{15}\epsilon_{\text{denitri}} = -15\%$ to solve in Eq. 7.

Similar to our $\delta^{18}\text{O}$ isotope mass balance, the initial NO_3^- $\delta^{15}\text{N}$ value was calculated using isotope mass balance (Eq. 8). For the $\delta^{15}\text{N}_0$ calculation, we first split into fractions of soil NO_3^- that was added as NO_3^- (f_{NO_3}) and that derived from N that was then oxidized to NO_3^- (f_{N}) and $^{15}\epsilon_{\text{nitrif}}$ is the enrichment factor for nitrification.

$$\delta^{15}\text{N}(\text{NO}_3^-)_0 = f_{\text{NO}_3} \delta^{15}\text{N}_{(\text{NO}_3^-)} + f_{\text{N}} (\delta^{15}\text{N}_{(\text{N})} + ^{15}\epsilon_{\text{nitrif}}) \quad \text{Eq. 8}$$

The $f_{\text{NO}_3} = f_{\text{NO}_3\text{atm}} + f_{\text{UAN}}$ were quantified above and the average f_{NO_3} was ~ 0.05 for the study period, and $f_{\text{N}} \sim 0.95$. The initial $\delta^{15}\text{N}_{(\text{NO}_3^-)}$ and $\delta^{15}\text{N}_{(\text{N})}$ values in Eq. 8 were the estimated using similar isotope mixing models (equation 9 and 10)

$$\delta^{15}\text{N}_{(\text{NO}_3^-)} = f_{\text{NO}_3\text{atm}} \delta^{15}\text{N}_{\text{NO}_3\text{atm}} + f_{\text{fert}} \delta^{15}\text{N}_{\text{NO}_3\text{fert}} \quad \text{Eq. 9}$$

$$\delta^{15}\text{N}_{(\text{N})} = f_{\text{NH}_3\text{atm}} \delta^{15}\text{N}_{\text{NH}_3\text{atm}} + f_{\text{Nfert}} (\delta^{15}\text{N}_{\text{Nfert}} + \epsilon_{\text{volit}}) + f_{\text{Soil N}} \delta^{15}\text{N}_{\text{Soil N}} \quad \text{Eq. 10}$$

The $\delta^{15}\text{N}_{\text{NO}_3\text{atm}}$ and $\delta^{15}\text{N}_{\text{NO}_3\text{fert}}$ values and f 's used in Eq. 9 were based on observations or literature values. The $\delta^{15}\text{N}$ values of NO_3^- and total N contained in UAN used by Midwestern US farmers averages value of $0.2 \pm 3.6\text{‰}$ (Michalski et al., 2015) and $-0.2 \pm 2.1\text{‰}$ (Bateman & Kelly, 2007; Vitòria et al., 2004) respectively. Thus, we will use a value of $0.0 \pm 3.6\text{‰}$ for the $\delta^{15}\text{N}$ of all N fertilizers. As noted above, the atmospheric NO_3^- deposition was $1.48 \text{ kg N ha}^{-1}$ and NO_3^- from UAN was $12.4 \text{ kg N ha}^{-1}$ for a total of $13.9 \text{ kg N ha}^{-1}$ added as NO_3^- . This yields $f_{\text{atm}} = 0.11$ and $f_{\text{UAN}} = 0.89$. The $\delta^{15}\text{N}_{\text{NO}_3\text{atm}}$ was assumed to be $-2.0\text{‰} \pm 6$, on based on $\delta^{15}\text{N}$ values measured in wet depositions (Elliott et al., 2007; Freyer, 1991; Garten, 1992). This results in an estimated $\delta^{15}\text{N}_{(\text{NO}_3^-)} = 0.0\text{‰}$ for Eq. 9.

The $\delta^{15}\text{N}_{\text{NH}_3\text{atm}}$, $\delta^{15}\text{N}_{\text{NH}_4+\text{fert}}$, and $\delta^{15}\text{N}_{\text{Soil N}}$ values used in Eq.10 values were based on observation or literature values. A $\delta^{15}\text{N}_{\text{NH}_3} = -5.0\text{‰} \pm 5$ was based on wet deposition measurements (Garten, 1992; Heaton, 1986). The $\delta^{15}\text{N}_{\text{Soil N}} = 5.7\text{‰} \pm 0.3$ was based on our measured soil core N. The $\delta^{15}\text{N}_{\text{Nfert}}$ was set to $0.0\text{‰} \pm 3.6\text{‰}$ from measurements by (Bateman & Kelly, 2007; Otero et al., 2004; Michalski et al., 2015). There is a large $^{15}\epsilon_{\text{volit}}$ ($\sim 30\text{‰}$) associated with NH_3 volatilization that may enrich residue NH_4^+ if volatilization occurs (Högberg, 1997). This would happen during the brief period after NH_3 injection in the Fall. Ammonia loss through volatilization is minimal if soils are moist, regardless of temperature, but even less occurs at low temperatures (Overdahl & Rehm, 1990; Sommer & Christensen, 1992). After injection, NH_3 is rapidly hydrolyzed to NH_4^+ , this binds to the negatively charged clay soil particles through cation ion exchange (Benke et al., 2012). Soil moisture data (Fig 5-4A) shows that during the dates of injection moisture content was high and temperatures were cool, suggesting there was minimal loss through NH_3 volatilization post injection. In a study on anhydrous ammonia

volatilization losses after injection, Sommer & Christensen, (1992) found less than 3% of ammonia was lost by moist soils. From this, we estimate there was only a trivial loss by volatilization, therefore $^{15}\epsilon_{\text{volit}}$ was ignored. This leads to Eq.11

$$\delta^{15}\text{N}_{(\text{N})} = f_{\text{NH}_3\text{atm}} (5.0\text{‰}) + f_{\text{Nfert}} (0\text{‰}) + f_{\text{Soil N}} (6\text{‰}) \quad \text{Eq. 11}$$

In order to evaluate the f values in Eq. 10 and 11, the total non-nitrate N added to the field was evaluated. The f_{fert} in Eq. 10 includes anhydrous ammonia, Urea-UAN, and NH_4^+ -UAN. Likewise, $f_{\text{NH}_3\text{atm}}$ includes both NH_3 and NH_4^+ deposition. NH_3 and NH_4^+ was added to the field by wet and dry deposition and was calculated using the same EPA CASTNET and NADP databases and methods to determine NO_3^- deposition. Atmospheric NH_3 added 0.003 ± 0.001 kg N ha^{-1} week $^{-1}$ by dry deposition and 0.06 ± 0.06 kg N ha^{-1} week $^{-1}$ by wet deposition for a NH_3 total deposition of 1.68 kg N ha^{-1} over the study period (93% from wet deposition and 7% from dry deposition). The total non-nitrate N added as fertilizer was 216 kg N ha^{-1} (24.8 kg N ha^{-1} as urea, 12.4 kg N ha^{-1} as UAN NH_4^+ and 179 kg N ha^{-1} of anhydrous ammonium).

Based on Fall and winter soil conditions we hypothesize that most of the anhydrous ammonia applied in the Fall remained within the soil until Spring, when nitrification begins to occur. Nitrification is a temperature dependent process, and studies have shown that nitrification rates decrease dramatically below 10°C until they are inhibited at freezing temperatures (Grundmann et al., 1995; Hwang & Oleszkiewicz, 2007; Sabey et al., 1956). The soil temperature at the knifing depths where anhydrous ammonia is applied at our site stayed below 10°C from late November to mid-April, except for a few days in December (Fig 5-4A). Additionally, anhydrous ammonium is toxic when injected into the soil, reducing the population of nitrifying bacteria (Eno et al., 1954; Overdahl & Rehm, 1990) thus nitrification would have been suppressed by ammonia toxicity early in the year. Based on these factors, we conclude that

minimal nitrification occurred prior to mid-April, but occurred rapidly once soil temperatures exceed this 10°C threshold. For example, it has been shown that 73-96% of added NH₃ will be nitrified within 20 days when soil temperatures exceed this 10°C threshold (Chalk et al., 1975; Sabey, 1968; Welch, 1969). In total, 218 kg N ha⁻¹ was added to the soil directly as new reduced N. If soil mineralization is ignored ($f_{\text{Soil N}}$), this yields $f_{\text{NH}_3\text{atm}} = 0.008$ and $f_{\text{fert}} = 0.99$, and thus $f_{\text{NH}_3\text{atm}}$ can be ignored and Eq.11 reduces to

$$\delta^{15}\text{N}_{(\text{N})} = f_{\text{fert}} (0\text{‰}) + f_{\text{Soil N}} (6\text{‰}) = f_{\text{Soil N}} (6\text{‰}) \quad \text{Eq. 12}$$

It is apparent from Eq. 12 that $f_{\text{Soil N}}$, soil N that is mineralized to NH₄⁺, which is difficult to quantify, will ultimately control the $\delta^{15}\text{N}_{(\text{N})}$ value. This difficulty is driven by soil heterogeneity which vary dramatically even within a 2m² plot (Stoyan et al., 2000). Hubner et al (1991) found that soils growing maize and treated with 180 kg N ha⁻¹ yielded an average of N mineralization rate of 0.34 kg N ha⁻¹ d⁻¹, which predicts a total of 61 kg N ha⁻¹ in our field. Likewise, Mary and Recous (2002) found a rate of 0.33 kg N ha⁻¹ d⁻¹ in a wheat field receiving an organic slurry. Based on these considerations the $f_{\text{Soil (N)}}$ soil was estimated to be 0.21.

From these considerations, Eq. 8 was reevaluated (Eq.13)

$$\delta^{15}\text{N}(\text{NO}_3^-)_0 = f_{\text{NO}_3} \delta^{15}\text{N}_{(\text{NO}_3^-)} + f_{\text{N}} (\delta^{15}\text{N}_{(\text{N})} + {}^{15}\epsilon_{\text{nitrif}}) = .05(0.0\text{‰}) + 0.95(1.3\text{‰} + {}^{15}\epsilon_{\text{nitrif}}) \approx 1.2\text{‰} + ({}^{15}\epsilon) \quad \text{Eq. 13}$$

where ${}^{15}\epsilon_{\text{nitrif}}$ are the enrichment factor for nitrification, which suggests that the $\delta^{15}\text{N}(\text{NO}_3^-)_0$ may be sensitive to ${}^{15}\epsilon_{\text{nitrif}}$. Over 95% of nitrate in this IML was formed through nitrification and lab studies have shown the value of ${}^{15}\epsilon_{\text{nitrif}}$ to range from -36‰ to -15‰ (see Högberg, 1997). This unique (ϵ_{nitrif}) signal was never observed in the tile drain nitrate, the lowest $\delta^{15}\text{N}$ value was -1.1‰. Furthermore, ϵ_{nitrif} is not observed in other field studies with ammonium as the main N source (Kellman, 2005; Kellman & Hillaire-Marcel, 2003). Therefore, its absence is likely

because nitrification is not the rate limiting step, rather it is desorption of NH_4^+ from clay (Högberg, 1997; Scherer, 1993). The desorption of NH_4^+ from clay is difficult because it does not readily exchange with other cations and induces only a small isotopic fractionation ($<0.5\%$) (Freney & Simpson, 1983; Högberg, 1997; Scherer, 1993). Thus, we hypothesize that equilibrium between pore water and clay bound that NH_4^+ is established, and that the pore NH_4^+ is completely nitrified to NO_3^- on a short timescale, thus there would be no isotope enrichment associated with nitrification. If nitrification were incomplete, then reactant NH_4^+ and the nitrification intermediate NO_2^- would be present in the tile discharge. Both of these ions were absent in the IML tile discharge and is evidence that complete nitrification of desorbed NH_4^+ occurred supporting the rate limit hypothesis. Based on this logic we assume that in $^{15}\epsilon_{\text{nitrif}} \approx 0$ (Eq.13) and the $\delta^{15}\text{N}(\text{NO}_3^-)_0 \approx 1.2\%$, which is close to the Spring tile NO_3^- values. This 1.2 ‰ value $\delta^{15}\text{N}(\text{NO}_3^-)_0$ was used in Eq. 7 to calculate f_{Lost} .

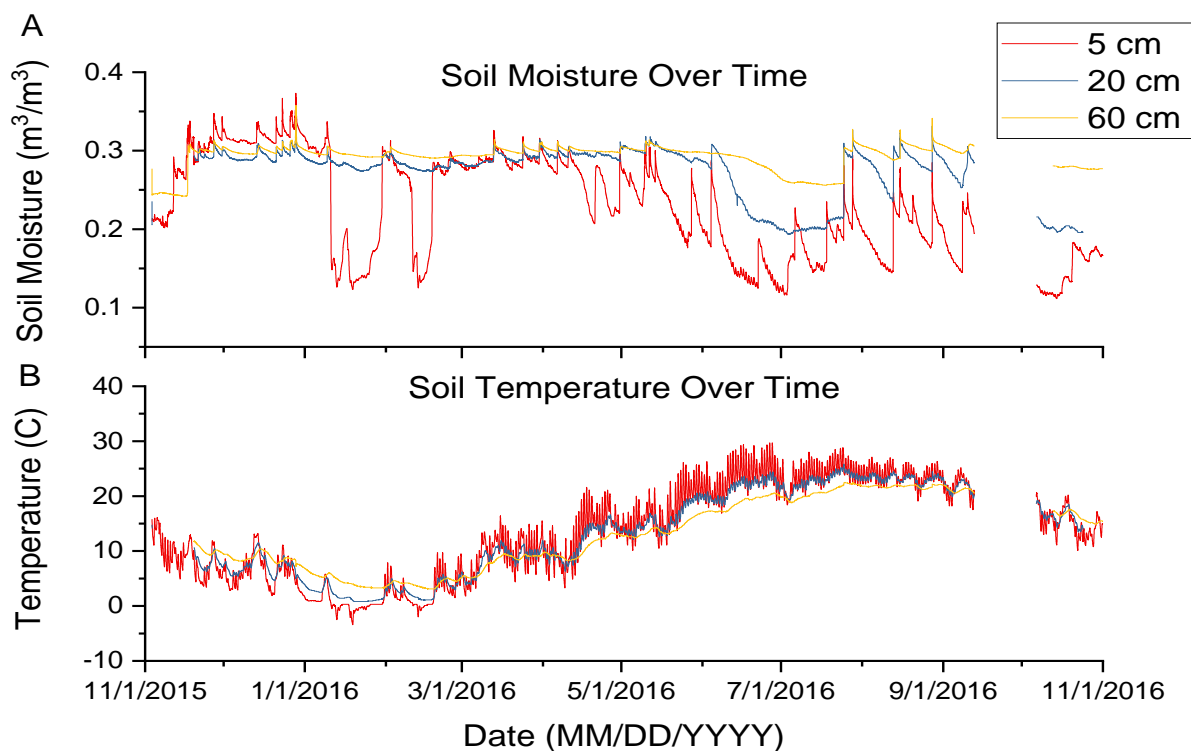


Figure 5-4 The study site's soil temperature (A) and soil moisture (B) at three depths (5cm, 20cm and 60cm) over a year.

The Rayleigh model (Eq. 7) was used to quantify the total amount of N lost via denitrification. The model inputs, $\delta^{15}\text{N}_0 = 1.2\text{‰}$, $^{15}\epsilon_{\text{denitri}} = -15\text{‰}$, and the tile nitrate $\delta^{15}\text{N}_f$ values were used (Eq. 7) to determine the f_{lost} of nitrate via denitrification. These fractions were then used with NO_3^- concentrations and discharge to quantify total N loss (Eq. 14 and 15).

$$\text{QL} = [\text{NO}_3^-] * \text{TF} * \Delta s \quad \text{Eq. 14}$$

$$\text{NO}_3^- \text{ denitrified (kg N ha}^{-1}\text{)} = \sum (\text{QL} / (f_{\text{lost}})) - \text{QL} \quad \text{Eq. 15}$$

Where QL is the quantity of nitrate lost (kg N), $[\text{NO}_3^-]$ is the nitrate concentration (kg N L⁻¹), TF is the average tile flow (L/s) in the interval Δs (the interval between sampling time in seconds) and f_{lost} is the fraction of nitrate lost by denitrification. The amount of N lost by denitrification between each sampling interval, and the cumulative N loss over the study period, are shown in Figure 5-5.

The model predicts that a total of $7.6 \pm 2.1 \text{ kg N ha}^{-1}$ was lost by field scale denitrification during the entire study period, 3.3% of the total N input. This estimated amount of denitrified nitrogen agrees well with values by Liang & Mackenzie, (1997) in a sandy clay loam in Canada growing corn who reported losses of 4 to 8 kg N ha⁻¹ from April to November in fields receiving N fertilizer at 170 to 400 kg N ha⁻¹. Our amounts of denitrification also agree with Nishio, (2002) who found that between <2 to 12% percent of fertilizer N was lost in a study of four different Japanese soils. Sainz Rozas et al, (2004) also reported similar N loss by denitrification (3.1 to 6.8%) in an Argentina soil. On the other hand, our findings are smaller than estimates by Ryden (1981) who determined losses of 11 to 29 kg N ha⁻¹ and Colbourn and Dowdell (1984) who estimated denitrification losses of 18 to 38 kg N ha⁻¹. These differences maybe attributed to soil type and management and environmental differences. In the Ryden (1981) study, plots received between 250 and 500kg of N ha⁻¹ in over 4 different application, and

soil moisture was greater, particularly during the highest temperature. The total N balance 230 kg N was added as fertilizer, 31 ± 0.9 kg N ha⁻¹ was leached, 195 kg was removed by corn uptake (determined using average N removal per bushel of corn and the average bushel harvest per ha in Illinois for 2016, see supplemental for calculation), and 7.6 kg N ha⁻¹ was lost by denitrified. This results in a net loss of 2.7 ± 2.0 kg N ha⁻¹ of N from the field. This agrees well with research that suggest IML fields under constant management are in N equilibrium without obvious accumulation or loss of N (Cassman & Walters, 2002).

The amount of denitrification varied from Spring to Fall. We find that a total 2.0 kg N ha⁻¹ was lost in the Spring at a daily rate of 43.5 g N ha⁻¹ d⁻¹, 4.8 kg N ha⁻¹ in the Summer at a daily rate of 98.0 g N ha⁻¹, and 0.9 kg N ha⁻¹ in the Fall at a daily rate of 19.2 g N ha⁻¹. All seasonal denitrification rates match well which with those by Elmi et al., (2000), whose measured denitrification rates by measuring evolved gases from soil cores. In total we find that 38.7 kg N ha⁻¹ or 16.6% of applied N was loss by leaching and denitrification, a value much lower than Sainz Rozas et al (2004) who measured between 33 and 36% of N loss. Of this 16.6% loss in our field, over 80% (31 kg N ha⁻¹) was from leaching. Yet, our leaching amounts are low compared to values by Randall (2001) who saw 214 kg N ha⁻¹ over a 4-year period. However, as observed by Frankenberger et al, (2004) leaching is heavily dependent on, crop, drain spacing, tillage, fertilizer N, fertilizer amounts, and precipitation amounts, thus comparisons of leaching much be used cautiously.

We emphasize that nitrogen loss by denitrification estimated using the Rayleigh model is a function of both f and the NO₃⁻ flux. For example, the higher NO₃⁻ flux in the Spring corresponds to a significant amount of N loss by denitrification (2.0 kg N ha⁻¹), despite low fractions of NO₃⁻ loss. The large variation in $\delta^{15}\text{N}$ and $\delta^{18}\text{O}$ values during the Spring suggest coupling of

denitrification and nitrification, as denitrification would cause an increase in $\delta^{15}\text{N}$ and $\delta^{18}\text{O}$ values.

Ultimately, this could result in the underestimation of N denitrified. However, this underestimation is partially made up by the increase in nitrate flux caused by high nitrification rate. During this period nitrate concentrations increase, a trend not seen in any other period. Thus, despite the low f values (0.1 to 0.25) in Spring, the high concentration result in over twice as much N loss compared to Fall when high f values (0.20 to 0.40) are observed.

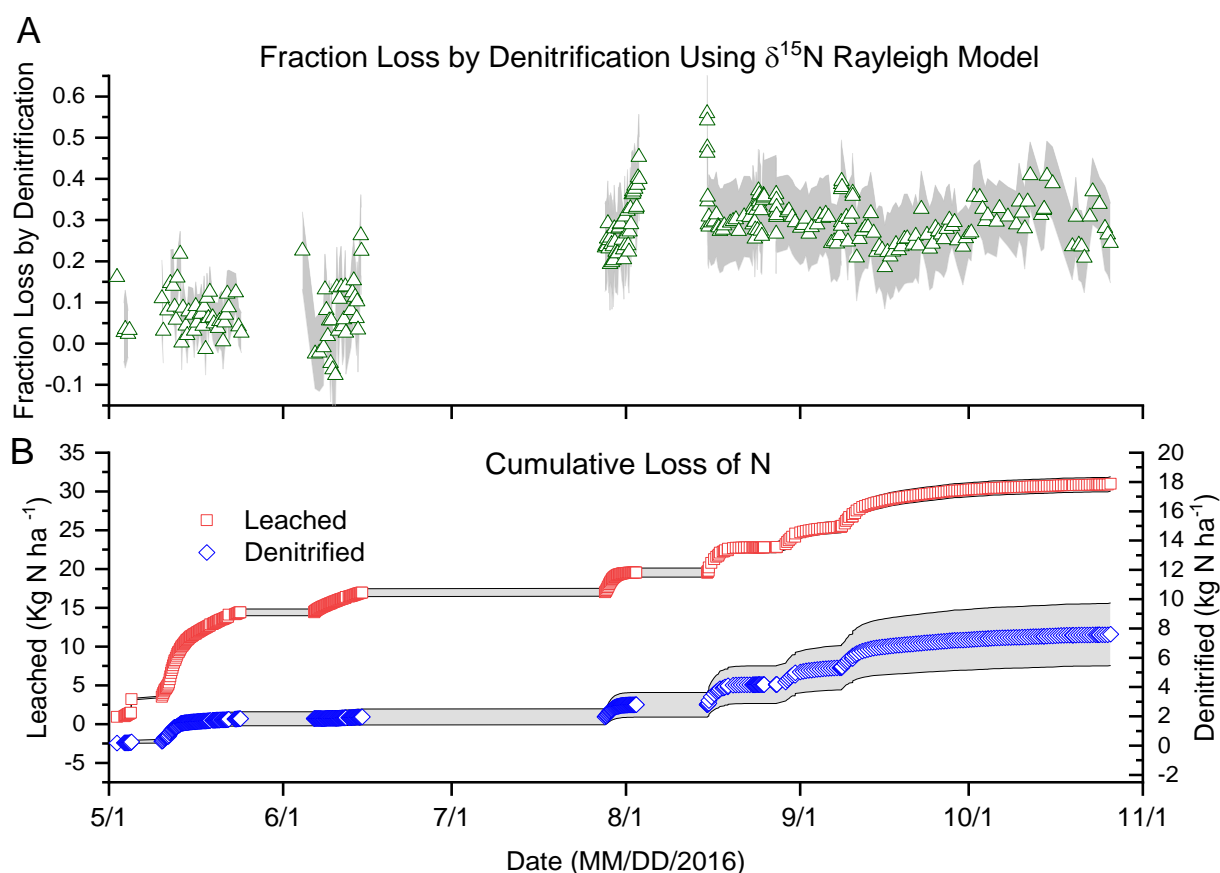


Figure 5-5(A) The fraction of nitrate loss through denitrification by the Rayleigh isotopic distillation model. Error bars are every other measurement point. (B) The cumulative loss of nitrate through leaching (red squares) and denitrification (blue diamonds) over the season. The grey area represents the error. The absence of data around 6/1 in figure 5B is due to no tile flow data collection

The Rayleigh model predicts the largest fraction of denitrification loss (nearly 60%) in the beginning of the summer period, when tile flow returned after a 43-day absence. After this period, the average nitrate concentrations decreased by 20 mg N/L relative to the average Spring concentration and the $\delta^{15}\text{N}$ and $\delta^{18}\text{O}$ values increased by 3‰ and 4‰. The cause of this high fraction of denitrification loss could be the result of 1 of 5 different scenarios. 1) denitrification has increased, and nitrification has remained the same 2) denitrification has remained the same but nitrification has decreased 3) denitrification has increased and nitrification has decreased 4) both denitrification and nitrification have increased but denitrification has increased more than nitrification to have a greater rate 5) both denitrification and nitrification have decreased but nitrification has decreased more than denitrification. Based on the time of year and results by Chalk et al. (1975), who found that applied ammonia was nitrified 1 to two months after application. Thus, the nitrification rate likely decreased and cases 1 and 4 can be eliminated. Additionally, from Spring to Summer soil temperatures increased while soil moisture at 20 cm depth remained the same, and with denitrification being dependent on these two factors we hypothesize that denitrification would have increased (Baker et al 2010; Pilegaard, 2013). Thus cases 2 and 5 can be eliminated leaving case 1 that denitrification rate has increased while nitrification has decreased.

Fall had the highest fraction of denitrification (0.3) but the lowest amount of total denitrification (0.9 kg N ha^{-1}), a result of low nitrate concentrations (12 mg N/L). This is likely due to the confluence of corn senescence, lower soil temperatures in the Fall, and a shift in soil N availability. Corn senescence provides a carbon source, reducing available inorganic N as mineralization decreases and immobilization increases (Recous et al., 1995). Meanwhile the reduced temperature of the Fall causes all soil microbial processes to slow, including nitrification

and denitrification. Reduced nitrification and mineralization will provide limited nitrate for denitrification allowing denitrification to easily cause large fractions of loss. However, the cooler temperatures will also reduce the rate of denitrification. Overall what is observed scenario 5 from above where a large fraction of loss caused by limited denitrification due to low concentrations from limited nitrification.

The overall uncertainty for our model for fraction loss (f) and kg N denitrified ha^{-1} can be seen in figure 5-5. This maximum uncertainty for fraction loss was 0.11 and the highest uncertain for kg N denitrified ha^{-1} was 2.1. This uncertainty is due to the propagation of error from $\delta^{15}\text{N}_0$, $\delta^{15}\text{N}_f$, $^{15}\epsilon_{\text{denitri}}$, and QL. The uncertainty of $\delta^{15}\text{N}_f$ and QL were based on analytical error and was $\pm 0.5\%$ and $\pm 3\%$ respectively. The $^{15}\epsilon_{\text{denitri}}$ was $\pm 4\%$ and based on deviation in the literature for $^{15}\epsilon_{\text{denitri}}$ soil. $\delta^{15}\text{N}_0$ was calculated using initial measure value in combination with the initial N mixing ratios performed above from this is was determined the standard deviation of $\delta^{15}\text{N}_0$ could be $\pm 2.0\%$. Simulations using high and low values were then run to calculate error in f loss and amount denitrification. Sensitivity testing showed that the overall error of fraction loss and amount of N denitrified was strongly controlled by $\delta^{15}\text{N}_0$. However, the standard deviation of $^{15}\epsilon_{\text{denitri}}$ also contributed to error.

5.6 Conclusion

In this study, the amount of denitrification was estimated from the stable isotopes of $\delta^{15}\text{N}$ and $\delta^{18}\text{O}$ which are steadily enriched from initial Spring values of 1.2‰ and 0.5‰ to Summer highs of 13.5‰ and 11.2‰, respectively. Isotopic increases are often accompanied by decreases in NO_3^- concentrations, Spring highs of 27 mg N/L to Summer lows of 3 mg N/L, qualitatively demonstrating denitrification. The amount of N denitrified was quantified via a Rayleigh isotopic distillation model and estimated at 7.6 kg N ha^{-1} or 3% of added N loss by denitrification.

Our estimates of N loss by denitrification in this IML using nitrate $\delta^{15}\text{N}$ and $\delta^{18}\text{O}$ values can help resolve the uncertainties of field scale denitrification. Our denitrified N loss values are in agreeance with our N balance as well as values measured by Sainz Rozas et al, (2004) and Nishio, (2002), and overall suggest that denitrifying conditions were not readily present within our field. Other studies growing corn and receiving similar amount of N fertilizer estimated losses of 30 kg N ha^{-1} by denitrification (Liang & Mackenzie, 1997). These differences can be attributed to form and application rates of N, climate differences, and stage of corn growth during events.

The research demonstrated that both $\delta^{15}\text{N}$ and $\delta^{18}\text{O}$ values of nitrate were required to reduce the uncertainty when determining the fraction of N loss by denitrification. Many studies that have used nitrate $\delta^{15}\text{N}$ values did not reach definitive conclusions about whether denitrification was present, let alone quantify the amount. The nitrate $\delta^{15}\text{N}$ shift to higher values in the Summer/Fall in our IML could have been attributed to a shift towards nitrification of mineralized soil N. We were able to exclude this by using the nitrate $\delta^{18}\text{O}$ values, because they are independent of the source of reduced N used by nitrifying Bacteria. In doing so we were able to use the well-defined $^{15}\epsilon_{\text{denitrif}}$ and the Rayleigh model to quantify the fraction of nitrate lost to denitrification. This would not have been convincing without the nitrate $\delta^{18}\text{O}$ measurements, which reinforces the power of the dual isotope ratio approach.

The dynamical nature of $\delta^{15}\text{N}$ and $\delta^{18}\text{O}$ values of nitrate during individual storms and over the entire season highlights the limitation of applying simple mixing models to N in some ecosystems. Our detained isotope and mass balance showed that, in this IML, nitrification was nearly the sole source of NO_3^- in the tile discharge. Using the tile discharge nitrate $\delta^{15}\text{N}$ and $\delta^{18}\text{O}$ values as “end-members” in simple linear mixing models or Bayesian models, which are often

used as a statistical “black box”, would have suggested source mixing, when the entire isotope variation can be attributed to subtle differences in proportions of nitrification and denitrification. This suggests that incorporating isotope effects into process based N cycling module contained in hydrologic models might be a more useful tool to understand N cycling than using purely statistical approaches.

This research has also demonstrated that to effectively use nitrate $\delta^{15}\text{N}$ and $\delta^{18}\text{O}$ values to assess field scale denitrification that collecting other, complimentary data, is essential. Monitoring nitrate concentrations at high temporal resolution was shown to be important. This is because of the heterogeneity of denitrification and nitrification in time and space (Groffman et al., 2009; T. H. Nielsen & Revsbech, 1998). Changing nitrate concentrations as a function of tile discharge time, and amount, reflects this heterogeneity, and this information would be lost collecting monthly or total event samples (Brouder et al., 2005; Kellman & Hillaire-Marcel, 2003). Based a number of studies, it is becoming apparent that the $\delta^{18}\text{O}$ value of nitrate produced by nitrification is ecosystem dependent (Kool et al., 2011; Kool et al., 2007). Since nitrification is usually the main source of NO_3^- , particularly in IMLs, an experimental determination of nitrification $\delta^{18}\text{O}$ would be essential for assessing denitrification using $\delta^{18}\text{O}$ and $\delta^{15}\text{N}$. Given this, it is therefore critical to determine the $\delta^{18}\text{O}$ value of the tile discharge water, since that is used during soil nitrification and controls the nitrification $\delta^{18}\text{O}$ value (Mayer et al., 2001). Using modeled or archived $\delta^{18}\text{O}$ value of precipitation introduces uncertainty because precipitation $\delta^{18}\text{O}$ values can vary significantly between events and evaporation can modify the initial precipitation $\delta^{18}\text{O}$, factors that are avoided by measuring the tile water $\delta^{18}\text{O}$ value (Bowen & Revenaugh, 2003; Craig et al., 1963; Gat, 1996). Monitoring the N deposition flux was shown to be important for assessing whether it is a significant fraction of N input to an ecosystem. In this

IML it was shown to be trivial, but this may not be true in natural ecosystems (Fenn et al., 2003). Because a fraction of N deposition is NO_3^- , determining its $\delta^{18}\text{O}$ value can be useful for minimizing the uncertainty when determining the fraction of atmospheric NO_3^- input to an ecosystem. For example, a measured range of 50-65‰ will have less uncertainty in the f_{atm} factor compared to using the 30-100‰ range published in the literature that may not be relevant to the ecosystem of interest (Michalski et al., 2012). We showed that not only were the fertilizer N application amounts important, but also its chemical form (i.e. UAN, NH_3) and the timing of application were relevant. While it was not important in our IML, nitrate contained in fertilizers, like UAN and NH_4NO_3 , have elevated $\delta^{18}\text{O}$ values that might be useful for tracing their transport through other IMLs (Michalski et al., 2015). On the other hand, they obfuscate attempts to use $\delta^{18}\text{O}$ to infer denitrification. Thus, we have demonstrated that if these other data types are collected, along with determining the nitrate $\delta^{15}\text{N}$ and $\delta^{18}\text{O}$ values in discharge, researchers can potentially evaluate denitrification loss of N at field, or even watershed, scale, something that has thus far been elusive.

Given the power of the dual isotope ratio approach for quantifying field scale denitrification, future research aimed at reducing the uncertainties in this approach are warranted. Though several studies have investigated the ^{18}O composition of NO_3^- during nitrification, ambiguity still exist especially within soil nitrification were only a few studies have been performed with varying $f_{\text{H}_2\text{O}}$, from 0.32 to 1 (Kool, 2011; Mayer et al., 2001). Likewise, constraints are needed on the $^{15}\epsilon_{\text{denitri}}$ of soil as value range wildly from -7‰ to -20‰, and Rayleigh models are heavily dependent on these values (Osaka et al., 2018). This research was able to limit these uncertainties by incubation experiments. Furthermore, a comparison study of

different methods used to quantify denitrification needs to be performed as simple method comparisons to other studies is limited by plot and climate differences.

5.7 Acknowledgments

The authors thank funding support from the National Science Foundation (Grant EAR1331906) and the Purdue Climate Change Research Center. The lead author would also like to thank the ASEE SMART scholarship for its funding. The authors also thank the Illinois State Geology Survey and Illinois State Water Survey for their support in this research. Lindsey Crawley at the Purdue Stable Isotope lab for running $\delta^{18}\text{O}\text{-H}_2\text{O}$ samples. Data can be accessed through the University of Illinois CLOUDER open source database (<http://data.imlczo.org/clowder/>).

CHAPTER 6. CONCLUSION AND FUTURE DIRECTIONS

The research within this dissertation focused on improving our understanding of the stable isotopes of nitrate within Midwestern soils and their ability to be used as tracers to source and assess microbial processes within soil, particularly nitrification and denitrification. Determining the $^{15}\epsilon$ during both denitrification and nitrification in Midwestern soils is an advancement because most studies have focused primarily on pure bacteria cultures or denitrification and nitrification occurring in marine environments. The few studies on the $^{15}\epsilon$ of nitrification and denitrification within soil systems, report a large range of values, and are limited. This dissertation uses the observed $\delta^{15}\text{N}$ and $\delta^{18}\text{O}$ values of nitrate to evaluate microbial soil denitrification and nitrification.

6.1 $^{15}\epsilon_{\text{NO}_3^-/\text{NH}_4^+}$ of nitrification and source of oxygen

The $^{15}\epsilon_{\text{NO}_3^-/\text{NH}_4^+}$ was determined for nitrification occurring within a Midwestern agricultural soil. Also, the sources of oxygen used during the oxidation of NH_4^+ during nitrification was determined under several incubations using three isotopically different H_2O . In each of these incubations, the nitrogen isotopes in NO_3^- produced from NH_4^+ were isotopically light yielding $^{15}\epsilon_{\text{NO}_3^-/\text{NH}_4^+} = -25\text{‰}$. The negative $\delta^{15}\text{N}$ values of NO_3^- produced during nitrification is a result of enzymes favorably oxidizing $^{14}\text{NH}_4^+$ compared to the heavier $^{15}\text{NH}_4^+$. This isotopic enrichment is important because the $\delta^{15}\text{N}$ is also used to differentiate between NO_3^- from manure, fertilizer NH_4^+ , and soil N. For example, nitrate formed from nitrification of NH_4^+ that has a $\delta^{15}\text{N}$ value of -25.46‰ , similar to manure, could show NO_3^- $\delta^{15}\text{N}$ values near 0‰ and without considering the $^{15}\epsilon_{\text{NO}_3^-/\text{NH}_4^+}$, this nitrate could be misinterpreted to be from soil N or NH_4^+ fertilizer ($\delta^{15}\text{N} = 0\text{‰}$).

The incubations showed that the $\delta^{18}\text{O}$ value of NO_3^- from the nitrification NH_4^+ was reflected in the $\delta^{18}\text{O}$ value of H_2O . The fraction of NO_3^- oxygen derived from H_2O was 0.82, greater than the 0.66 predicted by current mechanistic models of nitrification. The greater fraction of oxygen from H_2O was due to equilibrium isotope exchange that occurs between the NO_2^- intermediate and H_2O prior to its oxidation into NO_3^- . This isotopic oxygen exchange, like $^{15}\epsilon_{\text{NO}_3^-/\text{NH}_4^+}$, can have profound effects on the final $\delta^{18}\text{O}$ value of NO_3^- from nitrification. Often NO_3^- $\delta^{18}\text{O}$ values are used to apportion NO_3^- sources between inorganic, atmospheric, and organic NO_3^- . However, if equilibrium isotope exchange between NO_2^- and H_2O occurs and is not considered, then the fractions of NO_3^- sources may be incorrectly allocated. For example, the $\delta^{18}\text{O}$ value of H_2O used during soil nitrification in a field will reflect the $\delta^{18}\text{O}$ value of precipitation, which in the United States typically spans -24 to 0‰ and rarely exceeds +5‰ (Vachon et al., 2010). Therefore, oxygen isotope exchange between H_2O and NO_2^- would cause the $\delta^{18}\text{O}$ value of nitrate to be lower than that calculated, since the O atom derived from $\text{O}_2 = +23‰$ is being exchanged with an oxygen from H_2O that has a much lower $\delta^{18}\text{O}$ value (-24 and 5‰). This would cause the under prediction of contribution of organic NO_3^- compared to other sources. It's also important to mention that the degree of oxygen equilibrium exchange is a pH dependent process and may be more prevalent in acidic soils as opposed to alkaline soils. The findings from this study are particularly important in soils system where NH_4^+ additions are large and in soils that tend to have a lower pH. This describes Midwestern soils where NH_4^+ is the dominant source of N fertilizer and the pH of soils range from 6.5 to 6.0. Thus, stable isotope sourcing studies that involve nitrate from soils may be more prone to enrichment by $^{15}\epsilon_{\text{NO}_3^-/\text{NH}_4^+}$ and equilibrium isotope exchange of oxygen compared to other locations throughout the U.S.

6.2 $^{15}\epsilon_{\text{NO}_3^-}$ and $^{15}\epsilon_{\text{NO}_2^-}$ of denitrification

The effect of denitrification on the $\delta^{15}\text{N}$ of NO_3^- and NO_2^- was evaluated using a combination of experimental investigations and computational chemistry modeling. During denitrification of NO_3^- to gaseous N, two enzyme steps exist that can cause kinetic isotopic enrichment, the reduction of NO_3^- to NO_2^- ($^{15}\epsilon_{\text{NO}_3^-}$) and the reduction of NO_2^- to gaseous N ($^{15}\epsilon_{\text{NO}_2^-}$). From experimental results, the $^{15}\epsilon_{\text{NO}_2^-}$ was determined to be $9.1\text{‰} \pm 1.5$. The $^{15}\epsilon_{\text{NO}_2^-}$ was determined by measuring the fraction of NO_2^- loss and plotting against the change in $\delta^{15}\text{N}$ value. The presence of an $^{15}\epsilon_{\text{NO}_2^-}$ enrichment suggest that if nitrite concentrations are present in a significant molar ratio compared to NO_3^- than both NO_3^- and NO_2^- must be separated to performing accurate isotopic measurements of $\delta^{15}\text{N}$ and $\delta^{18}\text{O}$. The $^{15}\epsilon_{\text{NO}_3^-}$ was evaluated using four kinetic models that consisted of a first order, zero order, and two Michealis-Menten kinetic mechanism. Among all the models the Michealis-Menten models that account for enzyme kinetics were able to best reproduce the change in $\delta^{15}\text{N}$ values of $\text{NO}_{3/2}$. This suggest that for the most accurate modeling of changing the $\delta^{15}\text{N}$ by microbial processes, such as nitrification or denitrification, enzyme kinetics should be included. However, when compared to the first order model results where only marginally improved, R^2 of 0.95 vs 0.93, suggesting that the first order Rayleigh model is still an acceptable model to predict changes in $\delta^{15}\text{N}$ of $\text{NO}_{3/2}$.

6.3 Qualitative identification and quantification measured of denitrification by stable isotopes within an agricultural soil

This chapter studied denitrification across a 6.75 ha intensively managed landscape. Denitrification was evaluated, qualitatively and quantitatively, by measuring the stable isotope of nitrate in discharge collected from tile drain runoff from May to November. During this period the stable isotopes of $\delta^{15}\text{N}$ and $\delta^{18}\text{O}$ steadily enriched from initial Spring values of 1.2‰ and

0.5‰ to Summer highs of 13.5‰ and 11.2‰, respectively. These isotopic increases were regularly accompanied by decreases in NO_3^- concentrations, qualitatively demonstrating denitrification. The amount of N denitrified was quantified using a Rayleigh isotope distillation model paired with concentration data. An estimated 7.6 kg N ha^{-1} or 3% of added N was lost by denitrification. Given this small amount of denitrification loss it can be suggested denitrifying conditions were not readily present at the field site as other studies that have determined denitrified amounts as high as 30 kg N ha^{-1} . While many studies have measured the $\delta^{15}\text{N}$ and $\delta^{18}\text{O}$ values of NO_3^- from tile drain discharge this is the first study that quantitatively estimated denitrification by $\delta^{15}\text{N}$. Measurements of $\delta^{18}\text{O}$ proved useful to eliminate source mixing as a possible explanation for the observed increase in $\delta^{15}\text{N}$, reinforcing the ability of the dual isotope approach. While the $\delta^{15}\text{N}$ values were used to quantify denitrification. Furthermore, this research also emphasizes the importance of complimentary data. High temporal resolution of nitrate concentration, precipitation amounts, soils moisture, soil temperature, and N depositions flux, proved useful in identifying short-term changes in the soil system. Furthermore, collection of the $\delta^{18}\text{O}$ values of tile drain H_2O was found to be instrumental as it controls the $\delta^{18}\text{O}$ of NO_3^- from nitrification. Overall, within this chapter we demonstrated that if these other data types are collected, along with determining the nitrate $\delta^{15}\text{N}$ and $\delta^{18}\text{O}$ values in discharge, researchers can potentially evaluate denitrification loss of N at field, or even watershed, scale, something that has thus far been elusive.

6.4 Future Outlook

This research suggests the potential to use stable isotopes of NO_3^- to not only partition between NO_3^- sources but more importantly to evaluate the progression of reaction pathways of NO_3^- within soil. Future research should build on the work presenting in this dissertation by

further constraining the isotopic enrichment factors of denitrification and nitrification in different soils conditions. For example, the $^{15}\epsilon_{\text{NO}_3^-}$ value presented within this dissertation was just outside the range of reported literature value of other soils. An improvement of these studies would not only allow better delineation of NO_3^- sources but would also improve the precision when applying the $^{15}\epsilon_{\text{NO}_3^-}$ to qualitatively determine denitrification as performed in chapter 5. Likewise, a better understanding of $^{15}\epsilon_{\text{NO}_3^-/\text{NH}_4^+}$, and how soil condition affect, would prove immensely valuable particular within the Midwestern intensively managed landscapes (IMLs). Furthermore, a deeper understanding on not only the extent of equilibrium exchange in soils but also the parameters that influence it. Within this dissertation it was shown that between 46% to 100% of oxygen exchange can occur between NO_2^- and H_2O during nitrification, however, other studies have found exchange as high as 100% and as low as <1%. Furthermore, while it was not investigated within this dissertation equilibrium exchange of oxygen between NO_2^- and H_2O has also been observed during the process of denitrification. Thus, in addition to understanding what and how soil parameters control and influence exchange during nitrification, more studies are needed to understand if and how soils parameters influence exchange during denitrification. Last the quantitative method of estimating denitrification by $\delta^{15}\text{N}$ used in chapter 5 to estimate denitrification within an IML needs a comparison study to fully evaluate this new method. This comparison study should apply several methods to estimate denitrification such as chamber studies and long-range FT-IR at the same site to evaluate the performance of each approach.

REFERENCES

- Adams, P. J., Seinfeld, J. H., & Koch, D. M. (1999). Global concentrations of tropospheric sulfate, nitrate, and ammonium aerosol simulated in a general circulation model. *Journal of Geophysical Research Atmospheres*, *104*(D11), 13791–13823. <https://doi.org/10.1029/1999JD900083>
- Akunna, J. C., Bizeau, C., & Moletta, R. (2008). Nitrate reduction by anaerobic sludge using glucose at various nitrate concentrations: Ammonification, denitrification and methanogenic activities, *3330*. <https://doi.org/10.1080/09593339409385402>
- Aleem, M. I. H., Hoch, G. E., & Varner, J. E. (1965). Water as the source of oxidant and reductant in bacterial chemosynthesis. *Proceedings of the National Academy of Sciences of the United States of America*, *54*(3), 869–873. <https://doi.org/10.1073/pnas.54.3.869>
- Andersson, K., & Hooper, A. (1983). O₂ and H₂O are each the source of one O in NO₂⁻ produced from NH₃ by Nitrosomonas: ¹⁵N-NMR evidence. *FEBS Letters*, *164*(2), 236–240.
- Aravena, R., & Robertson, W. D. (1998). Use of Multiple Isotope Tracers to Evaluate Denitrification in Ground Water: Study of Nitrate from a Large-Flux Septic System Plume. *Groundwater*, *36*(6), 975–982. <https://doi.org/10.1111/j.1745-6584.1998.tb02104.x>
- Baily, A., Rock, L., Watson, C. J., & Fenton, O. (2011). Spatial and temporal variations in groundwater nitrate at an intensive dairy farm in South-East Ireland: Insights from stable isotope data. *Agriculture, Ecosystems and Environment*, *144*(1), 308–318. <https://doi.org/10.1016/j.agee.2011.09.007>
- Bateman, A. S., & Kelly, S. D. (2007). Fertilizer nitrogen isotope signatures. *Isotopes in Environmental and Health Studies*, *43*(3), 237–247. <https://doi.org/10.1080/10256010701550732>
- Benke, M. B., Goh, T. B., Karamanos, R., Lupwayi, N. Z., & Hao, X. (2012). Retention and nitrification of injected anhydrous NH₃ as affected by soil pH. *Canadian Journal of Soil Science*, *92*(4), 589–598. <https://doi.org/10.4141/cjss2011-108>
- Berg, J. M., Tymoczko, J. L., & Stryer, L. (2002). *Section 24.1, Nitrogen Fixation: Microorganisms Use ATP and a Powerful Reductant to Reduce Atmospheric Nitrogen to Ammonia. Biochemistry. 5th edition.* Retrieved from <http://www.ncbi.nlm.nih.gov/books/NBK22522/>
- Bergersen. (1986). Strain of *Rhizobium lupini* Determined Natural Abundance of ¹⁵N in Root Nodules of Lupinus, *18*(1), 3–7.

- Berman, E. S. F., Levin, N. E., Landais, A., Li, S., & Owano, T. (2013). Measurement of $\delta^{18}\text{O}$, $\delta^{17}\text{O}$, and ^{17}O -excess in water by off-axis integrated cavity output spectroscopy and isotope ratio mass spectrometry. *Analytical Chemistry*, 85(21), 10392–10398. <https://doi.org/10.1021/ac402366t>
- Betlach, M. R., & Tiedje, J. M. (1981). Kinetic Explanation for Accumulation of Nitrite, Nitric Oxide, and Nitrous Oxide During Bacterial Denitrification, *42*(6), 1074–1084.
- Blackburn, T. H., Blackburn, N. D., Jensen, K. I. M., & Risgaard-petersen, N. (1994). Simulation Model of the Coupling between Nitrification and Denitrification in a Freshwater Sediment, *60*(9), 3089–3095.
- Blackmer, A. M., & Bremner, J. M. (1977). Nitrogen isotope discrimination in denitrification of nitrate in soils. *Soil Biology and Biochemistry*, 9(2), 73–77. [https://doi.org/https://doi.org/10.1016/0038-0717\(77\)90040-2](https://doi.org/https://doi.org/10.1016/0038-0717(77)90040-2)
- Blum, P., Hunkeler, D., Weede, M., Beyer, C., Grathwohl, P., & Morasch, B. (2009). Quantification of biodegradation for o-xylene and naphthalene using first order decay models, Michaelis – Menten kinetics and stable carbon isotopes. *Journal of Contaminant Hydrology*, 105(3–4), 118–130. <https://doi.org/10.1016/j.jconhyd.2008.11.009>
- Böhlke, & Denver. (1995). Combined Use of Groundwater Dating, Chemical, and Isotopic Analyses to Resolve the History and Fate of Nitrate Contamination in Two Agricultural Watersheds, Atlantic Coastal Plain, Maryland. *Water Resources Research*, 31(9), 2319–2339. <https://doi.org/10.1029/95WR01584>
- Böhlke, Harvey, J. W., & Voytek, M. A. (2004). Reach-scale isotope tracer experiment to quantify denitrification and related processes in a nitrate-rich stream, midcontinent United States. *Limnology and Oceanography*, 49(3), 821–838. <https://doi.org/10.4319/lo.2004.49.3.0821>
- Böhlke, J. K., & Coplen, T. B. (1995). Interlaboratory comparison of reference materials for nitrogen-isotope-ratio measurements. International Atomic Energy Agency (IAEA). Retrieved from http://inis.iaea.org/search/search.aspx?orig_q=RN:27021334
- Böhlke, J. K., Mroczkowski, S. J., & Coplen, T. B. (2003). Oxygen isotopes in nitrate: New reference materials for ^{18}O : ^{17}O : ^{16}O measurements and observations on nitrate-water equilibration. *Rapid Communications in Mass Spectrometry*, 17(16), 1835–1846. <https://doi.org/10.1002/rcm.1123>
- Borah, D. K., Bera, M., & Shaw, S. (2003). Water, Sediment, Nutrient, and Pesticide Measurements in an Agricultural Watershed in Illinois During Storm Events. *Transactions of the ASAE*, 46(3), 657–674. <https://doi.org/10.13031/2013.13601>
- Bothe, H., Jost, G., Schloter, M., Ward, B. B., & Witzel, K. (2000). Molecular Analysis Of Ammonia Oxidation And Denitrification In Natural Environments. *FEMS Microbiology Reviews*, 24, 673–690. <https://doi.org/10.1111/j.1574-6976.2000.tb00566.x>

- Bothe, H., Ferguson, S., & Newton, W. E. (2006). *Biology of the nitrogen cycle*. Elsevier.
- Böttcher, J., Strelbel, O., Voerkelius, S., & Schmidt, H. L. (1990). Using isotope fractionation of nitrate-nitrogen and nitrate-oxygen for evaluation of microbial denitrification in a sandy aquifer. *Journal of Hydrology*, 114(3–4), 413–424. [https://doi.org/10.1016/0022-1694\(90\)90068-9](https://doi.org/10.1016/0022-1694(90)90068-9)
- Bouwman, A. F. (1998). Nitrogen oxides and tropical agriculture. *Nature*, 392, 866. Retrieved from <https://doi.org/10.1038/31809>
- Bouwman, A. F., Beusen, A. H. W., Griffioen, J., Van Groenigen, J. W., Hefting, M. M., Oenema, O., et al. (2013). Global trends and uncertainties in terrestrial denitrification and N₂O emissions. *Philosophical Transactions of the Royal Society B: Biological Sciences*, 368(1621), 20130112–20130112. <https://doi.org/10.1098/rstb.2013.0112>
- Bowen, G. J., & Revenaugh, J. (2003). Interpolating the isotopic composition of modern meteoric precipitation. *Water Resources Research*, 39(10), 1–13. <https://doi.org/10.1029/2003WR002086>
- Bowman, & Focht. (1974). The Influence of Glucose and Nitrate Upon Denitrification Rates in Sandy Soils.
- Boyer, E. W., Alexander, R. B., Parton, W. J., Li, C., Butterbach-bahl, K., Donner, S. D., et al. (2018). Modeling Denitrification in Terrestrial and Aquatic Ecosystems at Regional Scales. *Ecological Society of America* : <http://www.jstor.org/stable/40061946>, 16(6), 2123–2142.
- Brouder, S., Hofmann, B., & Morris, D. (2005). Mapping Soil pH: Accuracy of Common Soil Sampling Strategies and Estimation Techniques. *Soil Science Society of America Journal*, 69, 427–442.
- Bryan, B. A., Shearer, G., Skeeters, L., & Kohl, D. H. (1983). Variable Expression of the Nitrogen Isotope Effect Associated with Denitrification of Nitrite *, 258(14), 8613–8617.
- Buchwald, C., & Casciotti, K. L. (2010). Oxygen isotopic fractionation and exchange during bacterial nitrite oxidation. *Limnology and Oceanography*, 55(3), 1064–1074. <https://doi.org/10.4319/lo.2010.55.3.1064>
- Buchwald, C., Santoro, A. E., McIlvin, M. R., & Casciotti, K. L. (2012). Oxygen isotopic composition of nitrate and nitrite produced by nitrifying cocultures and natural marine assemblages. *Limnology and Oceanography*, 57(5), 1361–1375. <https://doi.org/10.4319/lo.2012.57.5.1361>
- Bundy, L. G. (1985). *Corn Fertilization*. University of Wisconsin--Extension.
- Burns, L. C., Stevens, R. J., & Laughlin, R. J. (1996). Production of Nitrite in Soils by Simultaneous Nitrification and Denitrification, 28(415), 609–616.

- Casciotti, & McIlvin, M. R. (2007). Isotopic analyses of nitrate and nitrite from reference mixtures and application to Eastern Tropical North Pacific waters. *Marine Chemistry*, 107(2), 184–201. <https://doi.org/10.1016/j.marchem.2007.06.021>
- Casciotti, Sigman, D. M., Hastings, M. G., Böhlke, J. K., & Hilkert, A. (2002). Measurement of the oxygen isotopic composition of nitrate in seawater and freshwater using the denitrifier method. *Analytical Chemistry*, 74(19), 4905–4912. <https://doi.org/10.1021/ac020113w>
- Casciotti, Sigman, D. M., & Ward, B. B. (2003). Linking diversity and stable isotope fractionation in ammonia-oxidizing bacteria. *Geomicrobiology Journal*, 20(4), 335–353. <https://doi.org/10.1080/01490450303895>
- Casciotti, Böhlke, J. K., McIlvin, M. R., Mroczkowski, S. J., & Hannon, J. E. (2007). Oxygen isotopes in nitrite: Analysis, calibration, and equilibration. *Analytical Chemistry*, 79(6), 2427–2436. <https://doi.org/10.1021/ac061598h>
- Casciotti, McIlvin, M., & Buchwald, C. (2010). Oxygen isotopic exchange and fractionation during bacterial ammonia oxidation (vol 55, pg 753, 2010). *Limnology and Oceanography*, 55(2), 753–762. [https://doi.org/DOI 10.4319/lo.2009.55.2.0753](https://doi.org/DOI%2010.4319/lo.2009.55.2.0753)
- Casciotti, K. L. (2009). Inverse kinetic isotope fractionation during bacterial nitrite oxidation. *Geochimica et Cosmochimica Acta*, 73(7), 2061–2076. <https://doi.org/10.1016/j.gca.2008.12.022>
- Cassman, K. G., & Walters, D. T. (2002). Agroecosystems , Nitrogen-use Efficiency , and Nitrogen Management Agroecosystems , Nitrogen-use Efficiency ,.
- Castellano, M. J., Helmers, M. J., Sawyer, J. E., Barker, D. W., & Christianson, L. E. (2012). Nitrogen, carbon, and phosphorus balances in Iowa cropping systems: Sustaining the soil resource. *Integrated Crop Management Conference - Iowa State University*, (October 2012), 145–156.
- Cey, E. E., Rudolph, D. L., Aravena, R., & Parkin, G. (1999). Role of the riparian zone in controlling the distribution and fate of agricultural nitrogen near a small stream in southern Ontario. *Journal of Contaminant Hydrology*, 37(1–2), 45–67. [https://doi.org/10.1016/S0169-7722\(98\)00162-4](https://doi.org/10.1016/S0169-7722(98)00162-4)
- Chalk, P. M., Keeney, D. R., & Walsh, L. M. (1975). Crop Recovery and Nitrification of Fall and Spring Applied Anhydrous Ammonia. *Agronomy Journal*, 67, 33–37. <https://doi.org/10.2134/agronj1975.00021962006700010009x>
- Chen, F., Jia, G., & Chen, J. (2009). Nitrate sources and watershed denitrification inferred from nitrate dual isotopes in the Beijiang River, south China. *Biogeochemistry*, 94(2), 163–174. <https://doi.org/10.1007/s10533-009-9316-x>
- Cline, J. ., & Kaplan, I. R. (1975). Isotopic Fractionation of Dissolved Nitrate During Denitrification in The Eastern Tropic North Pacific Ocean. *Marine Chemistry*, 3(1330), 271–299.

- Corey, J. C., Nielsen, D. R., & Kirkham, D. (1967). Miscible Displacement of Nitrate through Soil Columns. *Soil Science Society of America Journal*. [Madison, Wis.]: <https://doi.org/10.2136/sssaj1967.03615995003100040023x>
- Cottrell, T. L. (1958). *The strengths of chemical bonds*. Academic Press.
- Craig, H., Gordon, L. I., & Horibe, Y. (1963). Isotopic exchange effects in the evaporation of water: 1. Low-temperature experimental results. *Journal of Geophysical Research*, 68(17), 5079–5087. <https://doi.org/10.1029/JZ068i017p05079>
- Crutzen, Mosier, A. R., Smith, K. A., Winiwarter, W., Crutzen, P. J., Mosier, A. R., et al. (2007). N₂O release from agro-biofuel production negates global warming reduction by replacing fossil fuels To cite this version : HAL Id : hal-00303019 N₂O release from agro-biofuel production negates global warming reduction by replacing fossil fuels.
- Crutzen, P. (1974). A Review of Upper Atmospheric Photochemistry, 80302.
- David, M. M. B., Gentry, L. L. E., Kovacic, D. a., & Smith, K. M. K. (1997). Nitrogen balance in and export from an agricultural watershed. *Journal of Environmental Quality*, 26(4), 1038. <https://doi.org/10.2134/jeq1997.00472425002600040015x>
- Davidson. (2009). to atmospheric nitrous oxide since 1860. *Nature Geoscience*, 2(9), 659–662. <https://doi.org/10.1038/ngeo608>
- Davidson, W. ., Doughty, J. ., & Bolton, J. . (2006). Nitrate Poisoning of Livestock. *Extension Extra*, 2–5. Retrieved from https://www.dairylandlabs.net/media-library/documents/11-7-13-10-18_sdsu-nitrate-poisoning-of-livestock---vough2.pdf
- Delwiche, & Steyn, P. L. (1970a). Nitrogen Isotope Fractionation in Soils and Microbial Reactions. *Environmental Science and Technology*, 4(11), 929–935. <https://doi.org/10.1021/es60046a004>
- Delwiche, C. C., & Steyn, P. L. (1970b). Nitrogen isotope fractionation in soils and microbial reactions. *Environmental Science & Technology*, 4(11), 929–935.
- Dodds, W. K., Bouska, W. W., Eitzmann, J. L., Pilger, T. J., Pitts, K. L., Riley, A. J., et al. (2009). Eutrophication of U. S. freshwaters: Analysis of potential economic damages. *Environmental Science and Technology*, 43(1), 12–19. <https://doi.org/10.1021/es801217q>
- Dole, M., Lane, G. A., Rudd, D. P., & Zaukelies, D. A. (1954). Isotopic composition of atmospheric oxygen and nitrogen. *Geochimica et Cosmochimica Acta*, 6(2–3), 65–78. [https://doi.org/10.1016/0016-7037\(54\)90016-2](https://doi.org/10.1016/0016-7037(54)90016-2)
- Doner, H. E., Volz, M. G., & McLarkn, A. D. (1974). Column studies of denitrification in soil. *Soil Biology and Biochemistry*, 6(6), 341–346. [https://doi.org/https://doi.org/10.1016/0038-0717\(74\)90041-8](https://doi.org/https://doi.org/10.1016/0038-0717(74)90041-8)

- Doughton, J. A., Vallis, I., & Saffigna, P. G. (1992). An indirect method for estimating ^{15}N isotope fractionation during nitrogen fixation by a legume under field conditions. *Plant and Soil*, 144(1), 23–29. <https://doi.org/10.1007/BF00018841>
- Duffield, J. A. (2015). Effects of Policy on Ethanol Industry Growth. *U.S. Ethanol: An Examination of Policy, Production, Use, Distribution, and Market Interactions*, 1–9. Retrieved from <http://www.usda.gov/oce/energy/index.htm%0AUse>
- Einsiedl, F., Maloszewski, P., & Stichler, W. (2005). Estimation of denitrification potential in a karst aquifer using the ^{15}N and ^{18}O isotopes of NO_3^- . *Biogeochemistry*, 72(1), 67–86. <https://doi.org/10.1007/s10533-004-0375-8>
- Elliott, E. M., Kendall, C., Wankel, S. D., Burns, D. A., Boyer, E. W., Harlin, K., et al. (2007). Nitrogen isotopes as indicators of NO_x source contributions to atmospheric nitrate deposition across the midwestern and northeastern United States. *Environmental Science and Technology*, 41(22), 7661–7667. <https://doi.org/10.1021/es070898t>
- Elmi, A. A., Madramootoo, C., & Hamel, C. (2000). Influence of water table and nitrogen management on residual soil NO_3^- and denitrification rate under corn production in sandy loam soil in Quebec. *Agriculture, Ecosystems and Environment*, 79(2–3), 187–197. [https://doi.org/10.1016/S0167-8809\(99\)00157-7](https://doi.org/10.1016/S0167-8809(99)00157-7)
- Eno, C. F., Blue, W. G., & Joseph, G. (1954). The Effect of Anhydrous Ammonia on Nitrification and the Microbiological Population in Sandy Soils1. *Soil Science Society of America Journal*, 18(1), 178. <https://doi.org/10.2136/sssaj1954.03615995001800020016x>
- Environmental Protection Agency, U., & of Water, O. (2018). 2018 Edition of the Drinking Water Standards and Health Advisories Tables (EPA 822-F-18-001). *2012 Edition of the Drinking Water Standards and Health Advisories*, (March), 20. [https://doi.org/EPA 822-S-12-001](https://doi.org/EPA%20822-F-18-001)
- Fairley, D. (1999). Daily mortality and air pollution in Santa Clara County, California: 1989-1996. *Environmental Health Perspectives*, 107(8), 637–641. <https://doi.org/10.1289/ehp.99107637>
- Feigin, A., Shearer, G., Kohl, D. H., & Commoner, B. (1974). The Amount and Nitrogen-15 Content of Nitrate in Soil Profiles from two Central Illinois Fields in a Corn-Soybean Rotation1. *Soil Science Society of America Journal*. [Madison, Wis.]: <https://doi.org/10.2136/sssaj1974.03615995003800030026x>
- Fenn, M. E., Baron, J. S., Allen, E. B., Rueth, H. M., Nydick, K. R., Geiser, L., et al. (2003). Ecological effects of nitrogen deposition in the western United States. *BioScience*, 53(4), 404–420. [https://doi.org/10.1641/0006-3568\(2003\)053\[0404:EEONDI\]2.0.CO;2](https://doi.org/10.1641/0006-3568(2003)053[0404:EEONDI]2.0.CO;2)
- Fewtrell, L. (2004). Drinking-Water Nitrate, Methemoglobinemia, and Global Burden of Disease, *112*(14), 1371–1374. <https://doi.org/10.1289/ehp.7216>

- Finlayson-Pitts, B. J., & Pitts Jr, J. N. (1999). *Chemistry of the upper and lower atmosphere: theory, experiments, and applications*. Elsevier.
- Firestone, M. K., & Davidson, E. A. (1989). Microbiological Basis of NO and N₂O Production and Consumption in Soil. *Exchange of Trace Gases between Terrestrial Ecosystems and the Atmosphere*, (May), 7–21. <https://doi.org/10.1017/CBO9781107415324.004>
- Franche, C., Lindström, K., & Elmerich, C. (2009). Nitrogen-fixing bacteria associated with leguminous and non-leguminous plants. *Plant and Soil*, 321(1–2), 35–59. <https://doi.org/10.1007/s11104-008-9833-8>
- Freney, J. R., & Simpson, J. R. (1983). *Gaseous Loss of Nitrogen from Plant-Soil Systems*. Springer Netherlands. <https://doi.org/10.1007/978-94-017-1662-8>
- Freyer, H. D. (1991). Seasonal variation of ¹⁵N/¹⁴N ratios in atmospheric nitrate species. *Tellus B*. <https://doi.org/10.1034/j.1600-0889.1991.00003.x>
- Fukada, T., Hiscock, K. M., Dennis, P. F., & Grischek, T. (2003). A dual isotope approach to identify denitrification in groundwater at a river-bank infiltration site. *Water Research*, 37(13), 3070–3078. [https://doi.org/10.1016/S0043-1354\(03\)00176-3](https://doi.org/10.1016/S0043-1354(03)00176-3)
- Galloway. (1998). The global nitrogen cycle: Changes and consequences. *Environmental Pollution*, 102(SUPPL. 1), 15–24. [https://doi.org/10.1016/S0269-7491\(98\)80010-9](https://doi.org/10.1016/S0269-7491(98)80010-9)
- Galloway, Dentener, F. J., Capone, D. G., Boyer, E. W., Howarth, R. W., Seitzinger, S. P., et al. (2002). Nitrogen Cycles: Past, Present and Future. *Biogeochemistry*, 1–69.
- Galloway, Dentener, F. J., Capone, D. G., Boyer, E. W., Howarth, R. W., Seitzinger, S. P., et al. (2004). *Nitrogen cycles: Past, present, and future*. *Biogeochemistry* (Vol. 70). <https://doi.org/10.1007/s10533-004-0370-0>
- Galloway, Trends, R., Townsend, A. R., Erisman, J. W., Bekunda, M., Cai, Z., et al. (2008). Transformation of the Nitrogen Cycle : Potential Solutions. *Science*, 320(2008), 889–892. <https://doi.org/10.1126/science.1136674>
- Garcia-Ruiz, Garci, R., & Whitton, B. A. (1998). Kinetic Parameters of Denitrification in a River Continuum †, 64(7), 2533–2538.
- Garten, C. T. (1992). Nitrogen isotope composition of ammonium and nitrate in bulk precipitation and forest throughfall. *International Journal of Environmental Analytical Chemistry*, 47(1), 33–45. <https://doi.org/10.1080/03067319208027017>
- Gat, J. R. (1996). Oxygen and Hydrogen Isotopes in the Hydrologic Cycle. *Annual Review of Earth and Planetary Sciences*, 24(1), 225–262. <https://doi.org/10.1146/annurev.earth.24.1.225>
- Gat, J. R. (1998). Oxygen and Hydrogen Isotopes in the Hydrologic Cycle, 1–38. <https://doi.org/10.1146/annurev.earth.24.1.225>

- Gat, J. R., & Gonfiantini, R. (1981). *Stable isotope hydrology*.
- Ge, S., Peng, Y., Wang, S., Lu, C., Cao, X., & Zhu, Y. (2012). Bioresource Technology Nitrite accumulation under constant temperature in anoxic denitrification process: The effects of carbon sources and COD / NO₃⁻-N. *Bioresource Technology*, *114*, 137–143. <https://doi.org/10.1016/j.biortech.2012.03.016>
- Geisseler, D., Horwath, W. R., Joergensen, R. G., & Ludwig, B. (2010). Pathways of nitrogen utilization by soil microorganisms - A review. *Soil Biology and Biochemistry*, *42*(12), 2058–2067. <https://doi.org/10.1016/j.soilbio.2010.08.021>
- Gentry, L. E., David, M. B., Smith, K. M., & Kovacic, D. A. (1998). Nitrogen cycling and tile drainage nitrate loss in a corn/soybean watershed. *Agriculture, Ecosystems and Environment*, *68*(1–2), 85–97. [https://doi.org/10.1016/S0167-8809\(97\)00139-4](https://doi.org/10.1016/S0167-8809(97)00139-4)
- Gentry, L. E., David, M. B., Below, F. E., Royer, T. V., & McIsaac, G. F. (2009). Nitrogen Mass Balance of a Tile-drained Agricultural Watershed in East-Central Illinois. *Journal of Environment Quality*, *38*(5), 1841. <https://doi.org/10.2134/jeq2008.0406>
- Gericke, D. (1992). Frühdiagnose rettet Menschenleben--Zur Situation bei den kolorektalen Tumoren. *Versicherungsmedizin / Herausgegeben von Verband Der Lebensversicherungs-Unternehmen e.V. Und Verband Der Privaten Krankenversicherung e.V.*, *44*(2), 60–63. <https://doi.org/10.1073/pnas.1206191109>
- Ghaly, & Ramakrishnan. (2013). Nitrification of Urea and Assimilation of Nitrate in Saturated Soils Under Aerobic Conditions, (July). <https://doi.org/10.3844/ajabssp.2013.330.342>
- Gillam, K. M., Zebarth, B. J., & Burton, D. L. (2008). Nitrous oxide emissions from denitrification and the partitioning of gaseous losses as affected by nitrate and carbon addition and soil aeration. *Canadian Journal of Soil Science*, *88*, 133–143. <https://doi.org/10.4141/CJSS06005>
- Glass, & Sliverstein. (1998). Denitrification Kinetics of High Nitrate Concentration Water: pH Effect on Inhibition and Nitrite Accumulation, *1354*(March 2018), 1–10. [https://doi.org/10.1016/S0043-1354\(97\)00260-1](https://doi.org/10.1016/S0043-1354(97)00260-1)
- Golterman, H. L., & Chalamet, A. (2013). Effects of Environmental Factors on Denitrification. *Denitrification in the Nitrogen Cycle*. Boston, MA: https://doi.org/10.1007/978-1-4757-9972-9_2
- Goreau, T. J., Kaplan, W. A., Wofsy, S. C., Mcelroy, M. B., Valois, F. W., & Watson, S. W. (1980). Production of NO₂⁻ and N₂O by Nitrifying Bacteria at Reduced Concentrations of Oxygen, *40*(3), 526–532.
- Granger, J., & Wankel, S. D. (2016). Isotopic overprinting of nitrification on denitrification as a ubiquitous and unifying feature of environmental nitrogen cycling. *Proceedings of the National Academy of Sciences*, *113*(42), E6391–E6400. <https://doi.org/10.1073/pnas.1601383113>

- Granger, J., Vt, C., Sigman, D. M., Needoba, J. A., & Harrison, P. J. (2004). Granger & Sigman (2004)L&O .pdf, 49(5), 1763–1773. <https://doi.org/10.4319/lo.2004.49.5.1763>
- Granger, J., Sigman, D. M., Prokopenko, M. G., Lehmann, M. F., & Tortell, P. D. (2006). OCEANOGRAPHY : METHODS A method for nitrite removal in nitrate N and O isotope analyses, 205–212.
- Granger, J., Sigman, D. M., Lehmann, M. F., & Tortell, P. D. (2008). Nitrogen and oxygen isotope fractionation during dissimilatory nitrate reduction by denitrifying bacteria. *Limnology and Oceanography*, 53(6), 2533–2545. <https://doi.org/10.4319/lo.2008.53.6.2533>
- Groffman, P. M., Davidson, E. A., & Seitzinger, S. (2009). New approaches to modeling denitrification. *Biogeochemistry*, 93(1–2), 1–5. <https://doi.org/10.1007/s10533-009-9285-0>
- Grundmann, G. L., Renault, P., Rosso, L., & Bardin, R. (1995). Differential Effects of Soil Water Content and Temperature on Nitrification and Aeration. *Soil Science Society of America Journal*, 59(5), 1342. <https://doi.org/10.2136/sssaj1995.03615995005900050021x>
- Hagopian, D. S., & Riley, J. G. (1998). A closer look at the bacteriology of nitrification. *Aquacultural Engineering*, 18(4), 223–244. [https://doi.org/https://doi.org/10.1016/S0144-8609\(98\)00032-6](https://doi.org/https://doi.org/10.1016/S0144-8609(98)00032-6)
- Harms, T. K., & Grimm, N. B. (2008). Hot Spots and Hot Moments of Carbon and Nitrogen Dynamics in a Semiarid Riparian Zone. *Journal of Geophysical Research: Biogeosciences*, 113(1), 1–14. <https://doi.org/10.1029/2007JG000588>
- Hart, S., Stark, J. M., Davidson, E., & Firestone, M. K. (1994). *Nitrogen mineralization, immobilization, and nitrification. Nitrogen Mineralization, Immobilization, and Nitrification.*
- Hastings, M. G., Sigman, D. M., & Lipschultz, F. (2003). Isotopic evidence for source changes of nitrate in rain at Bermuda. *Journal of Geophysical Research: Atmospheres*, 108(D24), n/a-n/a. <https://doi.org/10.1029/2003JD003789>
- Hatfield, J. L., & Keeney, D. R. (2008). Chapter 1 . The Nitrogen Cycle , Historical Perspective , and Current and Potential Future Concerns. *Nitrogen in the Environment: Sources, Problems, and Management*, 1–18.
- Heaton, T. H. . (1986). Isotopic studies of nitrogen pollution in the hydrosphere and atmosphere: A review. *Chemical Geology: Isotope Geoscience Section*, 59, 87–102. [https://doi.org/10.1016/0168-9622\(86\)90059-X](https://doi.org/10.1016/0168-9622(86)90059-X)
- Her, J.-J., & Huang, J.-S. (1995). Influences of carbon source and C/N ratio on nitrate/nitrite denitrification and carbon breakthrough. *Bioresource Technology*, 54(1), 45–51. [https://doi.org/https://doi.org/10.1016/0960-8524\(95\)00113-1](https://doi.org/https://doi.org/10.1016/0960-8524(95)00113-1)

- Hoering, T. C., & Ford, H. T. (1960). The Isotope Effect in the Fixation of Nitrogen by Azotobacter. *Journal of the American Chemical Society*, 82(2), 376–378. <https://doi.org/10.1021/ja01487a031>
- Hoffman, B. M., Lukoyanov, D., Yang, Z. Y., Dean, D. R., & Seefeldt, L. C. (2014). Mechanism of nitrogen fixation by nitrogenase: The next stage. *Chemical Reviews*, 114(8), 4041–4062. <https://doi.org/10.1021/cr400641x>
- Hofstra, N., & Bouwman, A. F. (2005). Denitrification in agricultural soils: Summarizing published data and estimating global annual rates. *Nutrient Cycling in Agroecosystems*, 72(3), 267–278. <https://doi.org/10.1007/s10705-005-3109-y>
- Hogberg, P., Hogbom, L., Schinkel, H., Hogberg, M., Johannisson, C., & Wallmark, H. (1996). ¹⁵N abundance of surface soils, roots and mycorrhizas in profiles of European forest soils. *Oecologia*, 108(2), 207–214. <https://doi.org/10.1007/BF00334643>
- Högberg, P. (1997). Tansley review no. 95 natural abundance in soil-plant systems. *New Phytologist*, 137(2), 179–203. <https://doi.org/10.1046/j.1469-8137.1997.00808.x>
- Hollocher, T. C. (1984). Source of the oxygen atoms of nitrate in the oxidation of nitrite by Nitrobacter agilis and evidence against a P-O-N anhydride mechanism in oxidative phosphorylation. *Archives of Biochemistry and Biophysics*, 233(2), 721–727. [https://doi.org/10.1016/0003-9861\(84\)90499-5](https://doi.org/10.1016/0003-9861(84)90499-5)
- Horibe, Y., Shigehara, K., & Takakuwa, Y. (2018). Isotope separation factor of carbon dioxide-water system and isotopic composition of atmospheric oxygen. *Journal of Geophysical Research*, 78(15), 2625–2629. <https://doi.org/10.1029/JC078i015p02625>
- Hsieh, J. C. C., Chadwick, O. A., Kelly, E. F., & Savin, S. M. (1998). Oxygen isotopic composition of soil water: Quantifying evaporation and transpiration. *Geoderma*, 82(1–3), 269–293. [https://doi.org/10.1016/S0016-7061\(97\)00105-5](https://doi.org/10.1016/S0016-7061(97)00105-5)
- Hu, S., Zeng, R. J., Keller, J., Lant, P. A., & Yuan, Z. (2011). Effect of nitrate and nitrite on the selection of microorganisms in the denitrifying anaerobic methane oxidation process. *Environmental Microbiology Reports*, 3(3), 315–319. <https://doi.org/10.1111/j.1758-2229.2010.00227.x>
- Hwang, J. H., & Oleszkiewicz, J. A. (2007). Effect of Cold-Temperature Shock on Nitrification. *Water Environment Research*, 79(9), 964–968. <https://doi.org/10.2175/106143007X176022>
- Johnson, C., Albrecht, G., Ketterings, Q., Beckman, J., & Stockin, K. (2005). Nitrogen Basics – The Nitrogen Cycle. *Cornell University Cooperative Extension*. Retrieved from <http://nmsp.css.cornell.edu>
- Kanwar, R. S., Baker, J. L., Johnson, H. P., & Kirkham, D. (1980). Nitrate Movement with Zero-order Denitrification in a Soil Profile1. *Soil Science Society of America Journal*. [Madison, Wis.]: <https://doi.org/10.2136/sssaj1980.03615995004400050003x>

- Kanwar, R. S., Johnson, H. P., & Kirkham, D. (1982). Transport of Nitrate and Gaseous Denitrification in Soil Columns During Leaching, *55*(2058).
- Karamanos, R. E., & Rennie, D. A. (1978). Nitrogen isotope fractionation during ammonium exchange reactions with soil clay. *Canadian Journal of Soil Science*, *58*(1), 53–60.
- Kaushal, S. S., Groffman, P. M., Band, L. E., Elliott, E. M., Shields, C. A., & Kendall, C. (2011). Tracking nonpoint source nitrogen pollution in human-impacted watersheds. *Environmental Science and Technology*, *45*(19), 8225–8232. <https://doi.org/10.1021/es200779e>
- Keller, C. K., Butcher, C. N., Smith, J. L., & Allen-King, R. M. (2008). Nitrate in Tile Drainage of the Semiarid Palouse Basin. *Journal of Environment Quality*, *37*(2), 353. <https://doi.org/10.2134/jeq2006.0515>
- Kelley, C. J., Keller, C. K., Evans, R. D., Orr, C. H., Smith, J. L., & Harlow, B. A. (2013). Nitrate-nitrogen and oxygen isotope ratios for identification of nitrate sources and dominant nitrogen cycle processes in a tile-drained dryland agricultural field. *Soil Biology and Biochemistry*, *57*, 731–738. <https://doi.org/10.1016/j.soilbio.2012.10.017>
- Kellman, L. M. (2005). A study of tile drain nitrate - $\delta^{15}\text{N}$ values as a tool for assessing nitrate sources in an agricultural region. *Nutrient Cycling in Agroecosystems*, *71*(2), 131–137. <https://doi.org/10.1007/s10705-004-1925-0>
- Kellman, L. M., & Hillaire-Marcel, C. (2003). Evaluation of nitrogen isotopes as indicators of nitrate contamination sources in an agricultural watershed. *Agriculture, Ecosystems and Environment*, *95*(1), 87–102. [https://doi.org/10.1016/S0167-8809\(02\)00168-8](https://doi.org/10.1016/S0167-8809(02)00168-8)
- Kendall, C., & Aravena, R. (2000). *Environmental Tracers in Subsurface Hydrology*. <https://doi.org/10.1007/978-1-4615-4557-6>
- Kendall, C., & McDonnell, J. (1998). *Isotope Tracers in Catchment Hydrology*. *Isotope Tracers in Catchment Hydrology*. Amsterdam: Elsevier Science B.V. <https://doi.org/10.1016/B978-0-444-81546-0.50024-0>
- Kendall, C., States, U., & Survey, G. (2000). *Environmental Tracers in Subsurface Hydrology*. <https://doi.org/10.1007/978-1-4615-4557-6>
- Kimball, B. K., Boote, J., Hatfield, L. R., Ahuja, C., Stockle, S. V., Archontoulis, C., & Baron, B. B. (2016). Prediction of evapotranspiration and yields of maize: An inter-comparison among 29 maize models. Phoenix, AZ.
- Kirda, C., Starr, J. L., Misra, C., Biggar, J. W., & Nielsen, D. R. (1974). Nitrification and Denitrification during Miscible Displacement in Unsaturated Soil. *Soil Science Society of America Journal*. <https://doi.org/10.2136/sssaj1974.03615995003800050024x>

- Kladivko, E. J., Scoyoc, G. E. Van, Monke, E. J., Oates, K. M., & Pask, W. (1991). Pesticide and nutrient movement into subsurface tile drains on a silt loam soil in Indiana. *Journal of Environmental Quality*, 20(1), 264–270. <https://doi.org/10.2134/jeq1991.00472425002000010043x>
- Knöller, K., Vogt, C., Haupt, M., Feisthauer, S., & Richnow, H. H. (2011). Experimental investigation of nitrogen and oxygen isotope fractionation in nitrate and nitrite during denitrification. *Biogeochemistry*, 103(1), 371–384. <https://doi.org/10.1007/s10533-010-9483-9>
- Kool, van Groenigen, J. W., Wrage, N., & Oenema, O. (2007). Can ^{18}O analysis be used to distinguish N_2O producing pathways in the soil?
- Kool, Wrage, N., Oenem, O., Dolfing, J., & van Groenigen, J. W. (2007). Oxygen Exchange between (de)nitrification intermediates and H_2O and its implications for source determination of NO_3^- and N_2O : a review. *Rapid Communication in Mass Spectrometry*, 21, 3569–3578. <https://doi.org/10.1002/rcm>
- Kool, Wrage, N., Zechmeister-Boltenstern, S., Pfeffer, M., Brus, D., Oenema, O., & Van Groenigen, J. W. (2010). Nitrifier denitrification can be a source of N_2O from soil: A revised approach to the dual-isotope labelling method. *European Journal of Soil Science*, 61(5), 759–772. <https://doi.org/10.1111/j.1365-2389.2010.01270.x>
- Kool, Dolfing, J., Wrage, N., & Van Groenigen, J. W. (2011). Nitrifier denitrification as a distinct and significant source of nitrous oxide from soil. *Soil Biology and Biochemistry*, 43(1), 174–178. <https://doi.org/10.1016/j.soilbio.2010.09.030>
- Kool, D., Wrage, N., Oenema, O., Van Kessel, C., & Van Groenigen, J. W. (2011). Oxygen exchange with water alters the oxygen isotopic signature of nitrate in soil ecosystems. *Soil Biology and Biochemistry*, 43(6), 1180–1185. <https://doi.org/10.1016/j.soilbio.2011.02.006>
- Kroopnick, P., & Craig, H. (1972). Atmospheric Oxygen: Isotopic Composition and Solubility Fractionation. *Science*, 175(4017), 54 LP-55. Retrieved from <http://science.sciencemag.org/content/175/4017/54.abstract>
- Kumar, Nicholas, D. J. D., & Williams, E. H. (1983). Definitive ^{15}N NMR evidence that water serves as a source of “O” during nitrite oxidation by *Nitrobacter agilis*. *FEBS Letters*, 152(1), 71–74. [https://doi.org/10.1016/0014-5793\(83\)80484-0](https://doi.org/10.1016/0014-5793(83)80484-0)
- Kumar, P., Le, P. V. V., Papanicolaou, A. N. T., Rhoads, B. L., Anders, A. M., Stumpf, A., et al. (2018). Critical transition in critical zone of intensively managed landscapes. *Anthropocene*, 22, 10–19. <https://doi.org/10.1016/j.ancene.2018.04.002>
- Kuypers, M. M. M., Marchant, H. K., & Kartal, B. (2018). The microbial nitrogen-cycling network. *Nature Reviews Microbiology*, 16(5), 263–276. <https://doi.org/10.1038/nrmicro.2018.9>
- Laidler, J. (1955). Some kinetic and mechanistic aspects of hydrolytic enzyme action, 83–96.

- Lavaire, T., Gentry, L. E., David, M. B., & Cooke, R. A. (2017). Fate of water and nitrate using drainage water management on tile systems in east-central Illinois. *Agricultural Water Management*, *191*, 218–228. <https://doi.org/10.1016/j.agwat.2017.06.004>
- Ledgard, S. F. (1989). Nutrition, moisture and rhizobial strain influence isotopic fractionation during N₂ fixation in pasture legumes. *Soil Biology and Biochemistry*, *21*(1), 65–68. [https://doi.org/https://doi.org/10.1016/0038-0717\(89\)90012-6](https://doi.org/https://doi.org/10.1016/0038-0717(89)90012-6)
- Lehmann, J., & Schroth, G. (2002). Trees, crops and soil fertility: concepts and research methods. *Trees, Crops, and Soil Fertility*, 151–166. <https://doi.org/10.1079/9780851995939.0000>
- Liang, B. C., & Mackenzie, A. F. (1997). Seasonal denitrification rates under corn (*Zea mays* L .) in two Quebec soils. *Canadian Journal of Soil Science*, *77*(1), 21–25. <https://doi.org/10.4141/S96-018>
- Licht, M., & Archontoulis, S. (2017). Corn Water Use and Evapotranspiration.
- Limmer, & Steele. (1982). Denitrification Potentials : Measurement Seasonal Vaiation Using a Short-Term Anaerobic Incubations Technique, *14*, 1–6.
- Linn, D. M., & Doran, J. W. (1982). Effect of Water-Filled Pore Space on Carbon Dioxide and Nitrous Oxide Production in Tilled and Nontilled Soils 1, (1961), 1267–1272.
- Liu, T., Wang, F., Michalski, G., Xia, X., & Liu, S. (2013). Using ¹⁵N, ¹⁷O, and ¹⁸O To Determine Nitrate Sources in the Yellow River, China. *Environmental Science & Technology*, *47*(23), 13412–13421. <https://doi.org/10.1021/es403357m>
- Luxhøi, J., Fillery, I. R. P., Murphy, D. V., Bruun, S., Jensen, L. S., & Recous, S. (2008). Distribution and controls on gross N mineralization-immobilization-turnover in soil subjected to zero tillage. *European Journal of Soil Science*, *59*(2), 190–197. <https://doi.org/10.1111/j.1365-2389.2007.00969.x>
- Lynch, J. A., Bowersox, V. C., & Grimm, J. W. (2000). Acid rain reduced in Eastern United States. *Environmental Science and Technology*, *34*(6), 940–949. <https://doi.org/10.1021/es9901258>
- Macko. (1987). Isotopic Fractionation of Nitrogen and Carbon in the Synthesis of Amino Acids by Microorganisms, *9622*(December 2017). [https://doi.org/10.1016/0168-9622\(87\)90064-9](https://doi.org/10.1016/0168-9622(87)90064-9)
- Maggi, F., & Riley, W. J. (2009). Transient competitive complexation in biological kinetic isotope fractionation explains nonsteady isotopic effects: Theory and application to denitrification in soils, *114*, 1–13. <https://doi.org/10.1029/2008JG000878>
- Maggi, F., & Riley, W. J. (2015). The effect of temperature on the rate, affinity, and ¹⁵N fractionation of NO₃–during biological denitrification in soils. *Biogeochemistry*, *124*(1–3), 235–253. <https://doi.org/10.1007/s10533-015-0095-2>

- Mariotti. (1982). Nitrogen Isotope Fractionation Associated with the NO₂ to N₂O Step of Denitrification in Soils. *Canadian Journal of Soil Science*, (2).
- Mariotti, Germon, J. C., Hubert, P., Kaiser, P., Letolle, R., Tardieux, A., & Tardieux, P. (1981). Experimental determination of nitrogen kinetic isotope fractionation: Some principles; illustration for the denitrification and nitrification processes. *Plant and Soil*, 62(3), 413–430. <https://doi.org/10.1007/BF02374138>
- Mariotti, A., Landreau, A., & Simon, B. (1988). ¹⁵N isotope biogeochemistry and natural denitrification process in groundwater: Application to the chalk aquifer of northern France. *Geochimica et Cosmochimica Acta*, 52(7), 1869–1878. [https://doi.org/10.1016/0016-7037\(88\)90010-5](https://doi.org/10.1016/0016-7037(88)90010-5)
- Martens, D. A. (2005). Denitrification. In D. Hillel (Ed.), *Encyclopedia of Soils in the Environment* (pp. 378–382). Oxford: Elsevier. <https://doi.org/https://doi.org/10.1016/B0-12-348530-4/00138-7>
- Mayer, B., Bollwerk, S. M., Mansfeldt, T., Hütter, B., & Veizer, J. (2001). The oxygen isotope composition of nitrate generated by nitrification in acid forest floors. *Geochimica et Cosmochimica Acta*, 65(16), 2743–2756. [https://doi.org/10.1016/S0016-7037\(01\)00612-3](https://doi.org/10.1016/S0016-7037(01)00612-3)
- Mengis, M., Schif, S. L., Harris, M., English, M. C., Aravena, R., Elgood, R. J., & MacLean, A. (2005). Multiple Geochemical and Isotopic Approaches for Assessing Ground Water NO₃⁻ Elimination in a Riparian Zone. *Groundwater*, 37(3), 448–457. <https://doi.org/10.1111/j.1745-6584.1999.tb01124.x>
- Menyailo, O. V., & Hungate, B. A. (2006). Stable isotope discrimination during soil denitrification: Production and consumption of nitrous oxide. *Global Biogeochemical Cycles*, 20(3), 1–10. <https://doi.org/10.1029/2005GB002527>
- Michalski, G., Savarino, J., Böhlke, J. K., & Thiemens, M. (2002). Determination of the Total Oxygen Isotopic Composition of Nitrate and the Calibration of a Δ¹⁷O Nitrate Reference Material. *Analytical Chemistry*, 74(19), 4989–4993. <https://doi.org/10.1021/ac0256282>
- Michalski, G., Earman, S., Dahman, C., L Hershey, R., & Mihevc, T. (2010). *Multiple isotope forensics of nitrate in a wild horse poisoning incident*. *Forensic science international* (Vol. 198). <https://doi.org/10.1016/j.forsciint.2010.01.012>
- Michalski, G., Bhattacharya, S. K., & Mase, D. (2012). Handbook of environmental isotope geochemistry. In *Handbook of Environmental Isotope Geochemistry* (Vol. 1–2, pp. 1–951). <https://doi.org/10.1007/978-3-642-10637-8>
- Michalski, G., Kolanowski, M., & Riha, K. M. (2015). Oxygen and nitrogen isotopic composition of nitrate in commercial fertilizers, nitric acid, and reagent salts. *Isotopes in Environmental and Health Studies*, 51(3), 382–391. <https://doi.org/10.1080/10256016.2015.1054821>

- Moir, J. W. B. (2011). *Nitrogen cycling in bacteria: molecular analysis*. Horizon Scientific Press.
- Monod, J. (1949). The Growth of Bacterial Cultures. *Annual Review of Microbiology*, 3(1), 371–394.
- Moore, & Schroeder, E. D. (1971). The Effect of Nitrate Feed Rate on Denitrification. *Water Research*, 5, 445–452.
- Moore, H. (1977). the Isotopic Composition of Ammonia , Nitrogen Dioxide and Nitrate in the Atmosphere. *Atmosphpric Enuirontwnt*, 11, 1239–1243.
- Nadelhoffer, & Fry, B. (1994). N-isotope studies in forests. *Stable Isotopes in Ecology and Environmental Sciences.*, 22–62. https://doi.org/10.1007/978-3-642-10665-1_23
- NADP Program Office. (2012). National Atmospheric Deposition Program. Retrieved from <http://nadp.sws.uiuc.edu/nadpdata/annualReq.asp?site=AK97>
- National Agricultural Statistics Survey. (2018). Crop production 2017 summary, (January), 2017–2018. [https://doi.org/ISSN: 1057-7823](https://doi.org/ISSN:1057-7823).
- Nicol, G. W., & Prosser, J. I. (2010). Archaea rather than bacteria control nitrification in two agricultural acidic soils ´, 74, 566–574. <https://doi.org/10.1111/j.1574-6941.2010.00971.x>
- Nielsen, R. L. B. (2000). *Corn Growth & Development What Goes On From Planting To Harvest* (Vol. 07).
- Nielsen, T. H., & Revsbech, N. P. (1998). Nitrification, denitrification, and N-liberation associated with two types of organic hot-spots in soil. *Soil Biology and Biochemistry*, 30(5), 611–619. [https://doi.org/10.1016/S0038-0717\(97\)00211-3](https://doi.org/10.1016/S0038-0717(97)00211-3)
- Nikolenko, O., Jurado, A., Borges, A. V., Knöller, K., & Brouyère, S. (2018). Isotopic composition of nitrogen species in groundwater under agricultural areas: A review. *Science of the Total Environment*, 621, 1415–1432. <https://doi.org/10.1016/j.scitotenv.2017.10.086>
- Norton, J. M., & Stark, J. M. (2010). Regulation and measurement of nitrification in terrestrial systems. *Methods in Enzymology*, 486(C), 343–368. <https://doi.org/10.1016/B978-0-12-381294-0.00015-8>
- Oelmann, Y., Kreuziger, Y., Bol, R., & Wilcke, W. (2007). Nitrate leaching in soil: Tracing the NO₃⁻ sources with the help of stable N and O isotopes. *Soil Biology and Biochemistry*, 39(12), 3024–3033. <https://doi.org/10.1016/j.soilbio.2007.05.036>
- Osaka, K., Nakajima, Y., Suzuki, K., Eguchi, S., & Katou, H. (2018). Nitrogen and oxygen isotope enrichment factors of nitrate at different denitrification rates in an agricultural soil. *Soil Science and Plant Nutrition*, 64(5), 558–565. <https://doi.org/10.1080/00380768.2018.1504321>

- Ostrom, N. E., Knoke, K. E., Hedin, L. O., Robertson, G. P., & Smucker, A. J. . (1998). Temporal trends in nitrogen isotope values of nitrate leaching from an agricultural soil. *Chemical Geology*, 146(3–4), 219–227. [https://doi.org/10.1016/S0009-2541\(98\)00012-6](https://doi.org/10.1016/S0009-2541(98)00012-6)
- Ostrom, N. E., Pitt, A., Sutka, R., Ostrom, P. H., Grandy, A. S., Huizinga, K. M., & Robertson, G. P. (2007). Isotopologue effects during N₂O reduction in soils and in pure cultures of denitrifiers, 112, 1–12. <https://doi.org/10.1029/2006JG000287>
- Overdahl, C. J., & Rehm, G. W. (1990). *Using Anhydrous Ammonia in Minnesota*.
- Parkin, T. B. (1987). Soil Microsites as a Source of Denitrification Variability, 1–6.
- Paul, E. A., & Clark, F. E. (1989). Occurrences and distribution of soil organics. *Soil Microbiology and Biochemistry*. Academic Press, San Diego, 81–84.
- Pilegaard, K. (2013). Processes regulating nitric oxide emissions from soils. *Philos Trans R Soc Lond B Biol Sci*, 368(1621), 20130126. <https://doi.org/10.1098/rstb.2013.0126>
- Powlson, D. S., Addiscott, T. M., Benjamin, N., Cassman, K. G., de Kok, T. M., van Grinsven, H., et al. (2008). When Does Nitrate Become a Risk for Humans *Journal of Environment Quality*, 37(2), 291. <https://doi.org/10.2134/jeq2007.0177>
- Recous, S., Robin, D., Darwis, D., & Mary, B. (1995). Soil inorganic N availability: Effect on maize residue decomposition. *Soil Biology and Biochemistry*, 27(12), 1529–1538. [https://doi.org/10.1016/0038-0717\(95\)00096-W](https://doi.org/10.1016/0038-0717(95)00096-W)
- Reddy, K. R., Patrick, W. H., & Phillips, R. E. (1978). The Role of Nitrate Diffusion in Determining the Order and Rate of Denitrification in.
- Rihn, K. (2013). *Thesis / Dissertation Acceptance*.
- Robinson, D. (2001). $\delta^{15}\text{N}$ as an integrator of the nitrogen. *Trends in Ecology & Evolution*, 16(3), 153–162. [https://doi.org/10.1016/s0169-5347\(00\)02098-x](https://doi.org/10.1016/s0169-5347(00)02098-x)
- Sabey, B. R. (1968). The Influence of Nitrification Suppressants on the Rate of Ammonium Oxidation in Midwestern USA field Soils. *Soil Sci. Soc. Am*, 32, 675–679.
- Sabey, B. R., Bartholomew, W. V., Shaw, R., & Pesek, J. (1956). Influence of Temperature on Nitrification in Soils. *Soil Science Society of America Journal*, 20, 357. <https://doi.org/10.2136/sssaj1956.03615995002000030016x>
- Samet, J. M., Dominici, F., Curriero, F. C., Coursac, I., & Zeger, S. L. (2000). Fine Particulate Air Pollution and Mortality in 20 U.S. Cities, 1987–1994. *New England Journal of Medicine*, 343(24), 1742–1749. <https://doi.org/10.1056/NEJM200012143432401>
- Santoro, A. E., & Casciotti, K. L. (2011). Enrichment and characterization of ammonia-oxidizing archaea from the open ocean: phylogeny, physiology and stable isotope fractionation. *The ISME Journal*, 5(11), 1796–1808. <https://doi.org/10.1038/ismej.2011.58>

- Sawyer, J., & Mallarino, A. (2007). Nutrient removal when harvesting corn stover. *Integrated Crop Management Newsletter*, 2012(30 January). Retrieved from <http://www.ipm.iastate.edu/ipm/icm/2007/8-6/nutrients.html>
- Scherer, H. W. (1993). Dynamics and availability of the non-exchangeable $\text{NH}_4\text{-N}$ — a review. *European Journal of Agronomy*, 2(3), 149–160. [https://doi.org/https://doi.org/10.1016/S1161-0301\(14\)80124-X](https://doi.org/https://doi.org/10.1016/S1161-0301(14)80124-X)
- Schlesinger, W. H. (2009). On the fate of anthropogenic nitrogen. *Proceedings of the National Academy of Sciences*, 106(1), 203–208. <https://doi.org/10.1073/pnas.0810193105>
- Sebilo, M., Billen, G., Mayer, B., Billiou, D., Grably, M., Garnier, J., & Mariotti, A. (2006). Assessing nitrification and denitrification in the seine river and estuary using chemical and isotopic techniques. *Ecosystems*, 9(4), 564–577. <https://doi.org/10.1007/s10021-006-0151-9>
- Seinfeld, J. H., & Pandis, S. N. (2006). Dynamics of Aerosol Populations. *Atmospheric Chemistry and Physics: From Air Pollution to Climate Change*, 588–627.
- Seinfeld, J. H., & Pandis, S. N. (2012). *Atmospheric chemistry and physics: from air pollution to climate change*. John Wiley & Sons.
- Selman, M., Greenhalgh, S., Diaz, R., & Sugg, Z. (2008). Eutrophication and Hypoxia in Costal Areas: A Global Assessment of the State of Knowledge. *WRI* (1), 1–6.
- Shearer, G., & Kohl, D. H. (1988). Nitrogen isotopic fractionation and ^{18}O exchange in relation to the mechanism of denitrification of nitrite by *Pseudomonas stutzeri*. *Journal of Biological Chemistry*, 263(26), 13231–13245.
- Sigman, D., Karsh, K., & Casciotti, K. (2009). Ocean Process Tracers: Nitrogen Isotopes in the Ocean. *Encyclopedia of Ocean Sciences*, 4138–4153. <https://doi.org/10.1006/rwos.2001.0172>
- Smith, & Tiedje, J. M. (1978). Phases of Denitrification Following Oxygen Depletion in Soil. *Soil Biol. Biochem*, 11, 261–267.
- Smith, M. F., Tiedje, R. B., & M, F. J. (1979). Influence of Nitrate, Nitrite, and Oxygen on the Composition of the Gaseous Products of Denitrification in Soil, The, (January 1979). <https://doi.org/10.2136/sssaj1979.03615995004300060016x>
- Smith, E. L., & Kellman, L. M. (2011). Examination of nitrate concentration, loading and isotope dynamics in subsurface drainage under standard agricultural cropping in Atlantic Canada. *Journal of Environmental Management*, 92(11), 2892–2899. <https://doi.org/10.1016/j.jenvman.2011.06.043>
- Snider, D. M., Schiff, S. L., & Spoelstra, J. (2009). $^{15}\text{N}/^{14}\text{N}$ and $^{18}\text{O}/^{16}\text{O}$ stable isotope ratios of nitrous oxide produced during denitrification in temperate forest soils. *Geochimica et Cosmochimica Acta*, 73(4), 877–888. <https://doi.org/10.1016/j.gca.2008.11.004>

- Snider, D. M., Spoelstra, J., Schiff, S. L., & Venkiteswaran, J. J. (2010). Stable Oxygen Isotope Ratios of Nitrate Produced from Nitrification: ^{18}O -Labeled Water Incubations of Agricultural and Temperate Forest Soils. *Environmental Science & Technology*, *44*(14), 100615134113072. <https://doi.org/10.1021/es1002567>
- Sobota, D. J., Compton, J. E., McCrackin, M. L., & Singh, S. (2015). Cost of reactive nitrogen release from human activities to the environment in the United States. *Environmental Research Letters*, *10*(2), 25006. <https://doi.org/10.1088/1748-9326/10/2/025006>
- Sommer, S. G., & Christensen, B. T. (1992). Ammonia volatilization after injection of anhydrous ammonia into arable soils of different moisture levels. *Plant and Soil*, *142*, 143–146. <https://doi.org/10.1007/BF00010184>
- Spalding, R. F., & Exner, M. E. (1993). Occurrence of Nitrate in Groundwater—A Review. *Journal of Environment Quality*, *22*(3), 392. <https://doi.org/10.2134/jeq1993.00472425002200030002x>
- Starr, J. L., & Parlange, J.-Y. (1975). Nonlinear Denitrification Kinetics with Continuous Flow in Soil Columns. *Soil Science Society of America Journal*. [Madison, Wis.]: <https://doi.org/10.2136/sssaj1975.03615995003900050026x>
- Starr, J. L., & Parlange, J.-Y. (1976). Relation Between the Kinetics of Nitrogen Transformation and Biomass Distribution in a Soil Column During Continuous Leaching. *Soil Science Society of America Journal*. [Madison, Wis.]: <https://doi.org/10.2136/sssaj1976.03615995004000030040x>
- Steele, K. W., Bonish, P. M., Daniel, R. M., & O'hara, G. W. (1983). Effect of Rhizobial Strain and Host Plant on Nitrogen Isotopic Fractionation in Legumes. *Plant Physiol*, *72*, 1001–1004. <https://doi.org/10.1104/pp.72.4.1001>
- Stoyan, H., De-Polli, H., Böhm, S., Robertson, G. P., & Paul, E. A. (2000). Spatial heterogeneity of soil respiration and related properties at the plant scale. *Plant and Soil*, *222*(1), 203–214. <https://doi.org/10.1023/A:1004757405147>
- Syakila, A., Kroeze, C., & Kroeze, C. (2011). The global nitrous oxide budget revisited The global nitrous oxide budget revisited, 0779. <https://doi.org/10.3763/ghgmm.2010.0007>
- Tiedje, J. M. (1988). Ecology of denitrification and dissimilatory nitrate reduction to ammonium. *Environmental Microbiology of Anaerobes*, (April), 179–244. <https://doi.org/10.1016/j.jacc.2011.09.010>
- Unkovich, M. (2013). Isotope discrimination provides new insight into biological nitrogen fixation. *New Phytologist*, *198*(3), 643–646. <https://doi.org/10.1111/nph.12227>
- USDA. (2009). *2007 Census of Agriculture*.
- USDA. (2017). Web Soil Survey Natural Resources Conservation Service, United States Department of Agriculture. Web Soil Survey.

- USEPA. (2018). United States Environmental Protection Agency Clean Air Status and Trends Network (CASTNet).
- Vachon, R. W., Welker, J. M., White, J. W. C., & Vaughn, B. H. (2010). Monthly precipitation isoscapes ($\delta^{18}\text{O}$) of the United States: Connections with surface temperatures, moisture source conditions, and air mass trajectories. *Journal of Geophysical Research Atmospheres*, *115*(21), 1–17. <https://doi.org/10.1029/2010JD014105>
- Vavilin, & Rytov. (2015). Chemosphere Nitrate denitrification with nitrite or nitrous oxide as intermediate products : Stoichiometry , kinetics and dynamics of stable isotope signatures, *134*, 417–426.
- Venterea, R. T., & Rolston, D. E. (2000). Mechanistic Modeling of Nitrite Accumulation and Nitrogen Oxide Gas Emissions during Nitrification. *Journal of Environment Quality*, *29*, 1741. <https://doi.org/10.2134/jeq2000.00472425002900060003x>
- Vitória, L., Otero, N., Soler, A., & Canals, A. (2004). Fertilizer characterization: Isotopic data (N, S, O, C, and Sr). *Environmental Science and Technology*, *38*(12), 3254–3262. <https://doi.org/10.1021/es0348187>
- Vitousek, P. M., & Matson, P. A. (1993). Agriculture, the Global Nitrogen Cycle, and Trace Gas Flux In: Oremland R.S (Ed.) (pp. 193–208). *Biogeochemistry of Global Change*. Boston, MA: Springer US. https://doi.org/10.1007/978-1-4615-2812-8_10
- Walters, & Power, J. F. (1991). Legume Residue and Soil Water Effects on Denitrification In Soils of Different Texture, *23*(12).
- Walters, W. W., Goodwin, S. R., & Michalski, G. (2015). Nitrogen stable isotope composition ($\delta^{15}\text{N}$) of vehicle-emitted NOx. *Environmental Science and Technology*, *49*(4), 2278–2285. <https://doi.org/10.1021/es505580v>
- Wanek, W. (2008). Short-term ^{15}N uptake kinetics and nitrogen nutrition of bryophytes in a lowland rainforest , Costa Rica, 51–62.
- Wang, A., Fang, Y., Chen, D., Phillips, O., Koba, K., Zhu, W., & Zhu, J. (2018). High nitrogen isotope fractionation of nitrate during denitrification in four forest soils and its implications for denitrification rate estimates. *Science of the Total Environment*, *633*, 1078–1088. <https://doi.org/10.1016/j.scitotenv.2018.03.261>
- Ward, B. B. (2011). Nitrification: an introduction and overview of the state of the field. In *Nitrification* (pp. 3–8). American Society of Microbiology.
- Wassenaar, L. I., Kumar, B., Douence, C., Belachew, D. L., & Aggarwal, P. K. (2016). Measurement of extremely ^2H -enriched water samples by laser spectrometry: Application to batch electrolytic concentration of environmental tritium samples. *Rapid Communications in Mass Spectrometry*, *30*(3), 415–422. <https://doi.org/10.1002/rcm.7459>

- Weier, K. L., Doran, J. W., Power, J. F., & Walters, D. T. (1984). Denitrification and the Dinitrogen / Nitrous Oxide Ratio as Affected by Soil Water , Available Carbon , and Nitrate the field solely from N₂O flux measurements ., (3).
- Welch, H. (1969). A Method for Marking the Point of Anhydrous Ammonia Release, (542), 1968–1970.
- Wilderer, P. A., Jones, W. L., & Daub, U. (2000). Competition In Denitrification Systems Affecting Reduction Rates and Accumulation of Nitrate, *21*(2), 239–245.
- William, D. (1998). Use of multiple isotope tracers to evaluate denitrification in ground ...
Library.
- Woo, D. K., & Kumar, P. (2017). Role of Micro-Topographic Variability on the Distribution of Inorganic Soil-Nitrogen Age in Intensively Managed Landscape. *Water Resources Research*, *53*(10), 8404–8422. <https://doi.org/10.1002/2017WR021053>
- World Health Organization. (2011). Guidelines for Drinking-Water Quality; World Health Organization, *1*, p342. [https://doi.org/10.1016/S1462-0758\(00\)00006-6](https://doi.org/10.1016/S1462-0758(00)00006-6)
- Wright, R. F., & Schindler, D. W. (1995). Interaction of acid rain and global changes: Effects on terrestrial and aquatic ecosystems. *Water, Air, & Soil Pollution*, *85*(1), 89–99. <https://doi.org/10.1007/BF00483691>
- Wunderlich, A., Meckenstock, R. U., & Einsiedl, F. (2013). A mixture of nitrite-oxidizing and denitrifying microorganisms affects the $\delta^{18}\text{O}$ of dissolved nitrate during anaerobic microbial denitrification depending on the $\delta^{18}\text{O}$ of ambient water. *Geochimica et Cosmochimica Acta*, *119*, 31–45. <https://doi.org/10.1016/j.gca.2013.05.028>
- Xia, Zhang, C., Zeng, X., Feng, Y., Weng, J., Lin, X., et al. (2011). Autotrophic growth of nitrifying community in an agricultural soil. *ISME Journal*, *5*(7), 1226–1236. <https://doi.org/10.1038/ismej.2011.5>
- Yang, X., Wu, X., Hao, H., & He, Z. (2008). Mechanisms and assessment of water eutrophication. *Journal of Zhejiang University Science*, *9*(3), 197–209. <https://doi.org/10.1631/jzus.B0710626>
- Yoshida, N. (1988). ¹⁵N-depleted N₂O as a product of nitrification. *Nature*, *335*(6190), 528–529. <https://doi.org/10.1038/335528a0>
- Yoshinari, T., & Wahlen, M. (1985a). Oxygen isotope ratios in N₂O from nitrification at a wastewater treatment facility. *Nature*, *317*, 349.
- Yoshinari, T., & Wahlen, M. (1985b). Oxygen isotope ratios in N₂O from nitrification at a wastewater treatment facility. *Nature*, *317*, 349. Retrieved from <http://dx.doi.org/10.1038/317349a0>

- Yun, S., & Ro, H. (2014). Soil Biology & Biochemistry Can nitrogen isotope fractionation reveal ammonia oxidation responses to varying soil moisture. *Soil Biology and Biochemistry*, 76, 136–139. <https://doi.org/10.1016/j.soilbio.2014.04.032>
- Yun, S., Ro, H., & Choi, W. (2011). Interpreting the temperature-induced response of ammonia oxidizing microorganisms in soil using nitrogen isotope fractionation, 1253–1261. <https://doi.org/10.1007/s11368-011-0380-1>
- Zhang, L. M., Hu, H. W., Shen, J. P., & He, J. Z. (2012). Ammonia-oxidizing archaea have more important role than ammonia-oxidizing bacteria in ammonia oxidation of strongly acidic soils. *ISME Journal*, 6(5), 1032–1045. <https://doi.org/10.1038/ismej.2011.168>

APPENDIX

SUPPLEMENTARY DATA CHAPTER 5

Equation to determine tile discharge rate

Tile discharge rates (Q) were determined using equations 1A, 1B, and 1C. The equation utilized dependent upon the height of the water upstream (H_{weir}) and down stream (H_{down}).

If $H_{down} > H_{weir}$ equation 1A was used

$$Q = C_d H^2 \tan \frac{\theta}{2} \sqrt{2g(H_{up} - H_{down})} \quad \text{Eq. 1A}$$

If $H_{up} \leq 0$ equation 1B was used

$$Q = 0 \quad \text{Eq. 1B}$$

Otherwise equation 1C was used

$$Q = \frac{8}{15} \sqrt{2g} C_d \tan \frac{\theta}{2} (H_{up} + k_h)^{\frac{5}{2}} \quad \text{Eq. 1C}$$

Where Q is discharge rates, C_d is the discharge coefficient for flow through a triangular orifice (0.58), K_h is a head correction factor (15mm). All heights are relative to the notch of the weir. H_{down} is the height of the water surface downstream. H_{up} is the height of the water upstream. H_{weir} is the height from the notch to the top of the weir. g is gravity ($g = 9.81\text{m/s}^2$).

N mass balance within field.

The 61 kg of N ha^{-1} from Soil N is counted as N turnover not added N.

Amount of N added = Amount of N loss.

N added = Fertilizers

N loss = Plant up take + Denitrification + Leaching

Fertilizers = Plant up take + Denitrification + Leaching

Plant up take was calculated using the average N removed per bushel of corn (0.4kg N) with the average bushels harvest per acre in Illinois in 2016 (490 bushel per hectare) = 196 kg N ha^{-1} (National Agricultural Statistics Survey., 2018; Sawyer & Mallarino, 2007).

232 kg N ha^{-1} = 196 kg N ha^{-1} (plant uptake) – 31kg N ha^{-1} (leached) – 7.6kg N ha^{-1} = -2.7 kg N ha^{-1}

We calculate the field had a net loss of 2.7kg N ha^{-1} .

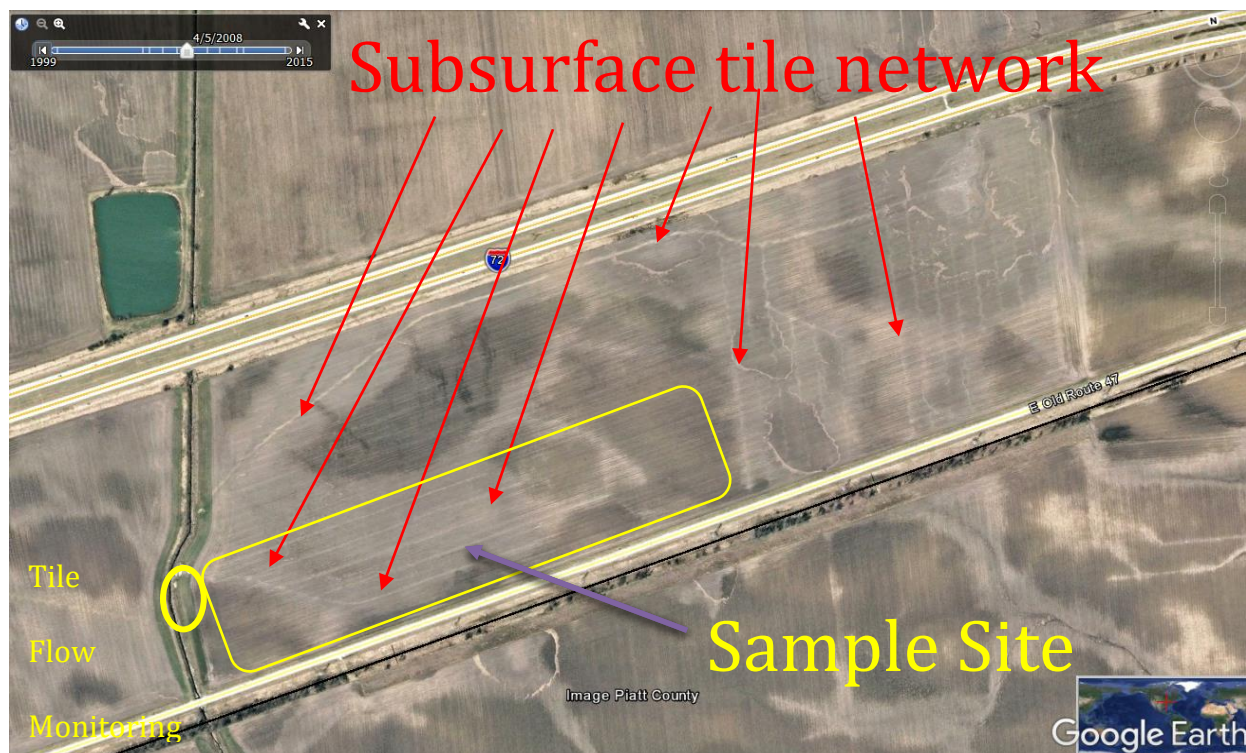


Figure S1. Aerial view (study area from April 5th, 2008 from Google Earth) of the experimental plot. Red arrows point out impressions in the soil due to tile drains. The yellow box represents the 6.75ha study site drainage area. The oval circle marks the location of tile discharge monitoring and sampling, and the collection of hydrological and meteorological data.

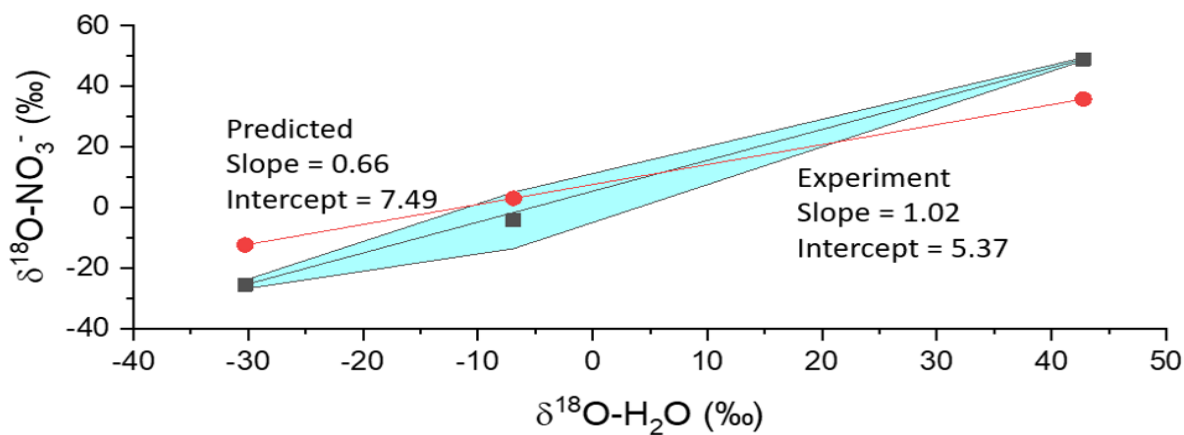


Figure S2. The slope of $\delta^{18}\text{O-NO}_3^-$ to $\delta^{18}\text{O-H}_2\text{O}$ of experiment is shown in the black squares/line. The slope represents the contribution of oxygen from H_2O . The theoretical slope of $\delta^{18}\text{O-NO}_3^-$ to $\delta^{18}\text{O-H}_2\text{O}$ based on the biochemical steps ($f_{\text{H}_2\text{O}} = 0.66$, $f_{\text{O}_2} = 0.33$) is shown in the red dots/line.

VITA

Benjamin Wilkins
 Purdue University
 Department of Chemistry
 560 Oval Drive
 West Lafayette, Indiana 47907
wilkin40@purdue.edu

Education:

Ph.D. Analytical Chemistry Purdue University Degree GPA: 3.99	2014 – 2019 West Lafayette, Indiana
B.S. In Chemistry University of New Orleans Degree GPA: 3.92 Summa Cum Laude	2010 – 2014 New Orleans, Louisiana

Peer Reviewed Papers (First Author):

Wilkins, B; Woo, D; Kumar, P; Keefer, D; Keefer, L; Fisher, M; Li, J; Hodson, T; Welp, L; Michalski, G. **Quantification of Field-Scale Denitrification by Stable Isotope Analysis of Nitrate and Water from Tile Drain Discharge.** *WRR*. 2019 (Submitted).

Wilkins, B; Yount, J; Michalski, G. **Determining the ¹⁵N Enrichment and Sources of Oxygen in Nitrate Produced by Nitrification in an Agricultural.** *EST*. 2019 (To be Submitted)

Wilkins, B; Vera, V; Michalski, G. **Determination of the ¹⁵N Enrichment and Source of Oxygen in Nitrate Produced by nitrification in an Agricultural Soil.** *JGR*. 2019 (To be Submitted)

Wilkins, B; Woo, D; Kumar, P; Keefer, D; Keefer, L; Fisher, M; Li, J; Hodson, T; Welp, L; Michalski, G. **Solute Transport and Evaporation within a Tile Drain Agricultural Field.** (In Prep).

Peer Reviewed Paper (Co-Author)

Li, J., Michalski, G., Davy, P., Harvey, M., Katzman, T., & Wilkins, B. (2018). **Investigating Source Contributions of Size-Aggregated Aerosols Collected in Southern Ocean and Baring Head, New Zealand Using Sulfur Isotopes.** *Geophysical Research Letters*, 45(8), 3717-3727.

Li, J; F, Wang; G, Michalski; Wilkins, B; (2018). **Atmospheric Depositions Across the Atacama Desert, Chile: Compositions, Source Distributions, and Interannual Variabilities** (Submitted).

Fraga, C; Primera-Pedrozo, C; Breton-Vega, A; Zumbach, M; Wilkins, B. **Adsorption and Desorption Study of a Nerve Agent Simulant from Office Materials for Forensic Applications (2019)** (To be Submitted)

Li, J; Wilkins, B; G Michalski. **Reduction of NO₃⁻ and NO₂⁻ by Titanium (III) to N₂O for Δ17O isotopic analysis. (2019)** (In Prep)

Oral Presentations (First Author)

Wilkins, B; Woo, D; Kumar, P; Keefer, D; Keefer, L; Fisher, M; Li, J; Hodson, T; Welp, L; Michalski, G. **Quantification of Field-Scale Denitrification by Stable Isotope Analysis of Nitrate and Water from Tile Drain Discharge.** (2018) Critical Zone Observatory-Intensively Managed Landscapes, Urbana, Illinois.

Wilkins, B; Pliskin, S. **Tracing Triacetin Migration by UPLC-MS.** (2018) Naval Weapons Station Seal Beach. Seal Beach California.

Wilkins, B; Fraga, C. **Dimethyl Methylphosphonate (DMMP) Sorption to Office Materials for Potential Isotopic Forensic Tracing** (2016). Pacific Northwest National Labs, Richland, Washington.

Oral Presentations (Co-Author)

Fraga, C; Primera-Pedrozo, O; Breton-Vega, A; Zumbach, M; Wilkins, B. **Adsorption and Desorption Study of a Nerve Agent Simulant from Office Material for Forensic Applications.** (2018) ACS. Boston, Massachusetts.

Michalski, G; Wilkins, B; Woo, D; Kumar, P; Keefer, D; Keefer, L; Li, J; Hodson, T; Welp, L. **Isotope Assessment of N Processing in a Corn/Soy Farm in the IML-CZO.** (2017) Critical Zone Observatory-Intensively Managed Landscapes, Urbana, Illinois.

Poster Presentations (First Author)

Wilkins, B; Woo, D; Kumar, P; Keefer, D; Keefer, L; Fisher, M; Li, J; Hodson, T; Welp, L; Michalski, G. **Nutrient Concentrations and Stable Isotopes of Runoff from a Midwest Tile-Drained Corn Field.** (2017) AGU Fall Meeting, New Orleans, Louisiana.

Wilkins, B, Li, J, Michalski, G; **Stable Isotopes in the Michalski Lab.** (2018) Purdue University, West Lafayette, Indiana.

Wilkins, B, Michalski, G. **Stable Isotopes and Nutrient Concentrations of a Midwestern Agricultural Soils.** (2017) Purdue University, West Lafayette, Indiana.

Wilkins, B, Katzman T, Michalski, G. **Research in the Michalski Lab.** (2016) Purdue University, West Lafayette, Indiana.

Wilkins, B, Katzman T, Michalski, G. **Research in the Michalski Lab.** (2015) Purdue University, West Lafayette, Indiana.

Poster Presentation (Co-Author)

Li, J., Michalski, G., Davy, P., Harvey, M., Katzman, T., & Wilkins, B. (2018). **Sulfur Isotopic Characteristics and Source Contributions of Size Aggregated Aerosols Collected in Baring Head, New Zealand.** (2017) AGU Fall Meeting, New Orleans, Louisiana.

Michalski, G; Wilkins, B; Vera, A; Yount, J. **Oxygen and Nitrogen Isotope Effects During Nitrification and Denitrification Occurring in Midwestern Soils.** (2017) AGU Fall Meeting, New Orleans, Louisiana.

Vera, O; Wilkins, B; Michalski, G. **Determining the Fractionation Factor of Denitrification in a Midwestern Maize Soil.** (2017) ABRCMS, Phoenix, Arizona.

Honors and Awards

DoD ASEE SMART Fellowship	2017
DHS-STEM Internship	2016
Purdue Incentive Grant	2016
Eppleton Teaching Award	2015
Purdue University Graduate Teaching Award	2015
Miller scholarship, University of New Orleans	2013
Undergraduate representative on grade appeal committee	2013
Founder of Alpha Chi Sigma University of New Orleans chapter	2013

Teaching

Teaching Assistant: CHM 111, General Chemistry, Fall 2014
 Supervisor Teaching Assistant: CHM 111/112, General Chemistry, Spring 2015-Spring 2017
 Teaching Assistant, EAPS 104, Oceanography, Summer 2015
 Guest Laboratory Instructor: EAPS591, Stable Isotope Instrumentation, Spring 2018

Mentorship

Purdue University Summer Undergraduate Research Fellowships – 2015,2017
 Purdue University Research Experiences for Undergraduates – 2017
 Purdue Undergraduates Research Experience 2015-2019 (8 total)

Research Experience:

Research Assistant
Purdue University

August 2014 – Present
West Lafayette, Indiana

- Collaborated development of N₂O Off-Axis Integrated Cavity Output Spectroscopy (OA-ICOS) laser research on the forensic applications of stable isotopes of Nitrogen and Oxygen focusing on NO₃⁻ and reduced products, development of peripherals for concentrating and separating compounds for analysis, Proper maintenance of GC-IRMS and OA-ICOS, developed isotope standards, separation by cyro-trapping.

Analytical Chemist
Naval Surface Warfare Center – Crane

May 2018 – August 2018
Crane, Indiana

- Utilized ultra-performance liquid chromatograph/ photo diode array/ mass spectrometry for separation and detection of molecules.

Teaching Assistant
Purdue University

August 2014 – August 2017
West Lafayette, Indiana

- Prepared labs for students, created quizzes, exams, and keys, sought proper lab safety for students, coordinated with professors and prep lab, led instructed teaching assistants, performed weekly labs and recitations.

Analytical Chemist
Pacific Northwest National Laboratory

June 2016 – August 2016
Richland, Washington

- Used inverse gas chromatography mass spectrometry/ flame ionization detection to understand the interaction of nerve gas simulates with various common office material.

Research Assistant
University of New Orleans

January 2014 – May 2014
New Orleans, Louisiana

- Synthesis of new layered oxides and perovskites, performed topochemical reactions, characterization using x-ray crystallography and elemental analysis.

Analytical Chemist
Thionville Laboratories

August 2013-December 2013
Harahan, Louisiana

- Analysis of various grain and oil commodities for the following: metals and other elements using ICP, Pesticides using GC/MS and HPLC, Hexane Residues using GC. Tocopherols and tocotrienols by HPLC, assay toxins, unsaponifiable matter, total fatty acids, solidification point, specific gravity and density, saponification value, refined and bleached color, phosphorus, peroxide value, moisture and volatile matter, iodine value, free fatty acids, p - anisidine values, and unsapaonifiable matter.

LaACES Program
University of New Orleans

August 2012- May 2013
New Orleans, Louisiana

- Performed research on atmospheric conditions, payload package, calibrated instruments, wrote, recorded, and kept documents, aided in software programming.

Analytical Chemist
St. Tammany Parish Sheriff's Office Crime Lab

January 2013 – May 2013
Covington, Louisiana

- Analysis of unknown suspected drug compounds, by GC/MS, FT-IR, and microscopy, running daily QC and standards, making of dilutions and standards, Analysis of Gunshot residues by SEM, firearm and tool analysis by comparison microscopy, extraction of digital forensics evidence, latent print analysis, and hair and fiber analysis.